HHS Public Access

Author manuscript

Anat Rec (Hoboken). Author manuscript; available in PMC 2020 September 01.

Published in final edited form as:

Anat Rec (Hoboken). 2020 September ; 303(9): 2415–2475. doi:10.1002/ar.24326.

Comparative dental anatomy in newborn primates: Cusp mineralization

Kelsey Paddock[1], **Larissa Zeigler**[1], **Brianna Harvey**[1], **Kristen A. Prufrock**[2,3], **Jordan M. Liptak**[1], **Courtney M. Ficorilli**[1], **Russell T. Hogg**[4], **Christopher J. Bonar**[5], **Sian Evans**[6], **Lawrence Williams**[7], **Christopher J. Vinyard**[8], **Valerie B. DeLeon**[9], **Timothy D. Smith**[1]

[1]School of Physical Therapy, Slippery Rock University, Slippery Rock, Pennsylvania [2]Department of Pathology and Anatomical Sciences, University of Missouri, Columbia, Missouri [3]Center for Functional Anatomy and Evolution, Johns Hopkins University School of Medicine, Baltimore, Maryland [4]Department of Rehabilitation Sciences, Florida Gulf Coast University, Fort Myers, Florida [5]Dallas Zoo, Dallas, Texas [6]DuMond Conservancy, Miami, Florida [7]Department of Veterinary Sciences, UT MD Anderson Cancer Center, Michale E. Keeling Center for Comparative Medicine and Research, Bastrop, Texas [8]Department of Anatomy and Neurobiology, Northeast Ohio Medical University, Rootstown, Ohio [9]Department of Anthropology, University of Florida, Gainesville, Florida

Abstract

Previous descriptive work on deciduous dentition of primates has focused disproportionately on great apes and humans. To address this bias in the literature, we studied 131 subadult nonhominoid specimens (including 110 newborns) describing deciduous tooth morphology and assessing maximum hydroxyapatite density (MHD). All specimens were CT scanned at 70 kVp and reconstructed at 20.5–39 μm voxels. Grayscale intensity from scans was converted to hydroxyapatite (HA) density (mg HA/cm^3) using a linear conversion of grayscale values to calibration standards of known HA density (R^2 = .99). Using Amira software, mineralized dental tissues were captured by segmenting the tooth cusps first and then capturing the remainder of the teeth at descending thresholds of gray levels. We assessed the relationship of MHD of selected teeth to cranial length using Pearson correlation coefficients. In monkeys, anterior teeth are more mineralized than postcanine teeth. In tarsiers and most lemurs and lorises, postcanine teeth are the most highly mineralized. This suggests that monkeys have a more prolonged process of dental mineralization that begins with incisors and canines, while mineralization of postcanine teeth is delayed. This may in part be a result of relatively late weaning in most anthropoid primates. Results also reveal that in lemurs and lorises, MHD of the mandibular first permanent molar (M_1) negatively correlates with cranial length. In contrast, the MHD of M_1 positively correlates with cranial length in monkeys. This supports the hypothesis that natural selection acts independently

Correspondence Timothy D. Smith, School of Physical Therapy, Slippery Rock University, Slippery Rock, PA 16057. timothy.smith@sru.edu.

SUPPORTING INFORMATION

Additional supporting information may be found online in the Supporting Information section at the end of this article.

on dental growth as opposed to mineralization and indicates clear phylogenetic differences among primates.

Keywords

catarrhine; deciduous; dentition; platyrrhine

1 | INTRODUCTION

Our understanding of mammalian dentition has been gleaned through painstaking methodologies. Three-dimensional reconstructions of developing jaws have informed us of early tooth morphogenesis. These models were at first produced by stacking aligned physical cross-sections (e.g., composed of wax plates or paper) based on histological sections (Ahrens, 1913; Blechschmidt, 1954; Luckett & Maier, 1982; Ooë, 1979). Computer generated models, also based on histology, have produced further insights in more recent years (e.g., Radlanski, 1995). in vitro or immunohistochemical data can be embedded within these models to identify genetic control or signaling mechanisms (e.g., Jernvall, Kettunen, Karavanova, Martin, & Thesleff, 1994). Similarly labor-intensive procedures, such as clearing and staining whole tooth germs, have helped us to understand patterns of cusp mineralization (e.g., Tarrant & Swindler, 1973; Winkler, Schwartz, & Swindler, 1991). The germs are painstakingly dissected out of the jaws and stained by soaking in alizarin red S solution. Then the outer collagenous capsule, the follicle, is cut open to reveal the mineralized portion of the crown, which may include only cusp tips. Radiological methods have historically failed to identify some teeth in such early stages of mineralization (see Garn, Lewis, & Polacheck, 1959; Winkler et al., 1991). More recently, micro-computed tomography (μ-CT) has significantly increased knowledge on dental development, particularly regarding the dentition of small-bodied primates, including both living and extinct taxa, and increased scan resolution has allowed detailed study of deciduous teeth in smaller primates (e.g., Franzen et al., 2009; Smith et al., 2011). In this study, we use μ-CT to further our understanding of the extent of cusp mineralization in primates at birth, a timeframe for which we currently lack a broad comparative perspective.

Compared to our understanding of the sequence in which teeth pierce the gingiva (gingival emergence) and transition from within alveolar crypts into occlusion (dental eruption), we have a far poorer comparative understanding of how the crown forms. Prior to the widespread availability of μ-CT, our most extensive and detailed observations centered on larger and medium-sized primates, which could be studied grossly or as whole-mount stained specimens (e.g., Kraus & Jordan, 1965; Tarrant & Swindler, 1973). The most comprehensive descriptions have focused on human deciduous teeth (e.g., Kraus & Jordan, 1965), but our extant and extinct closest relatives have also attracted much attention (e.g., Macchiarelli et al., 2006; Mann, 1988). The rare studies of smaller primates have relied on histologically sectioned material (e.g., Luckett & Maier, 1982). The advantages of histological methods are the fine resolution through microscopy and the ability to identify tissue types using a variety of staining procedures. However, the resolution of μ-CT has improved, now reaching interslice distances that can match that achieved during routine

paraffin histology. In this study, we use μ-CT in a comparative study of maxillary and mandibular tooth crowns in perinatal primates.

1.1 | Dentition of the newborn

In the newborn primate, there is most likely a mix of deciduous and permanent teeth that have at least initiated mineralization (Smith et al., 2015). For simplicity, our terminology here divides teeth into three groups: deciduous teeth (i1, i2, dc, dp2-dp4), "replacement" teeth (I1, I2, C, P2, P3, P4, i.e., the secondary teeth), and "permanent" teeth (the molars M1, M2, M3). Maxillary teeth are denoted by superscript numbers (e.g., M^1) and mandibular teeth are denoted by subscript numbers (e.g., M_1). The nomenclature used for postcanine deciduous teeth, "deciduous premolars," is meant to facilitate a discussion of tooth location in the developing jaw. These teeth are often discussed as "deciduous molars" in the literature (morphologically, this is a more appropriate term for the primary teeth replaced by the adult premolars, e.g., Schwartz, 2007).

Nearly all newborn primates possess at least one partially mineralized permanent tooth at birth: M1 (Smith et al., 2015). This is one trait that distinguishes primates from altricial mammals such as scandentians. However, primates vary enormously in the rate at which replacement teeth mineralize and erupt. In some, deciduous teeth have already been shed at birth, and replacement teeth have initiated crown formation; in others, deciduous teeth are maintained postnatally to weaning age and beyond (Godfrey, Samonds, Jungers, & Sutherland, 2001; Godfrey, Samonds, Jungers, Sutherland, & Irwin, 2004; Luckett & Maier, 1982; Smith et al., 2015). The extent of variation may relate to the relatively protracted parenting period for primates compared to most mammals. The newborn primate is at first fully dependent on, and later supplemented by maternal milk for a variable amount of time. This might be thought to give natural selection an unusually light hand on the dentition of the newborn. However, certain specializations can be observed at birth, such as precocious mineralization of cusps in folivorous primates (Smith et al., 2015). Hence, we expect certain adaptive characteristics of primate tooth cusps may be already apparent at birth.

1.2 | Crown mineralization in newborn anthropoid primates

The literature on crown mineralization in primates is centered mostly on hominoid primates (apes and humans). Using whole mount preparations that stained enamel and dentin, Kraus and Jordan (1965) studied developing tooth crowns of fetal and neonatal humans. The teeth of newborn great apes were studied by Seibert and Swindler (1991) and Winkler et al. (1991) using similar methods and radiography. In hominoids, mineralization of deciduous tooth crowns is well underway at birth, but the roots have yet to develop; the deciduous incisor crowns are the most complete, while deciduous canine and premolar crowns are still forming, particularly in the cervical region. Maxillary or mandibular dp4 may lag behind dp3 in mineralization (e.g., only two to three cusps of dp^4 are mineralized in some newborns). Seibert and Swindler (1991) note that all cusps of mandibular dp_4 of *Pan troglodytes* are mineralized, but the central basin is incomplete. Among three extant hominoids studied, Pongo (Winkler et al., 1991) may be more advanced than *Pan* and *Homo*, although great apes have not been studied using large samples. M^1/M_1 cusp mineralization is

initiated (at least more mesial cusps), but has not yet extended to the tooth basin at birth. Replacement teeth have not commenced mineralization.

Other anthropoids studied regarding crown formation include *Alouatta caraya* (Tarrant & Swindler, 1973), *Macaca mulatta* (Swindler & McCoy, 1964), and *Papio anubis* (Swindler, Orlosky, & Hendrickx, 1968). In *A. caraya* the fetal stages were studied, but the state of mineralization of teeth in the largest specimens allows us to infer that most deciduous tooth crowns are nearly complete or complete in mineralization at birth. In the largest fetus, isolated cusps of all upper and lower permanent molars had formed. In the catarrhines, most detailed descriptions have centered on the deciduous premolars, and the crowns are described as fully formed in newborns, in terms of occlusal features at least.

The sequence of cusp mineralization has also been addressed in anthropoids. Seibert and Swindler (1991) describe the sequence of cusp mineralization in *Pan* as follows. For the maxillary dps and M^1: paracone, protocone, metacone, then hypocone. For the mandibular dps and M_1: protoconid, metaconid, hypoconid, entoconid, and hypoconulid (if present). This sequence of mineralization corresponds to that in humans (Kraus & Jordan, 1965). Moreover, the above pattern of cusp formation for M_1 applies to all extant hominoids (Oka & Kraus, 1969), *M. mulatta* (Swindler & McCoy, 1964), *P. anubis* (Swindler et al., 1968), and *Theropithecus gelada* (Swindler & Beynon, 1993), suggesting the sequence may be identical across Catarrhini. Whether the sequence of cusp mineralization is similar among all anthropoids, or all primates, is unknown. In *A. caraya* it is uncertain whether the metacone or protocone of dp^4 calcify first (Tarrant & Swindler, 1973). Tarrant and Swindler also observed that in *A. caraya*, the mesial cusp pair coalesces (i.e., the protocristid mineralizes) before the distal cusp pair initiates calcification. This is in contrast to other known anthropoids in which the primary cusps form prior to crests (e.g., Kraus & Jordan, 1965; Swindler & McCoy, 1964). Since we have scarce information on platyrrhines, and no information on cusp morphology in strepsirrhines, common patterns and subtle variations among primates remain unclear.

In part, this study is intended to resolve the paucity of morphological observations on the deciduous teeth of nonhuman primates, as noted by Daris Swindler in his book, *Primate Dentition* (Swindler, 2002). As of that date, detailed observations accompanied by pictorial accounts were only available on hominoids, some catarrhines, a single platyrrhine (Swindler, 2002), and descriptions of Malagasy strepsirrhines (Tattersall & Schwartz, 1974). Unfortunately, this particular aim is only partially achieved, because the majority of our sample is of an age in which the extent of crown mineralization varies greatly. This relates to our second and more important aim: to further assess the state of crown maturation in newborn primates. In our previous work (Smith et al., 2015), we sought to definitively establish the presence of mineralized teeth using histology. Here, we expand the diversity of primates studied by using a larger sample of specimens examined with μ-CT, thereby creating a better context for understanding the far more detailed existing knowledge base on hominoid crown formation, and a point of comparison for information on deciduous teeth of extinct primates. We directly compare the capacity of histology and μ-CT to locate developing teeth and establish patterns of crown maturation using the latter method. Finally, we assess the sequence of cusp mineralization using selected species and compare the

trajectory of cusp mineralization at similar ages. In sum, we make a preliminary attempt to discern differences in the pace and pattern of mineralization achieved during gestation and early postnatal age.

2 | MATERIALS AND METHODS

2.1 | Sample

Specimens included a large sample of nonhuman primates that were previously examined to establish dental maturity (Smith et al., 2015), and more recently acquired samples. All specimens died of natural causes and were obtained as cadavers. In sum, 110 primates considered to be neonates (or newborns; for criteria, see Smith et al., 2015) and 21 fetal or older subadult specimens were studied. Throughout the text, subadult age is indicated in postnatal days (e.g., Day 1 = a 1-day-old), in months, or as "fetal," based on collection records at the point of origin.

The head of each specimen was μ-CT scanned at Northeast Ohio Medical University (NEOMED) using the Scanco vivaCT scanner (scan parameters: 70 kVp; 114 μA). The volumes were reconstructed using 20.5–25 μm cubic voxels with 8-bit grayscale values ranging from 0 to 255 (see DeLeon & Smith, 2014; Smith, DeLeon, Vinyard, & Young, in press). Three-dimensional digital reconstructions from the μ-CT volume for selected specimens were rendered using the Amira® 6.1 software (Thermo Fisher). Three-dimensional surfaces for the dentition shown in this paper are freely available for download at MorphoSource (https://www.morphosource.org/Detail/ProjectDetail/Show/project_id/879).

A histological sample of selected heads from this sample was consulted to establish the identity of dental tissues (see below). The material was previously sectioned at 10 μm and stained with Gomori trichrome and other stains (see Smith et al., 2015 for further details).

Terminology for cusp morphology used throughout the text is primarily derived from Swindler (2002); see Supporting Information S1). In our tabulations of data, primate systematics are based on Fleagle (2013) except for Platyrrhini, which is arranged according to Rosenberger (2011).

2.2 | Identification of mineralized tissues using μ-CT

The grayscale intensity of teeth in microCT scans was converted to hydroxyapatite (HA) density with a linear conversion of grayscale values. Each grayscale value was converted to an HA density using the calibration standard of HA density (R^2 = .99). Using this regression equation ($y = 6.9269x - 222.8126$), HA density reaches 0 at approximately a gray level of 32. Based on this, we assume most of the μ-CT voxels below this gray level in the presumptive tooth are either predentin or noise.

To assess the ability of μ-CT to faithfully identify dentin and enamel, we compared μ-CT slices to histology of the same specimens. Because enamel becomes fragmented during sectioning, due to a lack of fibrous matrix (Nanci, 2007), we selected specimens in which the enamel survived decalcification and subsequent serial sectioning. In these specimens,

Amira 6.0 was used to align the volume of μ-CT image data with micrographs of serial histological sections of the same specimen (see DeLeon & Smith, 2014, for further details). As a result, we were able to make paired comparisons of serial histological sections to matching μ-CT slices (Figures 1 and 2).

Based on the comparisons at matching cross-sectional levels, crown thickness (Figure 1) and degree of mineralization (Figure 2) are potentially limiting factors for crown segmentation. One match (Figure 1a,b) is of a well-mineralized tooth. In the μ-CT slice, enamel and dentin are distinct in the protocone, especially near the tip, but this distinction fades near the base of the cusps, in the basins (Figure 1b) and closer to the cervical parts of the crown; this is true even in locations where histology confirms the presence of both tissues (e.g., Figure 1c).

Voxel size may be one limiting factor that prevents μ-CT-based discrimination of enamel and dentin at these locations, and may also limit the ability to detect dentin alone where it is especially thin (Figure 1d). However, since enamel in basins and nearer the crown base is deposited after cusp enamel (Swindler, 2002), it is also likely that the enamel and dentin of the basins and crown cervix have a greater overlap in range of HA density than at the cusps.

Generally, the least mineralized teeth in newborn primates are permanent molars. In newborn *Tarsius*, M^1 is actually highly mineralized (Figure 1), as are parts of M^2. M^3 has nascent mineralization of its protocone (Figure 2), and this tooth illustrates the capacity of μ-CT slices to identify teeth just entering the late bell stage. M^3 at first resides beneath the orbit with little/no ossification of the surrounding tissue (Figure 2a). The tooth still has plentiful stellate reticulum, and the paracone solely consists of dentin (Figure 2b), although newly secreted predentin is extending further toward the basin (Figure 2c). As a consequence, the paracone is an isolated small structure as detected in CT slices at matching levels (Figure 2d). Gray levels between 30 and 50 capture the entirety of the mineralized dentin, although likely at an exaggerated thickness by comparison to histology (Figure 2e); the cusp tip is captured at a narrower range of gray levels between 39 and 50 (Figure 2f).

2.3 | Correspondence between morphology as viewed in μ-CT and histology

The two methods used in our matched cross-sectional comparison each have advantages and disadvantages. For many tissues, histology remains the gold standard for microanatomical description, and for poorly mineralized or newly mineralizing tissue it remains the better method for discerning detail (Figure 2). However, μ-CT is approaching the ability to resolve fine structure of skeletonized tissues (Bouxsein et al., 2010; Reinholt, Burrows, Eiting, Dumont, & Smith, 2009). Using our matched comparisons, we assessed the advantages and disadvantages of μ-CT.

Both methods distort our view of dental tissues. Histological distortions depend on the methodology, but the commonly used procedure of paraffin embedding and sectioning produces both compositional alterations to tissue and physical artifacts. An example of the former is the change to enamel during decalcification, a required step for microtome sectioning. Dentin survives decalcification well because, like bone, it has a densely collagenous matrix, which stains intensely using connective tissue staining procedures (e.g., green in Gomori trichrome—Figures 1 and 2). Enamel lacks a fibrous extracellular matrix

and once decalcified it often shatters and flakes away during microtome sectioning, leaving the so-called enamel space, a gap between dentin and the outer enamel epithelium of teeth at the late bell stage (Nanci, 2007; although newly mineralized enamel survives decalcification far better). Shrinkage due to dehydration and folds or tearing are additional examples of physical alterations introduced by histology.

Imaging by μ-CT creates less severe distortions than histology, but scan parameters can affect the capacity to detect microanatomical detail (e.g., Bouxsein et al., 2010). Optimal energy levels used during radiographic methods such as μ-CT vary according to age, with subadult morphology better discerned with lower energy output than for adults. However, there is a tradeoff between discerning the presence of mineralized tissues and surface detail. Figure 3 shows μ-CT slices through the head of a neonatal marmoset (*Callithrix jacchus*) scanned at two energy levels. Matching slice levels at the level of deciduous anterior teeth (Figure 3a,b) and dp^4 (Figure 3c,d) illustrate a basic challenge of studying subadult dentition using radiological methods: teeth mature at different rates. In many anthropoids, the posterior deciduous teeth mineralize later than the deciduous incisors and canine cusp tips. Therefore, selecting a single parameter may provide optimal detail in one tooth but not another. This is not just an age-related phenomenon. Newborns of different species may vary to a similar degree in tissue-level maturity of any given tooth (Smith et al., 2015).

Each energy parameter shown in Figure 3 has advantages and disadvantages. The lower energy level (45 kVp) accentuates enamel, especially at the tip (Figure 3b), and also more clearly reveals thinner mineralized crown parts that are closer to the cervix (Figure 3d). However, the higher energy level (70 kVp) provides a clearer apical margin of the crowns (Figure 3a), with more distinct spaces between teeth compared to 45 kVp scan slices (Figure 3a, inset). Since our study focuses on crown mineralization patterns, we opted to use the higher energy level (70 kVp). We acknowledge a tradeoff: we are optimizing surface detail of the cusps, while potentially losing the ability to resolve the presence of the least mineralized or thinnest dentin and enamel.

With any energy level there are some voxels, especially near the pulp chamber, that are ambiguous in their composition, that is, whether they represent dentin. Thus, we assessed our ability to identify dentin using samples that were scanned and subsequently sectioned by doing a paired comparison of histology and μ-CT-derived measurements of dentin thickness. Using *Tarsius*, we selected dp^4 and M^1. Using *Saimiri*, we selected dp^4 (*in Saimiri*, the dentin-enamel junction [DEJ] could not yet be well distinguished in M^1). These teeth are all well-advanced in the late bell stage or erupted (*Tarsius* dp^4). In CT slices, enamel and dentin appeared to be distinguishable at the cusp tips and buccal marginal ridges, based on comparisons to matching histological levels (Figure 4a,b). A specific gray level range is needed to isolate dentin during segmentation. A low range in gray levels captures the least mineralized dentin, but excludes the more mature dentin of the cusps (Figure 4c). Expanding the gray level range to include all dentin may capture some enamel, and also bleed irregularly onto the apical surface, presumably capturing peripheral “noise” (Figure 4d). Thus, cusp dentin is best segmented using a range of gray levels that excludes both poorly mineralized dentin and enamel (Figure 4e).

To compare the two methods (histology and μ-CT), we measured buccal dentin thickness (along basoapical axis) for the buccal cusps and the marginal ridge in every histological section (amounting to every fifth 10-μmthick section) in which the cusp was present. Next, we measured the same distance using matching μ-CT slices. Measurements were made using ImageJ, after entering linear scale dimensions for each imaging method (histology scale: based on a stage micrometer photograph at the same magnification as the section; μ-CT scale: based on known voxel dimension of 20 μm). In μ-CT slices, dentin was first captured as a range of gray levels using the threshold function in ImageJ. For each μ-CT slice, we manually selected a gray level range that visually appeared to correspond to dentin. The lowest gray level was selected to produce a smooth dentin surface contour at the pulp cavity (irregular surfaces produce by wider ranges do not match the smooth histological contours). A peak gray level was selected to occur at the amelodentinal junction, as surmised by an abrupt change in gray level (Figure 4). Paired *t* tests reveal no significant ($p > .05$) differences between measurements of buccal apical dentin thickness using μ-CT slices versus histology (Saimiri dp^4: $t(19) = 1.49$; $p = .15$; *Tarsius* dp^4: $t(16) = 1.09$; $p = .29$; *Tarsius* M^1: $t(33) = 0.36$; $p = .72$). The measurements are correlated at $r = .83–.99$. Based on plots of the paired measurements for one buccal cusp, the paracone, there appears to be no systematic bias that would suggest μ-CT consistently under- or overestimates the thickness measured via histology (Figure 5). The degree of discordance between the two measurement series is virtually none for *Saimiri*, and limited for *Tarsius*. The measurements follow identical curves, suggesting that divergence could be explained by error in alignment of sections to μ-CT slices.

These results suggest that at least in regions where dentin is more mature (which tends to be in cusp regions of newborn), we may rely on thresholding to produce faithful reconstructions of the tooth crowns, with the caveat that the least mineralized portions of the tooth in our reconstructions may be somewhat exaggerated in the crown basins, and regions closer to the cervix. Interestingly, the close correspondence also suggests that dentin does not shrink significantly, even though distortions to soft parts of the tooth germ may be quite severe, especially in less mature germs (Figure 2).

Lastly, we assessed the reliability of two different observers (TDS and JML) to detect dentin in the same tooth (dp^4 of the newborn *Tarsius syrichta*). In the first trial, each observer selected a gray level range corresponding to dentin in all μ-CT slices along the apical margin on the buccal side. This was accomplished using the threshold function of ImageJ, and the pixel range corresponding to dentin was measured in basoapical distance. Observers visually identified the dentin of the buccal cusps and intervening crest in every fourth CT slice (total = 34 slices). Basoapical dentin height was measured from its pulp interface to its enamel interface. Results of the measurement series on identical μ-CT slices were highly correlated (Pearson $r = .97$).

2.4 | A step-wise (cusp-first) method for crown segmentation

The immaturity of dentin and enamel at the tissue level is a final issue complicating reconstruction of subadult teeth. Histology at matched levels of μ-CT slices indicates that the dentin and enamel surfaces (dentin facing the pulp cavity, at the DEJ, and apical enamel) are

smooth (Figures 1 and 4). And yet, using teeth that are not fully mineralized, threshold ranges that encompass all gray levels, from the softest dentin to cusp enamel, capture surface noise (Figure 6a,b). In erupted teeth, by contrast, all surfaces are far smoother within the threshold range. This difference may be explained by the process of enamel mineralization. In mature teeth, apical enamel is denser than that near the DEJ (He et al., 2011). However, during dental development, the enamel near the DEJ mineralizes first (Avery, 2002). As a result, most of the enamel at the apical surface is relatively less mineralized and this may lead to the tendency of some apical enamel to differentiate poorly from adjacent gray levels in terms of radio-opacity; because of this, reconstructions accomplished by segmentation using a large range of gray levels may recruit voxels from adjacent tissues or even scattered photons into the reconstructed volume (Figure 4d).

Based on these observations, we devised a sequence of segmentation using Amira 6.1 software which minimizes the capture of adjacent voxels at the tooth surface, and thus presumably producing contours with better fidelity to the actual apical enamel surface. In this step-wise method of segmentation, the cusp is captured first, using a relatively high range of grayscale values. This range varies by species, but in all cases the goal is to capture the cusp with smooth apical surfaces (Figure 6a). Subsequently, the remainder of the crown is captured at descending threshold ranges, which capture increasingly more basal parts of the crown (Figure 6b). Each descending range was chosen without allowing the selected voxels to “bleed” onto the apical surface and capture additional voxels presumed to be noise. Segmentation was complete when the last voxels in the cervical region or root (when present) were captured. Our reconstructions focus most on capturing the crown, and may exclude some of the deepest parts of the root since these were difficult to segment without capturing adjacent bone.

2.5 | Assessing maximum HA density on tooth crowns

Once teeth were reconstructed, we examined the crown to assess where HA densities are greatest or least. This was first assessed qualitatively in five percentile ranges: 0–25%, 25–50%, 50–75%, 75–85%, and 85–100% of maximum hydroxyapatite density (MHD). As explained above, 8-bit images allowed a range of possible grayscale values from 0 to 255. Based on our regression analysis against an HA standard, we exclude voxels below 30 as we presume them to represent unmineralized material. The total range of density for each tooth was from 30 to the peak for the individual tooth. For this total range, the gray level corresponding to the 25th, 50th, 75th, and 85th percentiles were calculated. Using Amira, these were then used to create five reconstructions of the upper and lower tooth rows in occlusal view: the portion of voxels of the tooth within (a) the 25–100% range, (b) the 50100% range, (c) the 75–100% range, (d) the 85–100% range, and (e) the 0 to 100% range (i.e., all tooth voxels).

Next, the first four ranges were sequentially superimposed over the last range, beginning with the entire tooth row (all tooth voxels), represented as a 2D white profile of the tooth crown. The four superimposed layers were colored and partially transparent to create “maps” of HA density for the entire tooth row (e.g., Figure 7 and see Supporting

Information S2). For each species, this map shows which parts of which teeth represent the highest density of HA, revealing patterns of mineralization across the tooth row at birth.

Qualitatively, HA density of the crowns was examined using occlusal views of at least one specimen of each species under study. In addition, MHD was recorded for a total of 86 neonates from our overall sample and then averaged for each of 40 species (20 haplorhines; 20 strepsirrhines). These were $\log_{10}$ transformed for normalization and then plotted against $\log_{10}$-transformed cranial length (prosthion-inion), used here as a proxy for body size. Previously, we found cranial length to be a good proxy for body size (Smith et al., 2015). This provides a means to test the hypothesis, based on that histological study, that small-bodied and folivorous primates have the most highly mineralized teeth at birth.

3 | RESULTS

3.1 | Morphology of the dentition in newborn catarrhine monkeys

3.1.1 | General considerations—

The crown morphology of all deciduous teeth as well as M^1/M_1 are clear in these catarrhine monkeys even at birth, because crown mineralization is at an advanced state (Tables 1–3). Di^1/di_1 is wider than di^2/di_2. In upper and lower jaws, di^2/di_2 is caniniform to a varying extent (Swindler, 2002). Thus, there is a varied gradation of morphology from di^1/di_1 to dc. A striking characteristic of the postcanine deciduous teeth is the bilophodont form, that is, there are pronounced transverse crests between mesial and distal cusp pairs, seen on dp^3/dp_3 and dp^4/dp_4, and beginning to mineralize on M1. Four primary cusps are present on deciduous premolars. But in the lower jaw, an additional cusplet may be present at the mesial end of the paracristid, a possible paraconid. This cusp, when present, is more buccally positioned than the paraconid in *Tarsius*. In addition, the paraconid is typically more mineralized than the paracristid, suggesting mineralization begins earlier. Thus, putative paraconids are included in the total count of primary cusps when present (Table 3), but more developmental work is needed to understand whether these form similarly to the other cusps. The only permanent tooth present in any of the cercopithecoids is M^1. Histological work has verified this, and neither M^2 nor any replacement teeth have even progressed to the bud stage (Smith et al., 2015).

Maps of the MHD of the crowns reveal contrasts with other primates. Cusps, transverse crests, and even the marginal ridges are intense foci of HA density, whereas the primary cusps are more of an emphasis of MHD in other anthropoids. This suggests that perhaps aside from the sequence of primary cusp mineralization, there are subtle differences in crown mineralization patterns among primates. Further consideration of HA density follows morphological descriptions.

3.1.2 | Maxillary dentition

Subfamily Cercopithecinae

Allenopithecus nigroviridis, neonate.: Di^1 has a slightly rounded incisal border (Figure 7). The incisal margin of di^2 reaches a central rounded tip and has a slight distal heel. Dc has a nearly conical cusp, slight distal and mesial marginal ridges, and a lingual cingulum. Each of the incisors has a lingual cingulum with a spike-like tubercle near its base. Much of the

crowns of the anterior teeth, especially apically and near the cingulum, have at least 50% MHD. The incisal margins of the incisors and the tip of dc reach 85% MHD.

Dp^3 and dp^4 are roughly quadrate in shape. Dp^3 is more rounded and slightly compressed in an ovoid contour on the mesial side. A trigon basin is present, as are mesial and distal fovea. Both maxillary dps also have the following features: the mesial and distal pairs of cusps are connected by transverse crests; well demarcated marginal ridges border anterior and posterior fovea; parastyles and metastyles are present. The anterior transverse crest of dp^3 is raised prominently compared to that of the posterior transverse crest. Both transverse crests of dp^4 resemble that of dp^3. All cusps of dp^3 reach or exceed 85% of MHD. Dp^4 is less mineralized than Dp^3 because only a single cusp (the paracone) reaches MHD of 85%. The trigon basin of dp^3 is also more highly mineralized than that of dp4. M^1 has four well-mineralized cusps and transverse crests that are almost mineralized, but the trigon basin is as yet, not mineralized. The paracone and a very small portion of the protocone of M^1 reach 50% MHD.

Cercocebus atys, neonate.: Di^1 has a rounded incisal border; there is a slight lingual cingulum that is continuous with a vertical ridge that leads only partway toward the incisal margin (Figure 7). Its root is beginning to mineralize. Di^2 is caniniform with a slight distal heel. Dc has a slightly compressed cusp, with distal and mesial marginal ridges. Compared to the other anterior teeth, dc is the least mineralized near the crown base. All anterior teeth have extensive portions of the crown reaching at least 50% MHD. The apical margins of the incisors and the cusp tip of dc have particularly high densities of HA and reach the 85th percentile of MHD.

Dp^3 and dp^4 each have roughly quadrate well-mineralized crowns. The transverse crests are moderately raised on each, accentuating the basin and foveae. Both maxillary dps also have parastyles. M^1 has four mineralized cusps and the anterior transverse crest is mineralized, but the trigon basin is not. Buccal cusps of dp^3 reach or exceed the 85th percentile of MHD; the protocone reaches the 75th percentile while the hypocone is the least mineralized. The trigon basin of dp^3 reaches 50% MHD. Dp^4 is less mineralized than Dp^3. None of the cusps exceed the 50th percentile of MHD. The two buccal cusps and the tip of the protocone of M^1 reach 50% MHD.

Macaca mulatta, neonate.: Di^1 is spatulate with a rounded incisal border. Its root is beginning to mineralize. Di^2 is caniniform. The cusp tip of dc tapers slightly in the lingual direction. All anterior teeth have extensive portions of the crown reaching at least 50% MHD. The apical margins of the incisors and the cusp tip of dc reach the 85th percentile of MHD.

Dp^3 and dp^4 each have a well-delineated basin and foveae. Buccal cusps are slightly more robust and parastyles are present. The former is somewhat trapezoidal, being longer on the buccal margin than lingually; dp^4 is more quadrate. In both dps, the anterior transverse crest is more elevated than the posterior crest. Dp^3 is much more mineralized than dp^4, with all cusps but the hypocone reaching the 85th percentile of MHD. The transverse crests and the parastyle also represent peaks of mineralization in dp^3. In dp^4 the four primary cusps as well

as the anterior marginal ridge represent the peaks in MHD, with the paracone highest at 75% MHD. Four isolated crests of M^1 are mineralized with the two mesial cusps having the highest MHD, reaching 50% at the cusp tips.

Papio anubis, neonate.: Di^1 is wider with a rounded incisal border (Figure 7). Its root is beginning to mineralize. Di^2 is caniniform, with the cusp leading to mesial and distal ridges, and has a small shelf-like lingual swelling. Dc is poorly mineralized at the crown base; the cusp is buccolingually compressed. On all anterior teeth the apical margins reach the 85th percentile of MHD. Di^1 is the best mineralized overall, with most of the crown at >50% MHD.

Dp^3 and dp^4 each have transverse crests to delineate a trigon basin and mesial/distal foveae. Buccal cusps are slightly more robust and small parastyles are present. Both teeth are elongated mesiodistally and quadrate in shape. Four crests of M^1 are mineralized, with the proximal two already connected by a transverse crest. Dp^3 is much more mineralized than dp^4, with all cusps (with the exception of the hypocone) reaching at least the 75th percentile of MHD and the paracone reaching 85% MHD. The mesial transverse crest and the parastyle also have high levels of mineralization in dp^3 relative to adjacent areas of the crown. In dp^4 the four primary cusps represent the peaks in MHD, with them all reaching 50% MHD. Similarly, in M^1 all four cusp tips reach 50% MHD.

Subfamily Colobinae

Colobus guereza, neonate.: A single newborn is described based on a skeletonized hemisected head.

Di^1 has a straight incisal margin adorned with three mamelons. There is a low vertical lingual pillar with furrows on either side. These meet a lingual heel near the base of the crown. The mesial and distal margins are slightly raised lingually, but they are not distinct ridges. Di^2 comes to a caniniform apex, which tapers to rounded incisal margins. Dc is a partially mineralized crown, pyramidal in form, with a stout lingual pillar. The crown base appears mostly unmineralized.

Dp^3 and dp^4 each have a large central basin, with smaller fovea mesial and distal to transverse ridges. The mesial fovea of dp^3 is a triangular projection, while it has a rounded mesial margin in dp^4. The transverse crests are higher in dp^4 than dp^3. Dp^4 is less mineralized than dp^3, with a thin central basin, and a poorly mineralized posterior margin. Three cusps of M^1 are mineralized; the hypocone remains unmineralized.

Trachypithecus francoisi, neonate.: Di^1 has a rounded incisal margin (Figure 7). Di^2 has a more triangular, almost caniniform shape, except for the concave lingual fossa. Dc has pronounced mesial and distal marginal ridges tapering from the cusp, and a more rounded lingual surface compared to the incisors.

Dp^3 and dp^4 are both quadrate in shape. The anterior transverse crest of dp^3 is raised compared to that of the posterior transverse crest, and compared to either transverse crest of dp^4. There are weakly pronounced parastyles on each dp (parastyles and metastyles were

described as absent in colobines by Swindler, 2002). A trigon basin is present, as are mesial and distal fovea, separated from the latter by transverse crests. M^1 has four well-mineralized cusps; but the trigon basin is as yet, unmineralized. Transverse crests also remain barely mineralized and the marginal crests have not, as yet, started to mineralize. M^2 is not mineralized (and has not progressed to even the bud stage—Smith et al., 2015).

3.1.3 | Mandibular dentition

Subfamily Cercopithecinae

Allenopithecus nigroviridis, neonate.: Di_1 is tall and narrow (Figure 8). By comparison, di_2 is relatively lower, more rounded on the labial side, and the incisal margin reaches a pointed apex. Dc is broad at the base and slightly rounded on its lingual surface. Distal to the cusp there is a slight depression and then a raised heel with a small tubercle. The bulk of the crown is less erupted than adjacent teeth, save for the cusp tip. The cusp tips of all anterior teeth reach or exceed 85% MHD.

Dp_3 is compressed and ovoid in shape; dp_4 is nearly quadrate. Each has four primary cusps and a mesial marginal ridge that at least partly outlines the trigonid basin. In dp_3, the ridge is low on the lingual side, so that the basin is open adjacent to the metaconid. Dp_4 has much more prominent cusps than dp_3; the marginal ridge is raised on both lingual and buccal sides. In both deciduous premolars, the paracristid leads to a small cusp, a putative paraconid. Dp_3 has higher HA densities at each of the cusps as compared to dp_4. Three cusps of dp_3 (protoconid, hypoconid, and, to the least extent, the metaconid) are at or beyond the 85th percentile of MHD. The protoconid is the most mineralized of the four cusps in dp_4 (a small portion of the tip exceeds 85% MHD), and the hypoconid is the least mineralized. The small tubercle on the mesial marginal ridge is similar in MHD to the ridge as a whole. M_1 has four prominent cusps, with a possible fifth cusp mesially. None of these cusps exceed 50% MHD, and the hypoconid is least mineralized. M_2 is not observed.

No replacement teeth are mineralized.

Cercocebus atys, neonate.: Di_1 is spatulate with a straight incisive margin (Figure 8). By comparison, di_2 has a longer incisive margin, coming to a pointed apex leading to a slightly sloping mesial margin and a deeply sloping distal margin. The dc is rounded on its lingual side, rather than slightly concave like the deciduous incisors. Yet it still has mesial and distal marginal ridges, reminiscent of an incisal ridge. The marginal ridges or cusp tips of all anterior teeth reach or exceed 85% MHD.

Dp_3 is mesiodistally elongated. The mesial side is narrow compared to the wider and flatter distal end. The tooth is rotated obliquely compared to dp_4, such that the mesial side of dp_3 nearly faces in a buccal direction. This is true of all of the cercopithecines but especially so in this *C. atys* specimen. Dp_4 has a wider mesial end. Both deciduous premolars have a raised paracristid arcing around a mesial fovea and in dp_4 this leads to a small cusplet resembling a paraconid. Transverse crests are pronounced in dp_4, but not dp_3. Dp_3 is better mineralized than dp_4, with the mesial cusp pairs reaching the 85th percentile of MHD and the distal pair reaching 75% MHD. In dp_4, all cusps reach the 50th percentile of MHD; the

paracristid represents a peak in MHD relative to the adjacent basin. M_1 has four mineralized cusps. They are isolated although the mesial pair has nearly come in contact along a transverse crest. All cusps of M_1 except the entoconid reach the 50th percentile of MHD.

Macaca mulatta, neonate.: Both deciduous incisors are spatulate with broad incisal margins. Di_1 has a mostly flattened apex with three small mamelons. In di_2 the incisal margin slopes downward from a central peak to a distal heel. The dc is incompletely mineralized but a pointed distolingual heel is beginning to form. All anterior teeth reach the 85th percentile of MHD along the incisal margins, or in dc, at the cusp tip and along ridges departing the mesial and distal sides of the cusp.

Dp_3 is mesiodistally elongated with four prominent primary cusps and a raised paracristid. The mesial fovea is narrow compared to the distal fovea, but not as buccolingually compressed as in *C. atys*. There is a small cusplet at the end of the paracristid toward the lingual side of the mesial fovea. The distal fovea is small. Dp_4 has all of the same characteristics as dp_3 except the mesial end and the fovea within it are broader and roughly equal in breadth to the central (talonid) region. Transverse crests are equally pronounced in both deciduous molars. Dp_3 is better mineralized than dp_4, with the mesial cusp pairs and the hypoconid reaching the 85th percentile of MHD and the entoconid reaching 75% MHD. The mesial and distal foveae are more mineralized than the talonid basin. In dp_4, all cusps and the paracristid reach the 50th percentile of MHD. M_1 has four isolated mineralized cusps. The protoconid of M_1 is the only cusp to reach the 50th percentile of MHD, whereas the entoconid reaches <25% MHD.

Papio anubis, neonate.: The deciduous anterior teeth are all very well-rounded buccally, and the incisors have a more exaggerated lingual convexity than the other cercopithecine specimens we examined (Figure 8). The incisal margin of di_2 comes to a slight caniniform peak, and the cusp of dc leads to sharp mesial and distal marginal ridges. All three deciduous anterior teeth reach the 85th percentile of MHD, the dc only at the cusp tip.

Both deciduous premolars are mesiodistally elongated. Each has a large mesial fovea, mesiodistally elongate in dp_3 and rounded in dp_4. The talonid basin is bounded by transverse crests, and is open buccally and lingually via grooves between mesial and distal cusp pairs; the basin is larger in dp_4. The distal fovea is small in both premolars. Each deciduous premolar has four primary cusps and a rounded swelling at the mesial end, positioned slightly to the buccal side of the raised “paraconid shelf.” Dp_4 has a small cusplet distal to the metaconid, near the groove between the lingual primary cusps. Dp_3 is better mineralized than dp_4, with the protoconid reaching the 85th percentile of MHD, the metaconid and the hypoconid reaching 75% MHD, and the entoconid reaching 50% MHD. The mesial fovea is more mineralized than the talonid basin or distal fovea. M_1 has four isolated cusps with the mesial pair almost connected by the mineralizing transverse crest. In dp_4 and M_1, all cusps reach the 50th percentile of MHD.

Subfamily Colobinae

Colobus guereza, neonate.: Di_1 has straight incisal margin that inclines distally downward; centrally there is a slight notch that is continuous with an incisive fossa. By comparison, the

incisal margin of di_2 reaches a rounded central peak and there is a more rounded lingual surface and a distal, lingual heel. The dc has a mesial marginal ridge next to a slight lingual fossa. The cusp leads to a more rounded distal margin that leads in a straight line to the base of the mineralized crown. In di_1 and dc, this line of MHD reaches 75%. Di_2 reaches a MHD of 85% near the rounded apex of the incisal margin.

In occlusal view, dp_3 has a squared profile distally, but mesially the anterior marginal ridge comes to a triangular apex. The trigonid basin is thus quite elongated. Dp_4 is more closely quadrate, with higher cusps than dp_3; the trigonid basin is smaller than in dp_3, and the talonid basin is deep. Dp_3 has a MHD reaching 75% at the protoconid and metaconid. In dp_4 all four cusps reach a MHD of 50%. Three cusps of M_1 are mineralized with the protoconid reaching a MHD of 50%. The entoconid remains unmineralized.

No replacement teeth are mineralized.

Trachypithecus francoisi, neonate.: In di_1, the incisal margin is straight with a central depression (Figure 8). On both di_2 and dc the incisal margin reaches a central peak. Di_2 has a lingual longitudinal ridge. Anterior teeth lack prominent anterior and posterior marginal ridges.

The trigonid basin of dp_3 is more elongated than in dp_4. In the latter, the trigonid basin has a more pronounced ridge on the lingual side. From dp_3 to M_1, teeth become increasingly quadrate in the occlusal view. M_1 is present with four cusps and a mineralized crest between the mesial cusp pair. The tooth basin remains unmineralized.

3.2 | Morphology of the dentition in newborn platyrrhine monkeys

3.2.1 | General considerations—

There is arguably more ontogenetic dental variation among New World monkeys than among Old World monkeys. There is also much variation in the status of crown maturation in newborn platyrrhines (Tables 1–3). Callitrichines have the least mineralized postcanine teeth at birth (especially dp^4/dp_4 crowns), implying altricial mineralization. *Alouatta*, Aotus, and many other platyrrhines are far more advanced in cusp mineralization at birth.

3.2.2 | Maxillary dentition

Family Atelidae

Alouatta seniculus, neonate.: Di^1 has a rounded incisal margin (Figure 9). Di^2, though buccolingually compressed like di^1, possesses a caniniform cusp. Dc is very broad and flattened buccolingually near the cusp tip. Nearer the base it is broad and possesses a pronounced lingual cingulum. The tooth lacks the vertical lingual ridge described in *A. palliata* (Swindler, 2002). Dc is less erupted and displaced buccally relative to dp^2. The apices of di^1 and dc are the most mineralized parts of the anterior teeth, reaching the 85th percentile of HA density (of MHD for all teeth). Di^2 reaches 75% MHD.

Dp^2 and dp^3 are each broad with pronounced paracones. Each has a pronounced lingual cingulum with two or more small cusps; on each, one is positionally consistent with a small protocone. Swindler noted two cusps on dp^3 of *A. palliata*. Dp^4 has a quadrate shape and

four cusps. A distinct but low crista obliqua is present, which intersects the lingual side distal to the protocone and traverses to the base of the metacone. Three styles are present on the buccal side of dp^4 (para-, meso-, and metastyles), whereas only the parastyle is evident on dp^3. These cusplets may be common on the deciduous premolars of Alouatta (see also Swindler, 2002). The most mineralized cusp of each upper dp is the paracone, reaching or exceeding 85% MHD. The presumptive protocone of dp^2 and dp^3 reaches a MHD of 50%. On dp^4, the protocone and hypocone reach 75%; the hypocone is least mineralized, reaching 50% MHD. The basins of all dps are mineralized at 25–50% of MHD. Tarrant and Swindler (1973) noted that the styles of dps do not derive from their own calcification centers. Consistent with this observation, none of the styles observed here are notable “peaks” in HA density, distinguishing them from the ridge along which the styles form. M^1 has three isolated mineralized cusps, reaching 50% MHD for both the paracone and metacone. M^2 is not present or mineralized (also see Smith et al., 2015).

Histological observations reveal that the permanent incisors are at the cap or bud stage, and other replacement teeth are not even that advanced at birth (Smith et al., 2015).

Family Cebidae

Callithrix jacchus and C. penicillata, neonate.: Morphologically, deciduous teeth of the two *Callithrix* spp. are similar. Di^1 has a rounded apex. Di^2 is caniniform with a distally curving cusp and a distolingual heel (in specimens in which the crown base is mineralized). Dc is similar in form to di^2, but with a broader base; the base of dc may be deficient compared to the incisors. Di^1 is mostly mineralized at 50% MHD or higher, and the incisal margin reaches 85% MHD. In *C. jacchus*, di^2 reaches 75% MHD at the cusp tip and 50% along mesial and distal margins and at the lingual heel. Additionally, the MHD of dc is highly localized near the cusp, with the tip at 85% MHD or higher. In *C. penicillata*, all anterior teeth reach or exceed the 85th percentile of MHD at the cusp apex.

Dp^2 is nearly triangular in profile (occlusal view) with a highly projecting paracone and distinct mesial and distal ridges. Dp^3 also has a small protocone and a parastyle is visible in some but may not be mineralized in others. Hershkovitz (1977) also noted stylar cusps on older infants. Dp^4 has three cusps, with the paracone the most pronounced, and a sharp ridge connecting the two buccal cusps. The trigon basin is poorly mineralized as is the distal marginal ridge. The parastyle is present (and a mesostyle in *C. penicillata*) but other stylar cusps are as yet unmineralized in *C. jacchus*. However, a mesostyle is visible in *C. penicillata*. It is distinctly more molariform than dp^3 and dp^2. Dp^2 reaches a MHD of 50% at the cusp. Dp^3 reaches a MHD of 75% at the paracone. The paracone of dp^4 reaches a MHD of 75%. In all deciduous premolars, much of the crown base is at <25% MHD. M^1 is not mineralized.

No replacement teeth are mineralized in newborns.

Cebuella pygmaea, neonate.: *Cebuella* has the most advanced mineralization of deciduous teeth at birth compared to other callitrichines (Figure 9). Di^1 has a rounded incisal margin and has commenced root formation. Di^2 is rotated lingually compared to di^1 and caniniform. Dc is broad-based with a high, backwardly tilting cusp. In two specimens examined

regarding HA density, dc reached the 85th percentile of MHD. The cusps of di^1 and di^2 reach a HA density at the 50th–85th percentiles of MHD; in one specimen di^1 exceeds the MHD of di^2, and the reverse is true of the other specimen. The anterior teeth reach higher levels of MHD than the postcanine teeth.

Dp^2 resembles dc, except with pronounced cingula. Dp^3 possesses two cusps and in at least one subadult, a weakly developed parastyle. Dp^4 is triangular with three cusps. The trigon basin may be incompletely mineralized in dp^4, but in some newborns it appears to be nearly complete with poorly mineralized matrix. Two specimens have para- and mesostyles on dp^4 (in other cases the buccal cingula is not mineralized enough to locate them). On an older infant, a weakly pronounced metastyle is also observed. Older subadults also possess pronounced lingual cingula on dp^4, which is not yet mineralized in the newborns. Both dp^2 and dp^3 reach 75% MHD. In the one perinatal specimen examined for HA density, the paracone of dp^4 also reaches the 75th percentile of MHD, but in the other the paracone only reaches the 50th percentile. The paracone of M^1 is mineralized in two neonates (Day 0, Day 5), but is not detected in a third specimen of similar size (but unrecorded specific age). Previously, mineralization of M^1 was detected in a Day 0 newborn using histology (Smith et al., 2015). In a specimen possessing a mineralized paracone of M^1, the tip reaches the 25th percentile of MHD.

In the Day 0 and Day 5 neonates, no replacement teeth are mineralized. In an older infant (estimated at 1 month of age) the apical part of I^1 and C are mineralized.

Leontopithecus rosalia, neonate.: One neonate examined had cusp mineralization comparable to that of *Saguinus* spp. (see below). The deciduous teeth of this species were briefly described and figured by Hershkovitz (1977, fig. V.28). Deciduous incisors resemble those of other callitrichines (rounded di^1 apex, caniniform di^2). Dc is pictured as robust and having a vertical lingual ridge. Dc and deciduous premolars are indicated to possess parastyles and distostyles/metastyles. Hershkovitz (1977) wrote that the molarization of deciduous premolars was “more extensive” in *Leontopithecus* compared to the same teeth in other callitrichines. Smith et al. (2011) measured the dental follicle volume of maxillary postcanine teeth and found *Leontopithecus* has large deciduous premolars, significantly larger compared to Callithrix. In contrast, M^1 is poorly mineralized in *Leontopithecus* newborns—some fail to exceed the early bell stage of development (Smith et al., 2011, 2015).

Saguinus spp., neonates, juvenile.: Di^1 and di^2 are both buccolingually compressed. Di^1 has a rounded incisal ridge while di^2 is caniniform with a parastyle; in one S. *geoffroyi* neonate a small distostyle is apparent. Dc is a nearly conical cusp except for a slightly flattened lingual surface, and lacks any cingula at birth. In a Day 27 *S. oedipus* infant, para- and distostyles are present, as described in Hershkovitz (1977). In both *S. midas* and *S. oedipus*, the anterior teeth are of greater overall mineral density compared to postcanine teeth (the latter having more poorly mineralized crown bases, by comparison). Di^1 and di^2 reach 75% of MHD at the incisal margin in newborn *S. geoffroyi*, and reach the 85th percentile in the other two species. Dc reaches or exceeds the 85th percentile of MHD in all three species.

Dp^2 and dp^3 have broad cusps with incomplete mineralization of the base. Parastyles are typically beginning to mineralize at birth, but the lingual cingulum and the protocone of dp^3 may or may not be mineralized, as yet. In one *S. geoffroyi* neonate, para- and distostyles are present on dp^2 and dp^3, and the protocone of dp^3 has begun to mineralize. The Day 27 *S. oedipus* has a lingual heel on dp^2; dp^3 has a fully mineralized crown with a protocone, a parastyle, and a distostyle. At birth, dp^4 has three mineralized cusps and a parastyle. The basin is poorly mineralized. At best, the mesial margin and a portion of the trigon basin of the same side are mineralized. The buccal cusps are connected by a low, sharp crest. The crown of dp^4 is nearly completely mineralized at day 27 in *S. oedipus*, except for the lingual cingulum (shown by Hershkovitz, 1977 in this species). No metastyle is apparent. All deciduous premolars have more poorly mineralized crown compared to anterior teeth. Dp^2 and dp^3 reach a MHD of 75–85% at the paracone in *S. geoffroyi* and *S. oedipus*, while dp^4 reaches the 50th percentile of MHD at the two buccal cusps. M^1 is typically unmineralized at birth; M^1 paracone and protocone tips are mineralized in the day 27 *S. oedipus*. In *S. midas* all three of these teeth have a lesser MHD, perhaps reflecting their less mineralized state overall in the specimen studied.

Absence of replacement teeth at birth was histologically confirmed by Smith et al. (2015). The P27 *S. oedipus* has a mineralized I^1.

Saimiri boliviensis, neonate.: Di^1 has a rounded incisal margin. Di^2 is similar but the margin slopes distally, making the cusp taller and more rounded mesially. Both incisors have mesial crests. Dc is broad with a distally curved cusp, sharp mesial and distal ridges, and a flattened lingual surface. The crown base of the dc is only partially mineralized.

Features of the dps resemble the illustration (fig. V.28) provided by Hershkovitz (1977) for *S. sciureus*. Dp^2 has a large paracone and a smaller protocone; projecting para- and distostyles give it a triangular appearance in occlusal profile. With a more expanded cingulum, dp^3 and dp^4 all have a more quadrate appearance. Dp^3 has two primary cusps (paracone, protocone), para- and distostyles, and a metaconule. Dp^4 has four cusps, the paracone, protocone, metacone, and hypocone; para- and metastyles are also present. A crista obliqua is pronounced, traversing to the base of the metacone. The distolingual side of the deciduous premolars appears least mineralized, with the lingual cingulum of dp^3 and dp^4 incompletely mineralized in all newborns. In the newborn with the most mineralized deciduous premolars, dp^4 has a hypocone as well as a small cusplet lingual to the protocone. However, overall the crown base is far better mineralized than in callitrichines. Smith et al. (2011) demonstrated that the posterior-most deciduous premolars, especially dp^4, are large in *Saimiri* relative to their facial size. This may partially explain the absence of a maxillary sinus in the genus. The paracone and protocone of M^1 are mineralized.

Cebus apella (older infant, Day 15).: No perinatal material of Cebus spp. were available for description, but the morphology of the deciduous dentition described here is based on an older infant. Di^1 is broad with a lingual fossa and a slight lingual heel; the mesial margin is slightly raised as a ridge. Di^2 is similar but smaller. Both incisors have nearly flat incisal margins and partially formed roots. Dc has a tall pointed cusp with a slight distal marginal

ridge and a shallow lingual concavity. The distolingual part of the crown appears incomplete and the root is unmineralized.

Dp^2 has a pronounced paracone and a smaller but distinct protocone. Raised mesial and distal ridges help to define a shallow basin. On dp^3, the paracone and protocone are more close to equally sized, with the former being slightly larger. The basin is more expansive mesiodistally and there is a slight hypocone and indistinct metacone. Both dp^2 and dp^4 have small para- and distostyles. Dp^4 is the largest deciduous premolar and is almost quadrate, with four cusps. A distinct crista obliqua is present, intersecting the metacone.

Family Pitheciidae

Pithecia pithecia, neonate.: Di^1 and di^2 are broad at the crown apex, with roots beginning to mineralize (Figure 9). Di^1 is far wider than di^2 with a rounded incisal margin. Di^2 has a pointed apex at the center of the incisal margin. The dc is conical except for a vertical ridge on the distolingual border; the base of the crown remains poorly mineralized at birth. All anterior teeth reach or exceed the 85th percentile of MHD, di^1 at isolated points along the incisive margin, di^2 at the central apex, and dc at the very tip of the cusp.

Dp^2 has an oval profile, elongated buccolingually, with a raised paracone bordered by mesial and distal ridges that lead to distinct para- and distostyles. Lingually is a diminutive protocone. Dp^3 and especially dp^4 are more quadrate in form. Dp^3 has less distinct para- and distostyles than the other two premolars. A small tubercle on the postcingulum resembles the postprotostyle described on replacement premolars in *Pithecia* (Swindler, 2002). In dp^4 the same features are present except a distinct metacone is seen, and a more prominent cusp is seen on the postcingulum, constituting a hypocone in our view. A crista obliqua is distinct near the base of the metacone and transects the common border of the trigon and talon basins, before diminishing to a low ridge near the protocone. Small para- and metastyles are visible. In all deciduous premolars, the paracone is the densest part of the crown, reaching or exceeding 85% MHD. In dp^3 and dp^4, other cusps reach 50% MHD. The trigon basin of dp^3 also reaches 50% MHD. M^1 has four well-mineralized cusps and a trigon basin that has commenced mineralization and the talon is unmineralized. The paracone reaches 50% MHD, the protocone and metacone reach 25% MHD, while the hypocone and the periphery of the trigon basin are mineralized at <25% MHD.

The cusp tip of I^1 has commenced mineralization.

Callicebus cupreus, neonate.: Di^1 and di^2 each have rounded incisal margins. Dc is broad with distinct mesial and distal marginal ridges. Di^1 and di^2 reach at least the 75th percentile of MHD along the incisal margin. Dc reaches or exceeds a MHD of 85%.

Dp^2 and dp^3 both have a rounded shape in occlusal view with crests encircling the diameter. Each has a pronounced paracone; the lingual margin is raised with a small cusplets on dp^2 and a protocone on dp^3. Dp^4 is quadrate with three primary cusps; there is a widely flaring distolingual cingulum, but no distinct hypocone. Transverse crests extend lingually from the paracone and metacone, dividing the occlusal surface into three fossae. The deciduous premolars all reach or exceed a MHD of 85% at the paracone. M^1 is present and has four

cusps mineralized, including just the tip of the hypocone. The basin of M^1 has not yet mineralized. M^1 reaches a MHD of 50% at the paracone, and reaches the 25th percentile at the protocone and metacone.

I^1 is located distolingual to di^1. Only the incisal margin is mineralized, reaching a MHD of 25% at a pointed apex.

Aotus nancymaae, neonate.: Di^1 is apically broad with a slightly rounded incisal margin (Figure 9). Di^2 is smaller than di^1, and has one small cusp in the center of an otherwise rounded incisal margin. Dc has a conical cusp; the crown base is as yet poorly mineralized but appears to have a parastyle. Di^1 and dc each reach MHD at the 85th percentile or greater, while di2 varied in the two specimens examined for MHD (reaching the 50th percentile in one and exceeding the 85th percentile in a second specimen).

Dp^2 and dp^3 are both broad with a prominent paracone, and smaller protocone; each has a deep basin between the cusps. Dp^4 is quadrate with four primary cusps and a sharp crista obliqua demarcating the trigon basin. In one specimen the lingual cingulum is better developed, with a protostyle in addition to the hypocone. All deciduous premolars reach or exceed a MHD of 85% at the paracone. M^1 is present with three primary cusps, but the basin of the tooth is not yet mineralized. This tooth reaches the 50th percentile of MHD.

No replacement teeth are mineralized at birth.

3.2.3 | Mandibular dentition

Family Cebidae

Alouatta seniculus, neonate.: The incisal margin of di_1 is nearly straight whereas it comes to a rounded tip in di_2, similar to *Alouatta palliata* (Swindler, 2002; Figure 10). Dc is broad-based; the crown is less erupted than the incisors and only partially mineralized. Di_2 and dc reach 85% (of peak density for all teeth; MHD), whereas di_1 only reaches 75% MHD.

Dp_2 is nearly oval in occlusal profile, while dp_3 and dp_4 have a more quadrate shape. Dp_2 has one cusp connected to a raised longitudinal ridge (the protocristid), which descends toward the lingual margin where a small tubercle might be regarded as a rudimentary metaconid. On either side of the protocristid, mesial and distal marginal ridges create distinct foveae. In *Alouatta palliatta*, dp_2 is described as caniniform compared to the other dps (Swindler, 2002). In dp_3 and dp_4, four cusps are present. Dp_4 has more pronounced cusps compared to dp_3. The trigonid basin is larger than the talonid basin in dp_3, while this is reversed in dp_4 (described similarly in *A. palliatta*). Swindler describes dp_3 of *A. palliata* as relatively simple, in that it is bicuspid and lacks the cristid obliqua. In *A. seniculus*, dp_3 and dp_4 both have a cristid obliqua that connects to the protocristid near the protoconid. The mesial marginal ridge of dp_4 ends in a small cusplet near the lingual border, followed by a slight depression. On the distal marginal ridge of dp_4 there is a very small elevation that could be considered a rudimentary hypoconulid, which is rarely present in *Alouatta* according to Swindler (2002). The single prominent cusp in both dp_2 and dp_3 reaches 85% MHD, whereas dp_4 has portions of two cusps that reach 85% MHD (metaconid and protoconid). Along the distal marginal ridge, the small cusplet (rudimentary hypoconulid?)

corresponds to a small-elevated MHD along this border. M_1 has three mineralized cusps, each more prominent than in dp_4. M_2 is not mineralized or present. The metaconid and protoconid cusps of M1 are the most mineralized, reaching 50% MHD.

No replacement teeth are mineralized at birth.

Callithrix jacchus and Callithrix penicillata, neonate.: In both *Callithrix* spp., the anterior teeth are all buccolingually compressed; in this sense both dis are incisiform. Di_1 is has a rounded incisal margin that may reach a central point. Most have a broad cusp with an incisal ridge that comes to a point is the center. Di_2 is narrower, though still buccolingually flattened, with a small distolingual heel. Dc also has a somewhat flattened apical cusp, with a sharper cusp tip, and a distolingual heel. Marginal ridges are not prominent in the anterior teeth. All anterior teeth reach or exceed a HA density of 85% MHD. The peak for di_1 is more localized to the pointed center of the incisal ridge compared to di_2.

Dp_2 and dp_3 each have a highly projecting protoconid that is connected to mesial and distal marginal ridges. Hershkovitz (1977) indicated distinct distolingual heels for dp_2 and dp_3; these are nearly mineralized in one of the two neonates examined here, and are only partially mineralized in another. Dp_4 has four primary cusps and distinct basins. The trigonid basin is accentuated with a raised ridge along most of the perimeter; the talonid basin is completely or mostly mineralized at birth. It is distinctly more molariform than dp_3 and dp_2. *C. jacchus* neonate. Dp_2 and dp_3 both reach a MHD of 75% at the cusp apex. Dp_4 is less mineralized with a MHD of 50% in two of three specimens examined. Only the protoconid of M_1 is mineralized in most neonates; the metaconid tip is also mineralized in one. The protoconid of M_1 is at less than 25% of MHD in one specimen, but exceeds 25% MHD in two others.

No replacement teeth are mineralized at birth.

Cebuella pygmaea, neonate.: Di_1 has a broad flattened cusp with a rounded incisal margin. Di_2 is caniniform with a slightly curved cusp and, like the dc, possesses a distostyle (Figure 10). Dc has the same form but is more robust. It is a slight mesial swelling near the cusp base, but this is not a distinct projection (i.e., parastyle). Anterior teeth are more mineralized than the postcanine teeth. Both di_2 and dc reach or exceed 85% of MHD at the cusp tip. Di_1 reaches 75–85% MHD in the two newborns examined.

Dp_2 and dp_3 are both mesiodistally narrow with a high protoconid. Dp_2 resembles dc closely, but has a parastyle and a more projecting distostyle. Dp_3 has a small metaconid. Dp_4 is buccolingually broad with three to four prominent cusps mineralized at birth, and a cristid obliqua contacting the protocristid just buccal to the base of the protoconid. In one of the neonates the entoconid is as yet unmineralized. Mesially there is a pronounced paracristid that ends with a cusplet positionally consistent with a paraconid. Dp_2 is the most mineralized, reaching or exceeding 85% MHD. The protoconid of dp_3 and dp_4 reaches 75% MHD. M_1 is mineralized at the mesial cusp pair, the hypoconid, and a small rim of the mesial margin. Anterior teeth have a more mineralized protoconid than the postcanine teeth.

I_1 and I_2 have barely initiated mineralization (at <25% MHD), at the cusp tips alone, in a Day 5 newborn.

Leontopithecus rosalia, juvenile.: One neonate examined had cusp mineralization comparable to that of *Saguinus* spp. (see below). The deciduous mandibular teeth of this species were briefly described and figured by Hershkovitz (1977, fig. V.28). Deciduous incisors resemble those of other callitrichines. Dc is pictured as robust with a large distostyle/hypoconulid. Hershkovitz noted the conulids of dps were well developed in the single juvenile *Leontopithecus* he examined.

Saguinus spp., neonate.: Di_1 and di_2 each have three small swellings along the incisal margin, with di_1 being more spatulate, and di_2 have a sloping distal margin and a distostyle. Hershkovitz (1977) illustrated the same features in subadult *S. oedipus*, identifying the central cusp as protoconid, bracketed by the para- and distostylid. Dc is conical and as yet lacks any features of the crown base. A lingual cingulum, shown in dc of *S. oedipus* by Hershkovitz (1977) is not yet mineralized. The anterior tooth crowns are more fully formed than the postcanine teeth (especially the incisors, and reach the 75–85th percentile of MHD (dc, reaching the higher level).

Dp_2 has one primary cusp. Dp_3 has one to two primary cusps (protoconid, metaconid), a paracristid, and a protocristid, but it is incomplete lingually and distally. In an older (day 27) *S. oedipus* infant there are two primary cusps, as indicated by Hershkovitz (1977). In a weanling *S. oedipus*, the protocristid is especially raised and divides two basins; a small hypoconid is present. Thus, the degree of molarization of dp_3 may vary. Dp_4 has a cusplet at the end of the paracristid, in addition to the protoconid, metaconid and hypoconid. An entoconid is as yet unmineralized; it is present but miniscule in the day 27 infant. The trigonid basin is completely or nearly mineralized, but the talonid basin is unmineralized as birth. Dp_4 also has a cristid obliqua in a variable state of mineralization. In some newborns it is completely mineralized and intersects the protocristid buccal to the base of the protocone. The talonid basin is partially mineralized in one newborn. In *S. midas* and *S. oedipus*, dp_2 reaches the 75th percentile of MHD, whereas dp_3 and dp_4 only reach the 50th percentile. In *S. geoffroyi*, dp_2 reaches the 85th percentile of MHD, and dp_3 and dp_4 reach the 75th percentile. M_1 is not mineralized at birth in all but one newborn, a *S. geoffroyi* neonate, in which the protoconid is visible.

Saimiri boliviensis, neonate.: Di_1 and di_2 are both buccolingually flattened and slightly concave on the lingual side. Di_1 has a narrow apex with a flat incisal margin, while di_2 resembles the maxillary counterpart with its incisal border sloping distally. Dc is robust with a high cusp that tapers distally. A distolingual vertical ridge descends from the cusp to meet a pronounced lingual cingulum with a distostylid. The crown base is slightly deficient in mineralization on the mesiolingual margin.

Dp_2 and dp_3 are mesiodistally narrow. Dp_2 is nearly caniniform, but with a less projecting protoconid; it possesses a transverse ridge (positionally the same as the distolingual vertical ridge of dc) connecting the protoconid to a smaller metaconid. Dp_3 is bicuspid with cusps of more equal size, and a distal ledge with a distostylid. Dp_4 is quadrate with four primary cusps. A cristid oblique connects to the protocristid to the base of the protoconid. A paracristid extends mesially and arcs to the buccal side, demarcating the trigonid mesially and lingually. The talonoid basin is incompletely mineralized in some newborns; in

specimens where it is complete, a small hypoconulid is present. M_1 is present with two to three primary cusps, but no mineralized ridges or basins.

Cebus apella (Day 15).: Di_1 and di_2 expand apically to broad incisal margins; each has partially mineralized roots. Di_2 is larger with a more rounded apex and a more pronounced lingual heel. Di_2 is more robust than di_1. There are no marginal ridges. Dc has a curved pointed cusp emanating from a broad base. There is a ridge on the lingual surface. The root is unmineralized.

Dp_2 and dp_3 are nearly oval in occlusal profile, with two primary cusps (protoconid, metaconid) with a sharp, raised protocristid connecting them. The protocristid separates a broader mesial basin from a small distal basin. Small cusplets are found on the distobuccal side of each deciduous premolar, and also on the mesiobuccal side of dp_2. Dp_4 is quadrate in occlusal profile with four primary cusps, each pair parallel in mesiodistal position. The protoconid and metaconid are connected by a raised sharp crest, dividing a raised trigonid basin from a deeper talonid basin. M_1 presents with a protoconid and metaconid connected by a sharp protocristid, which is not as raised as in dp_4. The trigonid basin is partially mineralized. The hypoconid is an isolated cusp tip and the entoconid is as yet, unmineralized.

Family Pitheciidae

Pithecia pithecia, neonate.: Di_1 and di_2 each have straight incisal margins (Figure 10). Dc is conical with a sharp lingual crest projecting from tip toward the base of the crown. All anterior teeth reach or exceed the 85th percentile of MHD at the crown apex.

Dp_2 is bicuspid but with a weakly pronounced metaconid. The protoconid is prominent with a protocristid projecting partway toward a lingual shelf. Dp_3 is bicuspid, although distally there is a miniscule pair of cusps (reduced hypoconid, entoconid). A distinct protocristid divides trigonid and talonid basins. Dp_4 has four primary cusps, a small trigonid basin, and a broader talonid basin. In the dp_3 and dp_4, the trigonid basin is slightly more elevated and more mineralized compared to the talonid basin. The protocristid is relatively pronounced in all deciduous premolars, resembling *Callicebus* (see below). Dp_2 has the largest portion of 85% MHD compared to dp_3 and dp_4, which only the very tip of the protoconid reaching 85% of MHD. Four cusps of M_1 are present, but part of the talonid basin is unmineralized. Most of the cusps of M_1 reach 25% of MHD, except for the hypoconid (<25%). The protoconid of M_2 is visible (25% MHD), the only portion of that tooth that is mineralized. No replacement teeth are mineralized.

No replacement teeth are mineralized.

Callicebus cupreus, neonate.: Di_1 is narrow with a straight incisal margin. Di_2 is slightly broader than di_1 with a marginally rounded distal margin. Dc has a conical cusp that leads to a sharp mesial ridge; there is a flaring heel distolingually. Dc has the highest mineralization of each of the anterior teeth, reaching a MHD of 85%. Di_1 and di_2 reach a MHD of 50%.

Dp_2 and dp_3 are bicuspid and each have a prominent central crest running buccolingually, the protocristid; the metaconid is least pronounced in dp_2. Dp_4 has four cusps, well-mineralized basins, and a protocristid. The trigonid basin is elevated and bounded by raised marginal ridges; the talonid basin has deep grooves separating the distal cusp pair from the mesial pair. Distally the talonid basin lacks a marginal ridge; Thus, the talonid is "open" on all sides except for the protocristid on its mesial border. The protoconid of each deciduous premolar reaches or exceeds 85% MHD. On dp_4, the metaconid reaches 85% MHD at its tip, the hypoconid reaches 75% MHD, and the entoconid reaches 50% MHD. Three cusps of M_1 are mineralized. The entoconid is not apparent. The three cusps are as yet unconnected; a small portion of the protocristid descends lingually from the protoconid. M_1 reaches 50% of MHD at the protoconid and 25% at the metaconid.

The edges of the incisive margins of I_1 and I_2 are mineralized, reaching <25% MHD.

Aotus nancymaae, neonate.: Di_1 and di_2 each are buccolingually flattened; di_2 is broader at its apex (Figure 10). The incisal margin of di_1 is straight and level, while in di_2 is slopes distally. Each may have mamelons. The deciduous incisors lack marginal or longitudinal ridges and are poorly mineralized near the crown base. The dc is a conical cusp with slight marginal ridges; it is likewise poorly mineralized at the crown base. All anterior teeth reach at least the 75th percentile of MHD. In one specimen di_2 reaches or exceeds the 85th percentile, while in another specimen both deciduous incisors exceed that.

Dp_2 and dp_3 are roughly ovoid in occlusal view, and have two cusps. The metaconid of dp_2 is small at best, and indistinct in one newborn. Each has an elevated shallow trigonid basin, and a small distal shelf in lieu of a talonid basin. Dp_4 is quadrate with four primary cusps, a small trigonid, and a larger and deeper talonid basin. There is a metastylid on two of four specimens examined. The crown base of dp_3 and dp_4 is better mineralized than that of dp_2. Dp_2 reaches 85% MHD. Dp_3 reaches 75% MHD. Dp_4 varies from 75 to 85% MHD. In one specimen, the protoconid of dp_4 reaches or exceeds a MHD of 85%. M_1 varies in its state of mineralization in newborns. In the least mineralized specimen, there are three isolated cusp tips. In another, there are four cusps and a protocristid. The protoconid and metaconid of M_1 reaches a MHD of 50%; the hypoconid differs in the two specimens studied (reaching the 25 or 50th percentile of MHD).

No replacement teeth are mineralized at birth.

3.3 | Morphology of the dentition in newborn tarsiers

3.3.1 | General considerations—

Mineralization of permanent teeth is on an advanced schedule in tarsiers compared to nearly all other primates (Tables 1–3). Cusps are a particular focus of mineralization as opposed to crests. Tarsiers have an advanced mineralization schedule of replacement teeth. However, M^1/M_1 is more advanced in mineralization than any deciduous or replacement tooth.

3.3.2 | Maxillary dentition

Tarsius syrichta, *neonate*: Di^1 has a minute peg-shaped cusp and full root; although di^2 is not visible in the reconstruction (Figure 11), it was previously identified in the

reconstruction of the contralateral side of this specimen (Smith et al., 2015). Dc has a conical cusp and a slight cingulum distolingually, with a partially resorbed root.

Dp^2 is absent, as reported for *T. bancanus* by Luckett and Maier (1982). Dp^3 has one cusp with a pronounced cingulum on all sides. A parastyle is present and roots are nearly completely formed. Dp^4 is triangular in occlusal profile, with a large paracone and smaller metacone and protocone; a parastyle is present. A sharp crest connects the buccal cusps. Roots are nearly completely formed. M^1 is well mineralized at birth, although the cingulum is incompletely mineralized, and one newborn has a small gap in the center of the trigon basin. M^2 has three mineralized cusps; the basin is unmineralized. The paracone of M^3 is mineralized.

I^1, I^2, P^2, P^3, and P^4 are all partially mineralized at birth. Luckett and Maier (1982) note only I^1, I^2, and P^2 in a perinatal *T. bancanus*.

3.3.3 | Mandibular dentition

Tarsius syrichta, *neonate*: Di_1 has a small rounded cusp and full root; di_2 is absent or represented by a small vestigial fragment (Figure 12). The dc has a conical cusp, a lingual heel, and a nearly complete root.

Dp_2 is absent. Both dp_3 and dp_4 have highly projected protoconids. Dp_3 is a single-rooted, caniniform tooth. Dp_4 has one prominent cusp, no observable metaconid, and two stout roots. M_1 is fully mineralized at birth except for parts of the cingulum. Part of the buccal cingulum is visible in a Day 6 specimen. M_2 is mineralized except for the middle of the talonid basin and the cingulum. The protoconid and metaconid of M_3 are mineralized in two Day 0 specimens. In a Day 6 specimen, five primary cusps of M_3 are mineralized (including the paraconid).

I_1, C, P_2, P_3, and P_4 are partially mineralized at birth. The crowns and a portion of the roots of I_1 and P_2 are mineralized, in the remainder of the replacement teeth the base of the crown is poorly mineralized.

3.4 | Morphology of the dentition in newborn lemuroid strepsirrhines

3.4.1 | General considerations—Lemurids stand apart from other strepsirrhines in having relatively less mineralized M^1/M_1 at birth compared to other families, although there are variations among lemurids in the degree of mineralization of M^1/M_1 and the replacement teeth at birth (Tables 1–3). Cheirogaleids and galagids have advanced mineralization of certain replacement teeth at birth. The single available lorisid has the most well mineralized replacement teeth of any primates aside from indriids and tarsiers.

In dp_4, strepsirrhines, like some cercopithecoids, possess a cusp on the leading edge of the paracristid—a possible paraconid. In no species is it as large as most of the other primary cusps. More work is needed to assess its degree of variation.

3.4.2 | Maxillary dentition

Family Cheirogaleidae

Cheirogaleus medius, neonate.: Di^1 and di^2 are both small, especially the peg-like di^1. Dc is mesiodistally broad with a tall pointed cusp. Portions of the roots of all anterior teeth have begun to mineralize. Di^1 and di^2 both have a MHD reaching the 50th percentile. Dc reaches a MHD of 75%.

Dp^2 is caniniform but smaller than dc; its root has initiated mineralization. Dp^3 is broader than dp^3 with a pyramidal cusp. Lingually there is a vertical ridge with a vertical groove on either side. There appears to be a parastyle present, but the base of the crown looks poorly mineralized as yet, rendering a complete description impossible. Dp^2 reaches a MHD of 50% and dp^3 reaches a MHD of 85% located at the cusp. Dp^4 is triangular shaped with three primary cusps; the trigon basin is incompletely mineralized in both specimens examined and no trace of a cingulum can be seen, if present. Dp^4 reaches a MHD of 85% in the paracone. M^1 is present with three cusps and reaches a MHD of 50% at the paracone tip.

The tip of the I^1 cusp is mineralized adjacent to di^1. As in *Microcebus*, I^2 is distinctly less developed than I^1, showing no mineralization as yet (early bell stage). C is larger than I^1 and is located lingually to dc. The mineralized part of P^2 is larger than I^1, but smaller than C. I^1, C, and P^2 each reach a MHD of 25%.

Microcebus murinus, neonate (Figure 13): Di^1 and di^2 are both small and narrow and rounded on their buccal sides. Dc is caniniform, yet buccolingually compressed. Whether there are marginal ridges on the anterior teeth is unclear, and this may owe to the limits of resolution with the small specimen. All anterior teeth are beginning to form roots. Di^1 and di^2 both reaching 50% of MHD. Dc reaches a MHD of 75%.

Dp^2 is larger than dp^3, but they both have a single, tall cusp. Dp^3 is more triangular in profile (as noted by Tattersall & Schwartz, 1974) and yet appears partially unmineralized at the base of the crown. Because of this, the presence of stylar cusplets cannot be confirmed, although a parastyle has been attributed to dp^3 in cheirogaleids (Tattersall & Schwartz, 1974). Both dp^4 and M^1 are represented by three cusps at birth; neither possesses a mineralized hypocone, as yet, which was noted in these teeth by Tattersall and Schwartz (1974). In dp^4, the entire trigon basin and the distal margin are unmineralized. In M^1, the three cusps are isolated. Dp^2 and dp^3 reach a MHD of 75%. Dp^4 reaches or exceeds a MHD of 85% at the paracone. The metacone has a MHD of 50% and the protocone has a MHD of 25%. The paracone of M^1 reaches a MHD of 50%, whereas the rest of the tooth has a MHD of at most 25%. The paracone of M^2 is mineralized at the tip and reaches a MHD of less than 25%.

The apical part of C is mineralized, reaching 25% MHD at the tip. Although no other secondary teeth are shown in our reconstruction, histology of a specimen from the same litter reveals that I^1 is at the late bell stage (whereas I^2 is at the early bell stage). Regarding replacement premolars, histological observations show that P^2 is the most advanced, but is only at the early bell stage at birth (Smith et al., 2015).

Family Lemuridae

Eulemur collaris, E. mongoz, and E. rubriventer, neonate.: Di^1 and di^2 are small and buccolingually flat (Figure 13). Dc is broad and buccolingually compressed, with sharp mesial and distal margins. The roots of all anterior teeth have initiated mineralization in *E. mongoz*. In all newborns of *Eulemur* spp., di^1 and di^2 reach the 50th percentile of MHD; dc reaches the 75th percentile.

Dp^2 is small, caniniform, and buccolingually compressed, though not to the degree of dc. Dp^3 is rounded buccally and has a lingual vertical ridge. Tattersall and Schwartz (1974), in describing *E. rubriventer*, noted the dp^3 is "laterally compressed" like dp^2. This is not the case in any of our *Eulemur* infants. Dp^3 is much larger and pyramidal, with a slightly concave distolingual surface. A comparison to older infants (day 30 *E. collaris*, day 24 *E. mongoz*) reveals that dp^2 and dp^3 have only partially mineralized crowns. The older infants have a cingulum on the buccomesial and linguodistal border, and para and distostyles. Dp^4 is triangular in profile with three primary cusps. There is some variation in the smaller cusps of dp^4, which is difficult to attribute as species-specific based on the small samples. In *E. collaris*, a parastyle and smaller metastyle are present, as is a small paraconule (the latter is present in only two of the three neonates and also the older infant). The crista obliqua is incomplete; at day 30 it only weakly connects to the metacone, near its base. Lingual to the protocone are two isolated cusplets, the incipient protostyle and hypocone. By day 30, these can be visualized as projections from a lingual cingulum. In *E. mongoz*, a parastyle and a smaller metastyle are present. The crista obliqua is low and connects to the base of the metacone and bears a small metaconule. The trigon basin is unmineralized in the center at birth and fully mineralized by day 24. In a single newborn *E. rubriventer*, a pronounced parastyle is present, as is a small paraconule. The crista obliqua is distinct (far more so than in *E. collaris*) and bears two metaconules. Distal to the protocone is a triangular shelf; because it is distinct from the partially mineralized lingual cingulum, and this specimen is different from the other *Eulemur* spp. in this respect. Such a cusp was called a "pseudohypocone" by Swindler (2002); but see Anemone, Skinner, & Dirks, 2012 regarding the validity of this term). There are also two small cusps on an incipient lingual cingulum, the protostyle and a small true hypocone. The trigon basin is poorly mineralized. In representative specimens of all species, dp^2 reaches a MHD of 75%. Dp^3 and dp^4 reach or exceed a MHD of 85% at the paracone.

M^1 is present with three cusp tips mineralized. In the day 30 *E. collaris*, the crown of M^1 is well-mineralized, and three cusps of M^2 are mineralized. The basin of M^1 remains unmineralized in the day 24 *E. mongoz* and M^2 is not yet apparent. The M^1 paracone is the most mineralized (25th–50th percentile MHD) and the metacone is the least mineralized cusp.

No portions of I^1, I^2, or replacement premolars are mineralized at birth, and C is only beginning to mineralize in one newborn, *E. mongoz*, which reaches the 25th percentile of MHD. The cusp tip of C is also mineralized in a day 30 *E. collaris*.

Hapalemur griseus, neonate.: Di^1 is peg-like with a pronounced concavity lingually. Di^2 is similar and more rounded on its buccal side than di^1. In the two specimens studied, di^1

reaches a MHD of 25th and 75th percentile. Di^2 reaches and MHD of 25 and 50%. Dc is broad-based, elongate mesiodistally, flattened buccolingually, and possesses a slight distal heel. Lingually it has a sharp vertical ridge that runs from the crown base to the tapered and distally curved cusp tip; distal and parallel to this ridge is a deep groove. In both specimens, the dc reaches a MHD of 85%.

Dp^2 is caniniform but more pyramidal in form than dc. Like dc, it has a vertical lingual ridge with a groove distal to it. Dp^3 has a single cusp that connects to pronounced ridges mesially, distally, and lingually. In lingual view it resemble dp^2, with basin-like concavities that border the mesial ridge. The distolingual border is not completely mineralized. Dp^4 is broad and triangular shaped with three prominent cusps, as seen in M^1 (Swindler, 2002). Tattersall and Schwartz (1974) note that the metacone is the largest of the three cusps. This is true in our samples in terms of the cusp height, but in breadth, it is nearly matched by the protocone. The trigon basin is shallow and a crista obliqua is lacking. Three stylar cusps are present along the buccal margin of dp^4; a parastyle is visible on the first two dps, but the distal portion of these teeth is too poorly mineralized to detect a metastyle. The lingual cingulum is pronounced although the protostyle is quite small, and the hypocone is absent (as reported for M^1 by Schwartz and Tattersall (1985) and Swindler (2002)). In one specimen, all deciduous premolars reach a MHD of 85%. In the other, dp^2 reaches the 50th percentile while dp^3 and dp^4 reach the 75th percentile. Dp^2 and dp^3 each reach a MHD of 85%. Dp^4 reaches a MHD of 85% that is predominantly observed in the paracone. M^1 has three cusps and a mostly unmineralized basin, especially distally. At maximum, M^1 reaches a MHD of 50% found at the paracone and metacone. In both dp^4 and M^1, the buccal cusps are more mineralized (at higher MHD) or are more extensively mineralized than the protocone.

There are no replacement teeth mineralized at birth. In *Hapalemur* even the anterior maxillary teeth are less advanced (e.g., early bell stage) than in other lemurids (Smith et al., 2015).

Lemur catta, neonate.: Di^1 and di^2 are both small with irregular incisal margins. Dc is buccolingually narrow and elongated. It is simple and blade-like compared to *Eulemur* or *Hapalemur*, lacking a pronounced lingual ridge, and having a very shallow lingual groove. In di^1 and di^2, the crown has reached 50th and 25th percentile of MHD, respectively. Dc^1 has a MHD of at least 85%.

Dp^2 and dp^3 are both single-cusped, are rounded on buccal and lingual sides, and have sharp mesial and distal ridges; they. In the neonate, a parastyle can be seen on dp^2 but not on dp^3. However, both dp^2 and dp^3 are as yet incompletely mineralized near the crown base. In an older infant (day 28), dp^2 and dp^3 each have a parastyle and a small distostyle as well. Dp^4 has three primary cusps, a parastyle, and a smaller metastyle. A portion of the trigon basin is unmineralized at birth, but fully mineralized in the day 28 infant. The crista obliqua is not observed. The lingual cingulum is not mineralized in newborns, but is well-formed in the day 28 infant. A protostyle is absent (as observed for M^1—Schwartz and Tattersall, 1985) and in the region of the hypocone, there is only a slight swelling. Both of the dp^2 and dp^3 reach MHD of at least 85% at the cusp, more extensively so in dp^3. In dp^4, the most

mineralized cusp being the paracone (85%), followed by the metacone, and then the protocone (each of the latter reaching 75% MHD). M^1 has two mineralized cusps present. At day 28, there is an isolated, spiky ossified element in the region of the lingual cingulum, as yet not bridged to the protocone. The paracone of M^1 reaches 50% of MHD; the protocone and metacone of M^1 reach a MHD of 25%. M^2 is not mineralized at birth or at day 28.

In the day 28 infant, no replacement teeth are visible, but it is possible small cusp tips may be obscured by radio-opaque inclusions in incisor tooth crypts.

Varecia spp., neonate.: At birth, the state of mineralization of the maxillary tooth row in *Varecia rubra* and *Varecia variegata* is nearly identical. At birth, *Varecia* species have the least mineralized teeth of any primate that we have examined, and this is especially true of postcanine teeth.

At birth the crown of di^1 is visible, but only the apical part of the crown of di^2 is mineralized. In an older infant (day 25 *V. variegata*), the full crown of di^2 is mineralized and it is more rounded and peg-like than di^1. Dc is mesiodistally elongated and buccolingually compressed. There is no vertical lingual ridge (as in *Hapalemur*) and only a shallow vertical lingual groove (as in *Lemur*). A portion of the root of dc is seen at day 25.

Only a small portion of the cusp of dp^2 is mineralized in any of the newborns. A larger pyramidal portion of dp^3's single cusp is mineralized, with a rounded buccal side, a more flattened mesiolingual side, and a concave distolingual side. Dp^4 is visible as three isolated cusps; a portion of a parastyle may be connected to the paracone. The crown basin and lingual cingulum remain unmineralized. Form of the deciduous crowns is clear in the day 25 infant. Both dp^2 and dp^3 have vertical ridges on the lingual surface. Dp^2 is rounded mesial to this ridge and concave distal to this ridge. Much larger and broader than dp^2, dp^3 is now revealed to have a slight flaring of cingula on the buccal side. The basin and lingual cingulum of dp^4 are fully mineralized in the day 25 infant. The trigon basin is walled off mesially by a stout crest connecting the paracone and protocone. The basin is open distally. There is no crista obliqua. A small parastyle is present. A protostyle is lacking but there is a slight swelling consistent with a hypocone. Only the paracone of M^1 is mineralized in newborns. However, in the day 25 infant, M^1 has three isolated mineralized cusps.

At day 25, the apical part of the C cusp is mineralized.

Family Lepilemuridae: In newborn *Lepilemur leucopus* (Figure 13), one of the deciduous incisors is present. It is has a partial root and is further erupted than dc, possibly in the process of being shed. Dc reaches 50% MHD at the cusp tip; the di reaches the 25th percentile at the cusp.

All deciduous teeth have fully mineralized crowns and well-formed roots. Dp^2 has one cusp; it is buccolingually compressed with a small parastyle. In dp^3 there is one prominent cusp, which leads to mesial and distal ridge; a parastyle is present. In dp^4, three primary cusps are prominent; there is a parastyle and metastyle and a distinct lingual cingulum. The deciduous premolars are far less mineralized than permanent molars: dp^2 reaches only the 25th percentile of MHD, and dp^3 and dp^4 reach 50% MHD. In both M^1 and M^2 the majority of

the crown exceeds the 50th percentile of MHD and the three primary cusps all reach the 85th percentile of MHD. In M^3, the paracone reaches the 85th percentile while the remaining cusps each reach the 75th percentile of MHD.

The cusp apices of C and the three replacement premolars are present, reaching 25% MHD.

Family Indriidae

Propithecus coquereli, neonate.: Di^1 and di^2 are both small and buccolingually flat; di^1 comes to a pointed apex and di^2 has a more rounded incisal margin (Figure 13). Dc is broader and caniniform, with a slightly concave lingual surface and rounded buccal surface. However, dc is more buccolingually compressed than in other lemuroids, and seems proportionally far smaller. The deciduous anterior teeth reach a HA density of 50–75% MHD, the highest at dc.

Dp^3 is broad with one cusp that connects to mesial and distal marginal ridges; it is concave lingually. Dp^4 is broad with two prominent buccal cusps, a paracone and a metacone. Lingually there is a distinct protocone as well as a hypocone that varies in prominence. As a result, the tooth may be triangular or trapezoidal in profile, depending on how pronounced the hypocone is. In any case, the paracone is displaced far mesially relative to the rest of the cusps. As described in M^1 and M^2 (Tattersall & Schwartz, 1974), dp^4 possesses a well-developed buccal cingulum with three styles. The parastyle projects most prominently, while the metastyle is least prominent and is absent in some specimens. The contours of the crowns of M^1 and M^2 are nearly completely formed at birth. Moreover, the M^2 crown is nearly as well mineralized at birth as in one-month-old specimens; the former showed only small poorly mineralized or thin basins compared to one-month-old specimens. Two isolated cusps of M^3 are mineralized in one of the two newborns examined. Dp^3 reaches the 50th percentile of MHD. Dp^4 reaches or exceeds a MHD of 85% at the paracone. M^1 reaches a MHD of 85% at the paracone and metacone. M^2 has a MHD of 50% located in the paracone, metacone, and protocone. M^3 has a MHD of 25% at the paracone.

I^1 is very well mineralized, already revealing its spatulate shape in newborns. I^2 is as yet, unmineralized at birth. The cusp tip of C is present and lingual to dc. The paracone of P^4 is more advanced than P^3, and is already assuming a pyramidal shape and reaching a MHD of 50%. I^1 is the most advanced in mineralization, reaching a MHD of 85% at the incisal margin. In a day 32 infant, the tip of I^2 is visible; Thus, all replacement teeth are mineralizing by 1 month of age.

3.4.3 | Mandibular dentition

Family Cheirogaleidae

Cheirogaleus medius, neonate.: Di_1 and di_2 are narrow, pointed, and long with a longitudinal ridge running along the lingual side running from the tip toward a slight lingual heel. Dc is broader with a reduced longitudinal ridge, and a more flared lateral flange. Thus, the deciduous anterior teeth resemble the adult toothcomb, as described by Tattersall and Schwartz (1974). In two specimens examined, the anterior deciduous teeth each reach the 50th percentile of MHD.

Dp_2 is caniniform with a slight longitudinal ridge; the flanges are slightly larger than in the anterior teeth, and form marginal ridges. Dp_2 reaches the 50th–75th percentile of MHD at the cusp tip. Dp_3 is narrower near its apex compared to dp_2, and has a more pronounced longitudinal ridge. Distal to this ridge, this tooth becomes concave, and appears to form part of a basin; however, the lingual margins are as yet poorly mineralized (or unmineralized) and the outer margins of this basin cannot be visualized in the reconstructions. A lingual cingulum, described in *C. major* by Tattersall and Schwartz (1974), is likewise not visible if present. The cusp tip of dp_3 reaches the 50th percentile of MHD in one specimen and the 85th percentile the second specimen. Dp_4 is broad and has a prominent protoconid, hypoconid, and entoconid; the metaconid is present, but only barely elevated above the level of the protocristid. A cristid obliqua, projecting mesially from the hypoconid, is well-mineralized. This crest contacts the protocristid the base of the protoconid.

A “paraconid shelf” projects mesially, without a distinct cusp on its leading edge; it is more pronounced than the same region of M_1. The trigonid basin is shallower, elevated, and better mineralized than the talonid basin. There is a slight swelling on the crest forming the lingual margin of the talonid basin. This may be a metastylid, but detail is poor (perhaps due to limits of scan resolution in view of small tooth size). The protoconid of dp_4 reaches the 85th percentile of MHD; the entoconid is the least mineralized cusp. M_1 is represented by four cusps in one neonate. In a second neonate, the entoconid is not yet mineralized. Similar to dp_4, the protoconid of M_1 also has the highest MHD reaching the 50–75th percentile. One of the two mesial cusps of M_2 are present. The MHD of the cusp present in M_2 reaches 25% in one specimen.

The cusp tips of I_1, I_2, C, and P_2 are mineralized. Of the replacement teeth, I_1 is the most mineralized, reaching the 25th–50th percentile of MHD.

Microcebus murinus, neonate.: The deciduous anterior teeth resemble the adult toothcomb (Figure 14). Each of these teeth have a HA density reaching 50% of MHD.

Dp_2 is more robust than the dc and is caniniform with a pronounced lingual heel. Dp_2 reaches a MHD of 75%. Dp_3 is smaller than dp_2 with a prominent protoconid that leans distally; a vertical lingual ridge is present. Dp_4 has four primary cusps, and a deep talonid basin that is incompletely mineralized. A cristid obliqua intersects the protocristid near the protoconid. A small cusplet is present on the distal margin adjacent to the hypoconid. The protoconid of dp_3 and dp_4 reach a MHD of 85%. The entoconid of dp_4 is the least mineralized cusp. M_1 is present with three cusps, and a mineralized tip of the entoconid. The protoconid of M_2 is mineralized. Similar to dp_3 and dp_4, the protoconid is most mineralized (75%) cusp and the entoconid is least mineralized (25%) cusp on M_1. The protoconid of M_2 is mineralized at 25% MHD.

The cusp tips of I_1, I_2, and C are mineralized. I1 has the highest mineralization as 25% MHD.

Mirza coquereli, neonate.: The deciduous anterior teeth resemble an adult strepsirrhine toothcomb. Di_1 reaches the 75th percentile of MHD. Di_2 and dc reach a MHD of 85%.

Dp_2 is caniniform but more robust than the anterior teeth. The base of its crown is poorly mineralized lingually and the distal side. Dp_4 is larger than dp_2 and dp_3 with three well-mineralized cusps and the cusp tip of the entoconid. A cristid obliqua is mineralized and connects low on the protocristid. The trigonid basin is raised and with the mesial limit on the buccal side; the talonid basin is at yet unmineralized at birth. No smaller cusplets are evident. Three cusps of M_1 are mineralized, excluding the entoconoid. Dp_2 and the protoconid of dp_4 reaches or exceeds a MHD of 85%. Dp_3 reaches a MHD of 75%. M_1 reaches a MHD of 50%.

The cusp tips of I_1 and I_2 have begun to mineralize. They are at a MHD of <20%.

Family Lemuridae

Eulemur collaris (Figure 14), E. mongoz, and E. rubriventer, neonate.: Di_1 to dc resemble the adult toothcomb of *Eulemur* spp. The deciduous anterior teeth reach at least the 50th percentile of MHD. In one *E. collaris*, di_2 and dc reach a MHD of 75% at their caniniform cusp tips.

Dp_2 is caniniform. A distal marginal ridge and a smaller mesial marginal ridge are present. At its base dp_2 is triangular in shape; lingually there is an angular ridge creating fossae on either side. In some specimens the distolingual margin is incompletely mineralized. At birth, dp_3 has a single primary cusp, but with a broader base. However, a comparison to an older (day 30) *E. collaris* specimen reveals that in both dp_2 and dp_3, the crown is only partially mineralized in each of three newborns examined. Dp_2 expands mesially and distally into a buccolingually compressed, peg-like tooth. Dp_3 is more molariform in a day 30 *E. collaris*, since the distal portion is mineralized as an elongated shelf in this older infant. The distal concave surface is expanded to a talonid basin. The mesial surface expands to form a shallow trigonid basin. In the day 30 infant, dp_3 has a protoconid, metaconid, and hypoconid. A small paraconid is present.

Dp_4 is the most molariform deciduous tooth, with multiple cusps, and some variation among specimens. In *E. collaris*, the protoconid and hypoconid are prominent. On the lingual margin there are multiple cusps, including a small cusplet on the mesiolingual corner near the end of the paracristid, after a small gap. Distal to this small cusp is a deep groove, such that the trigonid basin is open lingually. A cristid obliqua intersects the protocristid centrally between the mesial cusp pair. The number of small cusps lingual to the talonid varies from one to two. Distal to the metaconid is a small cusplet, and even more distally is a metastylid (the first of these is conspicuously missing in one of the three neonates). Distal to the metastylid is a deep groove, such that the talonid basin, too, is open lingually. Further distally on the lingual side of the talonid is another small cusp, which we consider a small entoconid, but it is not equally pronounced in all specimens. On the distal margin of the talonid basin is a final small cusp, perhaps the hypoconulid. In the day 30 infant, there is a slight buccal cingulum on dp_4, not as pronounced as that of M_1. A neonatal and infant (P24) *E. mongoz*, are similar to the description above except neither of them has secondary cusps. In an *E. rubriventer* neonate, there are multiple cusps and smaller cusplets in addition to four primary cusps. One small cusplet on the mesiolingual margin. It is near the end of the paracristid, after a small gap. The paracristid is relatively elevated, with two small cusplets at

the mesial apex, one of which may be a paraconid. There is no cusplet closely opposed to the metaconid, as observed in other *Eulemur* spp. There are two cusplets mesial to the small entoconid on the crest bordering the lingual side of the talonid basin. No clear hypoconulid is visible. A small cusplet is present on the cristid obliqua, which meets the protocristid between the mesial cusp pair.

In newborn *Eulemur*, M_1 has three pyramidal primary cusps plus the entoconid tip. Additional small cusplet tips are visible in the newborn *E. collaris*. The crown of M_1 is entirely mineralized in the day 30 E. collaris infant.

The protoconid is the most mineralized cusp in all dps (reaching 85% MHD in *E. collaris* and *E. rubriventer*). The entoconid is the least mineralized of the primary cusps. Smaller cusplets on dp_4, such as the tuberculum intermedium and metastylid (if present) can be focal points of MHD, each reaching 50% while adjacent part of the lingual ridge are less dense. The trigonid basin is better mineralized than the talonid basin, reaching a MHD as high as 75% near the margins. The MHD of M_1 follows an identical pattern at the cusps, though lagging behind dp_4.

In *E. collaris* and *E. mongoz*, the cusp tips of I_1, I_2, and C_2 are mineralized at birth. In the older infant, each of these teeth is further mineralized and are beginning to form a longitudinal ridge and flanges. In the newborn *E. rubriventer*, only the cusp tip of C is mineralized.

Hapalemur griseus, neonate.: The deciduous anterior teeth resemble the adult toothcomb. In both specimens studied for HA density, the dc exceeds that of the deciduous incisors (although in one specimen, di1 has not scanned). In the specimen with all anterior teeth available, di1 and di2 reach a MHD of 50%, while the dc reaches 75% MHD.

Dp_2 and dp_3 are buccolingually compressed with only one distinct cusp. Dp_2 shares some similarities to the dc, but is more robust and has a less distinct longitudinal ridge, creating a shallow mesolingual depression and a deeper and broader buccolingual depression on either side. In dp_3 there is a distinct protocristid passing mesially from the protoconid, but lingually the metaconid is indistinct. Mesial to the protocristid is a descending triangular plane; distally is a shallow depression within a raised heel. No distinct anterior stylids, as mentioned by Tattersall and Schwartz (1974) could be detected. Dp_4 is extremely robust with prominent crests, a cristid obliqua and four primary cusps. Like dp_4, M_1 is also present with four cusps—with the protoconid being the most mineralized and the entoconid being the least mineralized. Mesially the dp_4 trigonid slopes distinctly upward to a pointed tip, consistent with a paraconid, as suggested by Tattersall and Schwartz (1974). There are multiple cusplets in both neonates; all are on the lingual side of dp_4. One is just distal to the metaconid (resembles the tuberculum intermedium described on P_4 and M_1 by Swindler). Distally to this cusplet is a smaller one, what might be called a metastylid along the lingual marginal crest bordering the talonid. Distal to the metastylid is a distinct notch, so that the basin is open lingually (as also true of M_1—Tattersall & Schwartz, 1974). Along the distolingual boundary, there is a pair of distinct cusps in both dp_4 and M_1. Observing these in M_1, Schwartz and Tattersall (1985) considered the more distal of the two to be a rather

distended entoconid, whereas Swindler (2002) appeared to be referring to the same structure as a hypoconulid. Here, we can observe that the more distal of the two has greater HA density, suggesting it may have formed first (in both dp_4 and M_1). All deciduous premolars reach a MHD of 85%. Dp_4 has a MHD of 85%, which mostly present in the cristids of the tooth.

The cusp tips of I_1, I_2, and C are mineralized.

Lemur catta, neonate.: The deciduous anterior teeth resemble the adult toothcomb. The anterior teeth reached at least the 75th percentile of MHD near the apex. In one of the two specimens studied, di2 and dc have small foci that have reached the 85th percentile of MHD.

Dp_2 and dp_3 both have one cusp that connects to mesial and distal ridges. Lingually, there is slight vertical swelling with a slight groove mesial and distal to it. A comparison to an older infant (day 28) reveals that the base of the crown is partially unmineralized at birth in both dp_2 and dp_3 (especially, the latter). Dp_4 has four primary cusps, including the protoconid, metaconid, hypoconid and a slightly smaller cusp on the distal side of the talonid basin. This cusp may correspond to what Swindler (2002) interprets as a hypoconulid on M_1. There is no clear entoconid; instead, there is a slight depression at the distolingual margin, such that the talonid basin is open lingually. Two smaller cusps are present. A metastylid is distinct on the lingual border of the talonid basin. Mesially, there is a small cusplet at the end of a distinct, arcing paracristid. Tattersall and Schwartz (1974) interpreted this as a paraconid. This cusp and the paracristid are notably more elevated in dp_4 compared to M_1, in which the trigonid slopes downward. A buccal cingulum is present on dp_4. M_1 has three cusps, the largest being the protoconid. A less mineralized, smaller cusp is present on the lingual side, the presumptive metastylid. No mineralization occurs distally as yet; neither the floor of the talonid basin nor the hypoconulid of M_1 are mineralized in day 4 and day 8 infants. The hypoconulid is present at day 28 and the talonid basin in mineralized except at the center. The buccal cingulum of M_1 is beginning to mineralize at day 28. Postcanine deciduous teeth are more mineralized than anterior teeth. The paracones of all deciduous premolars reach 85% of MHD at the cusp tip. On dp_4, the tip of the metaconid also reaches or exceeds 85% of MHD; the hypoconid reaches 75% of MHD. The hypoconulid reaches 50% MHD; in one of the two specimens examined for HA density, it is an isolated focus of MHD relative to the adjacent crown. The trigonid basin is better mineralized (50–75% MHD) compared to the talonid basin (reaching a MHD of 25%). M_1 reaches and maximum of 50% MHD at the protoconid, and in one of the two specimens, also the metaconid.

No replacement teeth are mineralized at birth. In the day 28 infant, I_1 and I_2 cusp tips are mineralized.

V. rubra and V. variegata neonate.: At birth, the state of mineralization of the mandibular tooth row in *V. rubra* and *V. variegata* is nearly identical. The species are described together. The morphology of the deciduous teeth is described based on an older infant *V. variegata*.

The deciduous anterior tooth resemble the adult toothcomb. In an older infant (day 25 *V. variegata*) each of the anterior teeth has initiated root formation.

The dp_2 and dp_3 are each more robust than dc but are similarly rounded buccally and somewhat curved toward the lingual side. Each of them has a vertical lingual ridge; distolingually to the ridge there is a concavity (these are less pronounced in dp_2). Dp_4 is much broader and more molariform than dp_2 and dp_3, with dp_4 having three primary cusps but no mineralization of the talonid basin or the distolingual margin. The trigonid basin is only partially mineralized, but already walled off buccomesially with a distinct paracristid. At the mesial end of the paracristid is a small cusplet. Only the protoconid of M_1 is mineralized. In the day 25 infant, dp_2 is revealed to be more caniniform than dp_3. A small heel is seen distolingually. In dp_3, the distolingual concavity now has the appearance of a shallow basin. Three primary cusps are present on dp_4; a distinct entoconid is not present. The scan resolution for the infant was lower than for the newborn, perhaps preventing clear visualization of these small cusps. Distolingually, there is a slight groove, opening the talonid basin, as described in M_1 (Tattersall & Schwartz, 1974). As in the newborn, a small cusplet is seen at the mesial end of the trigonid basin. This might be interpreted as a paraconid. The protoconid and metaconid are closer to one another (thus a shorter protocristid) compared to M_1. The cristid obliqua tapers toward the crown base as it approaches the protoconid, and never meets the protocristid. In M_1, there are four mineralized cusps in the day 25 infant. The protocristid and part of the talonid basin are mineralized; the latter is far less raised than in dp_4. The presumptive entoconid is small but distinctly mineralized. It is clearly delayed relative to the other three cusps, and it might be noted that there is little difference between this cusp and the metastylids seen in other lemurids. It thus seems possible that *Varecia* lacks entoconids on dp_4 and M_1, as described in *Lemur* (Tattersall & Schwartz, 1974). In another subadult (day 140 V. *rubra*), scanned at the highest resolution, dp_4 bears no entoconid, nor any raised cusplet lingual to the talonid basin. There was a small-elevated cusplet on M_1 lingual to the talonid.

No replacement teeth are mineralized at birth. I_1, I_2, C_1, and P_2 have all initiated mineralization, but P_2 is only mineralized at the very apex of the cusp.

Family Lepilemuridae: In newborn L. *leucopus* (Figure 14), the deciduous anterior teeth resemble an adult toothcomb, and each cusp reaches the 25th percentile of MHD. The roots have initiated mineralization.

Dp_2 has one buccolingually compressed cusp. In dp_3 there is one prominent cusp, which leads to mesial and distal ridge that end in small cusps; there is a distal heel. In dp_4 three primary cusps are prominent, but there is no entoconid. The cristid obliqua is pronounced and intersects the protocristid at its center. M_1 and M_2 are both well mineralized, including the basins, with pronounced cusps. M_3 is also well-mineralized, except for the distolingual border where the entoconid is not yet apparent. Deciduous premolars reach only the 50th percentile of MHD. In both M_1 and M_2 the majority of the crown exceeds the 50th percentile of MHD and all primary cusps reach the 85th percentile of MHD. In M_3, only the protoconid reaches the 85th percentile of MHD.

I_1 and I_2 and C are all partially mineralized, reaching 50% MHD. The permanent premolars have initiated mineralization, P_2 and P_4 are more mineralized than P_3, reaching the 25th and 50th percentile of MHD, respectively.

Family Indriidae

Propithecus coquereli, neonate.: Di_1 and di_2 are narrow and possess a very subtle lingual longitudinal ridge that is only apparent in the upper half of the crown (Figure 14). The mesial and distal ridges are likewise only apparent along the more apical portion of the crown. The dc is far smaller than the deciduous incisors and peg-like. Di_1 and dc reach a MHD of 50–75% and di_2 reaches a MHD of 85%.

Dp_2 is has one cusp and mesial and distal marginal ridges; the cusp is triangular in buccal profile. Dp_3 is smaller with a slight lingual concavity. Both dp_2 and dp_3 reach 50% MHD at the cusp tip. Dp_4 is elongated with four primary cusps, a long shallow trigonid basin, and a deeper talonid basin. The cristid obliqua is pronounced and intersects the protocristid at its center. Dp_4 reaches a MHD of 50% on all four cusps and the paracristid; the talonid basin is better mineralized than the trigonid basin. M_1 and M_2 are both very well-mineralized, including the basins, and have far more pronounced cusps compared to the deciduous premolars. M_1 has a low curved protocristid, with the cristid obliqua intersecting it in the middle. The protocristid is lower still on M_2. M_1 reaches a MHD of 85% and is located in the metaconid and protoconid. M_2 has a MHD of 50% located in each of the cusps, but predominantly in the metaconid and protoconid.

Three cusps of M_3 are mineralized at birth and the entoconid is not yet apparent. At this point, M_3 reaches a MHD of 25%. In 1-month-old *Propithecus* the entire M_3 crown is mineralized but the protocristid is absent.

The crowns of I_1 and I_2 are advanced in mineralization, and exceed their deciduous counterparts in MHD. P_2 and P_4 are mineralized although only at the tip of the protoconid.

3.5 | Morphology of the dentition in newborn lorisoid primates

3.5.1 | Maxillary dentition

Family Galagidae: Otolemur crassicaudatus *and* Otolemur garnettii. In both species, di^1 and di^2 are both peg-like and slightly concave ventrally (Figure 15). Dc is much larger and broader with sharp mesial and distal marginal ridges. Lingually there is a broad, rounded longitudinal ridge with concave depressions on either side; buccally dc is convex. Di^1 and di^2 both reach a MHD of 75%. Dc reaches a MHD of 85%. In an older (1-month-old) O. *crassicaudatus*, the roots of di^1 and di^2 are nearly complete; dc has two roots.

Dp^2 is smaller than dc, with a buccolingually compressed plate leading to a single cusp. Distolingually, there is a small projecting stylar cusp. Dp^3 is triangular in occlusal profile. Part of the crown appears to be, as yet, unmineralized, although a small parastyle is present. Dp^4 is very large and has three primary cusps and an incompletely mineralized basin; a parastyle and metastyle are evident in all specimens. In addition, a paraconule is visible in our single specimen of *O. garnettii*. The tip of the hypocone is mineralized, but as yet unconnected to the rest of dp^4. Dp^2 and dp^3 both reach a MHD of 85%. Dp^4 reaches a MHD of 85% at the buccal cusps in a newborn *O. crassicaudatus*, most broadly on the paracone; in *O. garnettii* the paracone alone reaches the 85th percentile. The hypocone has commenced mineralization in the newborn *O. garnettii*. M^1 has three mineralized cusps. In M^1 of *O.*

crassicaudatus, the paracone reaches a MHD of 50%, while the metacone and protocone reach the 25th percentile. Only the tip of the paracone of M^2 is mineralized at <25%. In *O. garnettii*, two cusps of M^1 are mineralized and M^2 is not yet apparent. However, based on histology Smith et al. (2015) observed M^2 had reached the late bell stage in a newborn *O. garnettii*.

In the older (day 26) *O. crassicaudatus* infant, the root of dp^2 has started to form. Dp^3 is revealed to have a broad base and a wide lingual cingulum, still incomplete distolingually; a para- and distostyle are present. The trigon basin and hypocone are fully mineralized in dp^4 and a small parastyle is present. The crown of M^1 appears fully mineralized; M^2 now presents with three isolated mineralized cusps.

The apical cusp of C is mineralized at birth. The cusp reaches the 25th percentile of MHD in both *Otolemur* specimens. The tip of the cusp of P^2 is also present in a newborn *O. garnettii*. In the older infant *O. crassicaudatus*, I^1, I^2, and P^2 are mineralized, in addition to C.

Galago moholi and Galago senegalensis.: In both species, di^1 and di^2 are small and peglike. Dc is caniniform and broad. The deciduous incisors reach a MHD of 25%. The cusp of dc reaches 75% MHD.

Dp^2 is similarly shaped to dc but smaller. There is a small gap between dp^2 and dp^3. Dp^3 has one cusp and para- and distostyles. Dp^4 has four cusps; the hypocone is mineralized at the cusp tip; a parastyle and metastyle are present. A paraconule is present in *G. moholi*, but was not observed in *G. senegalensis*. The trigon basin is well-mineralized except at the center. M^1 has three cusps; the hypocone is not yet mineralized. The paracone of M^2 is present. In a day 30 *G. moholi* infant, dp^3 has a broader base of the crown. The lingual cingulum of dp^4 is now more expansive and the hypocone appears more prominent. M^1 has a greatly expanded mineralization in the day 30 infant. The entire trigon basin is mineralized as is the lingual cingulum and hypocone. In the day 30 infant, M^2 is also advanced, with three primary cusps, the paraconule, and an isolated cusp tip of the hypocone. The paracone of dp^2 and dp^3 reach a MHD of 50%. Dp^4 reaches a MHD of 85% (at the protocone in one *G. moholi* examined for HA density) or the 75th percentile (the paracone, protocone, and metacone). The hypocone is the least mineralized at 25% MHD. M^1 reaches a MHD of 75% in *G. moholi* and 85% in *G. senegalensis*, in both cases at the paracone. The paracone of M^2 reaches less than 25% of MHD in *G. moholi* and <25% in *G. senegalensis*.

The apical part of the cusp of C is present, reaching 25% MHD. A smaller mineralized portion of P^2 is also present at birth. In the day 30 *G. moholi* infant, I^1 and I^2 are now mineralizing, and the mineralized parts of C and P^2 are nearing the size of their deciduous precursors.

Family Lorisidae

Nycticebus pygmaeus.: Di^1 and di^2 are small, peglike teeth (Figure 15). Dc is larger and cylindrical except for a tapering, triangular tip. The deciduous incisors reach a MHD of 25%, and the dc reaches the 50th percentile at the cusp tip.

Dp^2 has a single cusp with short mesial and distal ridges emanating away from the tip; it is rounded buccally and more flattened lingually. Dp2 reaches a MHD of 50% MHD. Dp^3 has a conical paracone with an adjacent parastyle. Since both are only partially mineralized, it I s impossible to say whether either has cingula except for the buccal cingulum that supports the parastyle of dp^3. Dp^4 is a triangular shaped mass with three primary cusps, all merged. The trigon basin is unmineralized in the center and the hypocone is an isolated cusp, unsupported as yet by mineralized cingulum. A parastyle is present, as well as a prominent paraconule. A crista obliqua is not apparent, as yet, if there is one. Dp^3 and dp^4 reach a MHD of 85% at the paracone (and metacone of dp^4). M^1 is represented by three cusps and the tip of the paraconule. Neither the parastyle nor the hypocone has started to mineralize. The three cusps of M^1 reach MHD of 50% (buccal cusps) and 25% (protocone). *Nycticebus coucang* is reported to have a metastyle and distinct buccal cingulum on M^1 (Swindler, 2002), and these are not present (or not mineralized) on dp^4 or M^1 of the newborn *Nycticebus pygmaeus*. Conversely, the distinct paracone of dp^4 and M^1 was not reported or illustrated on *N. coucang* by Swindler (2002).

Four replacement teeth are mineralized, I^1, I^2, C^1, and P^2. Only the tip of the cusp of P^2 is seen. The anterior replacement teeth are far larger and better mineralized than their precursors: the incisors reach the 50th percentile and the C reaches the 85th percentile of MHD. P^2 appears to have just initiated mineralization, reaching 25% MHD.

Perodicticus potto, infant.: Specimen #CM69182 is a skeletonized skull in the collection of the Carnegie Museum, Section of Mammals. Obtained from the Pittsburgh Zoo, the specimen is of unrecorded precise age. Dentally, it is considerably more mature than the Day 0 newborn lorisoids described above. It is very comparable with the P26 infant *Otolemur crassicaudatus* described above in possessing completely mineralized M^1 crown. This specimen, an older infant, is used only to describe deciduous tooth morphology.

The crowns of di^1 and di^2 are lingually flat, with rounded buccal surfaces; incisal margins are rounded. The dc resembles that of other lorisoids, possessing a buccolingually flattened single cusp.

Dp^2 is caniniform, resembling dc, except with distinct para- and distostyles. Dp^3 has a conical paracone bracketed by para- and distostyles. It has a pronounced lingual cingulum with a slight swelling as a hypocone. Since both are only partially mineralized, it is impossible to say whether either has cingula except for the buccal cingulum that supports the parastyle of dp^3. Dp^4 is a triangular shaped mass with three primary cusps; there is a small cingulum flaring distolingually, but no hypocone. M^1 is fully mineralized. M^2 is not visible, but may well have mineralized cusps that are separated from the skull, as the last developing molars in sequence form in advance of an osseous crypt.

Two replacement teeth are clearly visible: C and P^2. I^1 and I^2 are not visible but are presumably in crypts hidden by the palate (premaxillary portion). A crypt for P^3 is visible, but small with no cusp within. There is no evidence of cusps for P^3 or P^4.

3.5.2 | Mandibular dentition

Family Galagidae

Otolemur crassicaudatus and O. garnettii.: The deciduous anterior tooth resemble the adult toothcomb (Figure 16). Di_1 and di_2 reach a MHD of 57 (*O. crassicaudatus*)–85% (*O. garnettii*). Dc reaches a MHD of 75% at the apex of the tooth.

Dp_2 is also long and caniniform, but more robust than dc. Dp_3 is less mineralized than adjacent premolars, especially distolingually. The two mesial cusps are present. In an older (day 26) *O. crassicaudatus*, the distal crown is mineralized as an extended shelf, including a hypoconid. At birth, dp_3 appears obliquely oriented in the tooth row. This may be a transient condition due to crowding because in the day 26 specimen, the axis is more in line with other postcanine teeth. Dp_4 has four primary cusps and two small cusplets along the paracristid ridge. The talonid basin is deep and poorly mineralized in the center; the trigonid is shallow and elevated by comparison. The paracristid arcs sharply to the buccal side where it ends at a moderately-sized cusp. Dp_4 resembles M_1 closely, except that in the latter there is no cusp at the leading edge of the paracristid. M_2 has two mineralized cusps. In the newborn. *O. crassicaudatus*, Dp_2 reaches a MHD of 85%, whereas dp_3 reaches a MHD of 75%. Dp_4 reaches a MHD of 85% predominantly located in the protoconid and metaconid. M_1 reaches a MHD of 75% at the metaconid. M_2 reaches a MHD of 25%. The newborn *O. garnettii* follows a similar pattern but since di_1 was absent, it is not precisely comparable. By day 26, the crown of M_1 appears fully mineralized. M_2 is mineralized except for the center of the talonid basin. M_3 has two mineralized cusps.

I_1, I_2, and C are all small and located lingually to di_1, di_2, and dc, respectively. The tip of the protoconid of P_2 is also mineralized. The deciduous anterior teeth reach the 25th percentile of MHD.

Galago moholi and G. senegalensis.: Di_1, di_2, and dc form the toothcomb, and closely resemble the replacement teeth. The roots of the anterior teeth are barely mineralized at birth, but have started to extend in an older *G. moholi* infant (day 30). The deciduous incisors reach a MHD of 25%. In the newborn, all have deciduous teeth have a MHD reaching 50%.

Dp_2 is caniniform but broader than dc with a distal heel. Dp_3 has a maximum of three cusps at birth. The largest, the protoconid, is rotated relative to its position in dp_4; the metaconid is present but far smaller. In both *Galago* species, a large cusp mesial to the protoconid resembles a paraconid. In the day 30 infant, dp_3 is revealed to have an elongated crown, with a now extended distal surface leading to a distolingual heel. Dp_4 is far larger and more molariform than dp_2 and dp_3, with four primary cusps, as well as a mesiobuccal cusp at the leading edge of the trigonid basin. M_1 is present with four cusps. Unlike dp_4, the trigonid basin slopes down toward the base of the crown. The talonid basin is poorly mineralized. M_2 is present with only the protoconid mineralized. In the day 30 infant, M_1 is fully mineralized and M_2 is mineralized except for the floor of the talonid basin; the protoconid and metaconid of M_3 are mineralized as isolated cusps. At birth, dp_2 reaches a MHD of 75%. Both dp_3 and dp_4 have a MHD of 85% (the latter at both mesial cusps). Similar to dp_4, M_1 has a MHD of

85% localized at the tip of the protoconid and metaconid. M_2 protoconid is mineralized to 25% MHD.

The toothcomb teeth have permanent counterparts (I_1, I_2, and C). A small part of the cusp of P_2 is present in a newborn *G. moholi*. I1, I2, and C1 reach 25% MHD in *G. moholi*; they are at <25% MHD in *G. senegalensis*. The day 30 infant possesses the same replacement teeth with more of the crowns mineralized.

Family Lorisidae

Nycticebus pygmaeus (Figure 16).: Di_1, di_2, and dc are all conical in shape. The dc is more robust than the incisors. The deciduous incisors each have a lingual longitudinal ridge and flanges flaring mesially and distally. The flanges are not clearly evident on dc, nor on C. Although this might be due to the limits of resolution, it is noteworthy that the crowns are not fully mineralized, Dc and C may simply have marginal ridges closer to the crown base, as illustrated in *N. coucang* (see fig. 5.13, in Swindler, 2002). Each of those teeth has a HA density reaching 50% MHD.

Dp_2 is caniniform and broader than dc with a slight lingual heel. Dp_3 has one cusp, the protoconid, and a smaller mesial cusp that could be a paraconid. Both dp_2 and dp_3 crowns are incompletely mineralized—the dp_2 reaches a MHD of 75% whereas the dp_3 reaches a MHD of 85%. Dp_4 and M_1 are quadrate shaped with four cusps. Dp_4 has a small cusplet between the protoconid and metaconid; the talonid basin is incompletely mineralized. In M_1, the two mesial cusps are mineralized and joined by a protocristid. However, the hypoconid and entoconid are isolated cusps as yet, since the adjacent basin is not mineralized. In *N. coucang*, a buccal cingulid is described in M_1 (Swindler, 2002). If present, it is not mineralized in newborn *N. pygmaeus*. In M_1, the two mesial cusps are better mineralized than the distal pair (75 and 50% MHD for the protoconid and metaconid, respectively); only a small portion of the entoconid reaches the 25th percentile of MHD. One of the two newborns (sibling pair) is better developed than the other, and has three cusps of M_2 mineralized (no entoconid), while in the other, only the protoconid is mineralized.

Most of the crown of I_1, I_2, C, and P_2 are mineralized at birth. The anterior replacement teeth are far larger and better mineralized than their precursors: all reach or exceed the 85th percentile of MHD. P2 reaches 50% MHD.

Perodicticus potto, infant.: The anterior teeth resemble an adult toothcomb.

Dp_2 looks similar to dc, but more robust. Dp_3 has a flattened, sharp protoconid; a large heel projects from the base of the crown distolingually. Dp_4 has four primary cusps; the paracristid is obscured by the more fully erupted dp_3. A cristid oblique intersects the protocristid close to the metaconid. The crown of M_1 appears fully mineralized.

Among replacement teeth, C and P_2 are partially mineralized; the permanent canine is more fully erupted. I_1 and I_2 are not visible. Small crypts for P_3 and P_4 are present with no cusps visible within.

3.6 | HA density of mandibular tooth rows

3.6.1 | MHD of crowns in perinatal or older infant specimens: No correlations with duration of fixation—

To ascertain whether prolonged fixation in formalin may demineralize the developing dentition, MHD measurement on 66 prosimian primates were plotted against the duration of fixation based on records of the Duke Lemur Center, or recorded date of transfer of frozen specimens to formalin fixation by the authors. MHD measurements were highly variable. The correlations were weak and nonsignificant for two mandibular teeth measured, including dp_4 ($r = .16$) and M_1 ($r = -.08$). The range of fixation was quite broad, from 9 to 13,822 days. Scatterplots indicate no apparent downward trend in MHD based on increasing duration of fixation, as might be hypothesized based on acidification of formalin over time. Instead, the minimum to maximum HD is similar at both ends of the range of fixation duration (Figure 17).

3.6.2 | Crown HA density in newborn specimens: Phylogenetic patterns—

Mean mandibular MHD measurements for 40 primate species (20 haplorhines; 20 strepsirrhines; Table 4) and *Tupaia* are plotted against cranial length in Figures 31A and 31B. *Tupaia belangeri* scales far below all primates in MHD of dp_4 and below strepsirrhines (with smaller anthropoids) for MHD of M_1 (Figure 18). For both teeth, MHD of *T. syrichta* scales to cranial length similarly to strepsirrhines of comparable head size. Scaling patterns differ strikingly between anthropoid monkeys and strepsirrhines (Figure 18). For both teeth, MHD of strepsirrhines is significantly and negatively correlated to cranial length (dp_4, $r = -.39$; M_1, $r = -.57$). In contrast, dp_4 of anthropoids bears no significant correlation to cranial length, while M_1 is positively correlated ($r = .51$) with cranial length. In the case of M_1, there are clear outliers for each group. If the folivorous *Lepilemur* and *Propithecus* are excluded, the M_1 of strepsirrhines has a stronger correlation of $r = -.72$. Among anthropoids, the M_1 of two tamarins (*Leontopithecus rosalia, Saguinus geoffroyi*) is of notably low MHD for their head size. Once tamarins are excluded, the correlation reaches .81.

Overall patterns of crown HA density reveal that the crowns with the densest HA are within the postcanine teeth of strepsirrhines; in most species MHD is located at the protoconid of dp_4 (Figure 19). The protoconid of dp_3 may reach a similar range of density. In two strepsirrhines, *Propithecus coquereli* and *L. leucopus*, M_1 has the densest crown (Figure 18, 19); this also describes *T. syrichta* (Figure 20). In contrast to strepsirrhines and tarsiers, in anthropoids the MHD of the anterior teeth may rival or exceed that of postcanine teeth (Figure 20).

Certain phylogenetic patterns are evident. For example, even though cheirogaleids have a relatively high MHD of postcanine teeth (Figure 18) much of the crown remains comparably poorly mineralized at birth. The most folivorous strepsirrhines do not consistently scale as having a higher or lower MHD than other strepsirrhines. The highest range of HA density (e.g., >50% MHD) is localized at the cusps, whereas the basins and the base of the crowns is <25% MHD (Figure 18). *Varecia* spp. exhibit the same pattern (Figures 19 and 21), but they are aberrant among the large-bodied lemuroids. In lemurids, mineralization of most postcanine tooth crowns is more advanced in the basins and crown base compared to

cheirogaleids. Exceptions include the talonid basin of dp_4, the crown base of dp_3, and M_1, each of which may be unmineralized or less mineralized than the rest of the crown. Newborn lorisoids have highly localized MHD at cusps of deciduous postcanine teeth, and tend to have poorly mineralized talonid basins. Cheirogaleids and lorisoids have advanced mineralization of replacement teeth, and in newborn *Nycticebus* the MHD of anterior replacement teeth actually exceeds that of their precursors (Figure 19).

Anthropoids have distinctive family- or subfamily-level patterns in crown mineralization. Callitrichines are distinguished by advanced mineralization of the deciduous incisors at birth (Figure 20). The crowns of these teeth are entirely mineralized, and the roots are more advanced in mineralization compared to other anthropoids. In contrast, the remaining teeth have completely unmineralized crown bases, and in dp_4 the talonid basin is partially or completely unmineralized in all callitrichines except *Cebuella* (Figures 10 and 20). Delayed mineralization of dp_4 is especially notable in newborn tamarins, in which the entoconid may be unmineralized as well. Aside from callitrichines, in most cebids the degree of mineralization appears to be more evenly advanced throughout the crown, with the entire crown of each deciduous tooth reaching at least 25% MHD. All cercopithecoids have a distinctly less mineralized dp_4 compared to more anterior teeth (Figures 7, 8, and 20).

In the most molariform teeth, the protoconid is typically the locus of MHD, followed by the metaconid; the entoconid is at the lowest HA density of all primary cusps. This is the case in nearly all primates. One exception is a Day 6 *Tarsius*, in which the paraconid of M_1 is the cusp at maximum density. However, in both M_2 and M_3 the protoconid is the site of MHD. In a Day 0 *Tarsius*, both the protoconid and metaconid exceed the paraconid in MHD.

3.6.3 | Progression of crown mineralization: Cross-sectional age samples—

Several cross-sectional age samples that bracket the newborn stage are shown in Figure 21. At the earliest time point examined (late fetal stage), both lemuroids have more advanced mineralization of the anterior teeth and dp_2 relative to more posterior postcanine teeth. Specifically, MHD of all mandibular teeth is found within the former group of teeth; in contrast, a greater proportion of the crown of dp_3 and dp_4 remains unmineralized (Figure 21). In the *Lemur* fetus (possessing a cranial length at 80% of that for average neonatal cranial length), the two mesial cusps of M_1 are mineralized. In *Varecia*, which may be somewhat less advanced (at 73% of neonatal cranial length), only the protoconid of M_1 is visible.

The fetal *Propithecus*, which appeared close to neonatal size (cranial length is unavailable, but palatal length is 87% of that for known neonates), has fully formed deciduous crowns. The crown of dp_4 (arrowheads) is the most uniformly well-mineralized of all deciduous teeth. The M_1 crown (open arrows) is nearly fully formed, but aside from cusp tips, the HA density is less than that in dp_4.

Our cross-sectional age samples indicate different postnatal progression of cusp mineralization. In *Lemur*, newborns have a more mineralized dp_4 relative to more anterior teeth, suggesting the former accelerates its rate of mineralization perinatally. *Varecia* also exhibits the same change, but it occurs later. At birth, and even at Day 12, dp_4 still has an

incomplete crown, unlike newborn lemurids (Figure 21). The crown of dp_4 in our Day 25 *Varecia* is at a stage comparable to similarly aged Lemur (Figure 21) and *Eulemur* spp. (not shown). In contrast to the lemurids, all deciduous teeth of *Propithecus* become *relatively* less mineralized postnatally. That is, the range of HA density in permanent teeth reaches the highest parts of the overall range in HA density (75—85% MHD at the cusp tips and some crests), while in deciduous teeth the entire crowns are <50% of the overall range. In contrast, M_1 is less mineralized compared to deciduous teeth in all specimens aged 0–25 days in *Lemur* and *Varecia*. In our sample, the protoconid of M_1 overlaps the HA density of dp_4 in a P28 *Lemur*, but not in a P25 *Varecia*. The wide disparity of crown mineralization rates among large-bodied lemurs is perhaps best emphasized in a comparison of a day 140 *Varecia* (a possible weaning age) with one-month-old *Propithecus*. In the *Varecia*, only M_1 and M_2 are mineralized as yet, and neither are in occlusion. In the much younger *Propithecus*, M_1 is in occlusion already, and all permanent molar crowns are fully formed (Figure 21).

4 | DISCUSSION

Knowledge of primate dental development has expanded considerably in the past several decades. In particular, observations on dental development (e.g., tooth eruption) have grown to encompass representatives of nearly all extant primate families (Godfrey et al., 2001; Smith et al., 2015; Smith, Crummett, & Brandt, 1994). Increased resolution of μ-CT in recent decades now provides a nondestructive means of expanding our knowledge of crown morphology and mineralization patterns.

4.1 | Methodological considerations

4.1.1 | MHD of teeth at pre-eruptive or late bell stages are unaffected by lengthy fixation in formalin—

We evaluated MHD measurements in two teeth that are in very different stages of ontogeny. The well-formed crowns of dp^4 are advanced to a pre-eruptive stage in most newborn or older infant primates, meaning the enamel is fully formed in most species (see Smith et al., 2015). In contrast, M^1 varies from a similar stage of maturity in highly folivorous species, to those that have just commenced the late bell stage (e.g., most callitrichines). Correlations reveal no significant influence of lengthy formalin fixation on MHD on these teeth. This may indicate that the densest regions of the crown are unlikely to be demineralized and softened, even by decades of storage in formalin. In contrast, bone is documented to lose fracture resistance after prolonged fixation in formalin (e.g., Kikugawa & Asaka, 2004), suggesting bone demineralization occurs. We cannot discount the possibility that enamel is unaffected whereas the less hard dentin and cementin are more affected. It is also possible that the thinner periphery of enamel and dentin (e.g., nearer the crown cervix) are more affected than the densest core of the cusp tip. However, our findings on a large sample of subadult prosimians suggest that MHD is a reliable indicator of the extent of mineralization in developing crowns, especially within the densely mineralized cusp and crests. Selected specimens were stored in ethanol, some for decades. Although our sample of ethanol-stored specimens was far smaller, these data points did not differ noticeably from formalin-stored specimens at the species level.

4.1.2 | Micro-computed tomography parameters—Numerous parameters affect radiographic visualization of mineralized tissues. Here we chose to standardize two variables: voxel size and energy levels. The majority of our volumes were reconstructed using 20.5 μm cubic voxels. Our voxel size range is within the range used recently to morphometrically study the teeth of adult *Tupaia* spp. (Selig, Sargis, & Silcox, 2019), mammals whose tooth crowns are similarly-sized to those of the smallest primates. That said, the unmineralized portions of some tooth crowns at birth prevent us from definitively determining presence or absence of some smaller cusps, especially those projecting from the cingula/cingulids.

HA density of human teeth, including deciduous premolars, has been assessed at 70 kVp (Elfrink, ten Cate, van Ruijven, & Veerkamp, 2013; He et al., 2011). Our efforts to differentiate surfaces of crowns using different energy levels (Figure 3) strongly suggest that our highest energy level of 70 kVp offered the best possible fidelity of the crown surface in subadults; an added benefit is that it also allows a comparison of HA density in human teeth to our data on nonhuman primates.

4.2 | Newborn primate dentition: Morphology of deciduous teeth

Previous work on deciduous teeth has provided much detail on catarrhine primates (e.g., Seibert & Swindler, 1991; Swarts, 1988; Swindler & McCoy, 1964; Winkler et al., 1991), very limited morphological detail on platyrrhines (Hershkovitz, 1977; Tarrant & Swindler, 1973), and only one detailed study on strepsirrhines (Tattersall & Schwartz, 1977).

Our results agree with previous findings, summarized in Swindler (2002) on morphology of the deciduous dentition in Old World monkeys. Of the two deciduous incisors, the di1 of each jaw possesses a rounded or flattened incisal margin, while the di2 has a more pointed cusp margin (caniniform). There is consistency of results at the genus level, for example, our description of deciduous incisors of *T. francoisi* is similar to that figured for *T. cristata* by Swindler (2002); see (fig. 4.4 therein). Some details may vary. For example, Swindler also described mesial and distal ridges on di_1 and di_2 in some cercopithecines, but these are not apparent in the *Allenopithecus* specimen described here. Reconciling descriptions of the deciduous canines is made difficult since the crown base of the canine is typically still mineralizing at birth. As in permanent molars, the deciduous premolars are each bilophodont, with transverse crests connecting mesial and distal cusp pairs. The crowns appear complete at birth, although mineralization patterns suggest dp3 of the upper and lower jaws has undergone further matrix maturation than dp4 (see below). They each have four primary cusps; this excludes a putative paraconid of dp_4, which will be discussed further below. Mandibular dp_3 is notably different than dp_4 in that the mesial cusp pair is more closely opposed than the distal cusp pair. Swindler noted that stylar cusps are rare on upper deciduous premolars of Old World monkeys, but noted cusplets that are positionally consistent with parastyles in at least one of the premolars of *Trachypithecus cristata* and *Cercocebus torquata*. Our findings concur on the absence of meso- and metastyles, but we observed parastyles in all but one (*Colobus guereza*) of the six species we studied. It is of note that Swindler's samples for descriptive study (Swindler, 2002) were of mixed age subadults; it is possible smaller secondary cusps were subject to more wear than other crown

structures. In the broad context provided by this study in combination with previous work on hominoids (e.g., Swarts, 1988), the close similarity is size of deciduous premolars is distinctive in catarrhines among all primates.

Our descriptions of deciduous teeth in platyrrhines must be considered incomplete in some cases. For example, callitrichines have notably undermineralized dps at birth, preventing definitive assessment of cingula/cingulids, and small associated secondary cusps. Except for *Cebuella*, for which we possess a broader range of subadult ages, we exclude callitrichines from our summary of accessory cusps (Table 2). However, readers are referred to Hershkovitz (1977, fig. V.28 therein), who indicated numerous deciduous teeth with stylar cusps, illustrating parastyles/metastyles on di^2, dc, and the deciduous premolars. His illustration also indicates metastyles on di^2 and dp^4 (but not clearly shown on dp^2, dp^3).

Broadly, the platyrrhines described here have caniniform di^2 in contrast to the rounded or flat incisal margin of di^1. Deciduous canines of both jaws are poorly mineralized at the crown base in newborns, and are thus poor subjects for morphological description. We confirm the abrupt transition from caniniform dp^2 and dp^3 to highly molariform dp^4 in callitrichines, as observed by Hershkovitz (1977). However, it can also be generalized that in all platyrrhines, dp^4 is distinct from other deciduous premolars in its close morphological similarity to M^1. The same is observed for the lower premolars. Thus, no platyrrhines has the near size parity of deciduous premolars observed for catarrhines. With the exception of *Aotus* and *Callicebus*, stylar cusps are far more common in the platyrrhines we studied compared to catarrhines (Table 2).

The present study examines the broadest sampling of strepsirrhines confirmed at newborn age to date. Here, we can confirm that dp4 of both jaws is abruptly more molariform and robust compared to more anterior premolars (an exception is *Propithecus* and *Lepilemur*, in which dp4 is much smaller than M1, though still more molariform than dp3). A raised mesial shelf is also visible in most mandibular dp_4s, and may possess a putative paraconid. The presence of accessory cusps can be confirmed in some species (Table 2), but in cheirogaleids the crown bases are too poorly mineralized to confirm presence or absence. The readers are referred to Tattersall and Schwartz (1974), who noted that *C. major* was the only cheirogaleid in their sample that lacked a parastyle on dp^4.

A final consideration is the putative paraconid. Swindler (2002) discussed a mesial cusp, at the leading edge of the paracristid in some catarrhines. He noted that paraconid is present 80% of the time on dp_3 of colobines, and that it was previously described in some cercopithecines. Tattersall and Schwartz (1974) described a paraconid in some strepsirrhines (e.g., *Hapalemur*), and similar cusps are visible on numerous strepsirrhine described here. We do not make a claim here of homology to the clear and pronounced paraconid observable in tarsiers. Yet, it is noteworthy that this cusp was at least weakly pronounced in most of the catarrhines examined here. Moreover, it is positionally similar to a small cusp in some other primates, as described below. The cusp is more buccally positioned than the paraconid of M_1 in tarsiers (as is the entire paracristid). A critical difference between M_1 and dp_4 of all extant primates described to date (except tarsiers) is the raised mesial edge of the latter, producing a mesial “shelf” that is lacking in M_1. This creates a vexing dilemma: any cusplet that forms

at the leading edge of this shelf, regardless of homology, projects upward similarly to a paraconid. That there is a distinct concentration of HA density in this cusp at birth suggests it may be a primary cusp, but further cross-sectional age studies are needed for confirmation.

4.3 | Sequence of crown mineralization in the perinatal period

The process of dental crown formation has been well-studied in humans (e.g., Kraus & Jordan, 1965) and several anthropoid species have been studied in some depth (Swindler et al., 1968; Swindler & McCoy, 1964; Tarrant & Swindler, 1973). Swindler (2002) described the pattern of cusp mineralization for both upper and lower molariform teeth in a common pattern: beginning with the buccomesial cusp (e.g., paracone), mineralization proceeds lingually, (protocone), then buccodistally, and finally distolingually. He emphasized some variation in the transition to the second and third cusps (e.g., whether protocone or hypocone mineralizes first).

Swindler's observations were based on a number of catarrhines and one platyrrhine. With the large sample examined here, this pattern appears to hold for primates broadly. Several observations support this. First, in cross-sectional age samples, if only one cusp of a molariform tooth is mineralized at a given age, it is invariably the buccomesial cusp (Figure 21). If only two cusps are mineralized, it is typically the two mesial cusps. If only one cusp remains unmineralized in mandibular molariform teeth, it is the distolingual cusp in all cases. Our samples also confirm some variation. For example, in one *Varecia* newborn the two buccal cusps are mineralized while both lingual cusps are not (Figure 21). A second line of evidence may be gleaned from HA densities observed in subadult crowns. The same patterns are observed: the greatest HA density is found buccomesially (or mesially, when both mesial cusps presumably have reached a similar density range), and then density is sequentially lower in the same sequence that cusps appear. This is likely only typical at early ages. Kraus and Jordan (1965) maintained that the rate of mineralization among cusps changes postnatally across human development. Supporting this, Kono, Suwa, and Tanijiri (2002) found that enamel thickness of the hypoconulid was greater than that of the protoconid in the human M_1.

4.4 | Phylogenetic patterns of crown mineralization

4.4.1 | Molariform teeth—Using histological material, the state of mineralization of the maxillary teeth at birth was recently discussed by Smith et al. (2015). Dp^4 is well-mineralized in most primates, except in most neonatal callitrichines and *Varecia*. M^1 of galagids, indriids, and tarsiers is at a more advanced state of mineralization than lemurids or anthropoids (see also Godfrey et al., 2004); M^1 is more mineralized in catarrhines than in most platyrrhines. Given that these teeth are equally molariform in primates and functionally similar, these observations illustrate that primates have different strategies in transitioning the role of dp^4 toward its successor.

Our new observations on mandibular tooth crowns agree with our previous histological work, but the present report expands observations to a broader array of primates. In nearly all primate genera studied, at least some neonates have initiated mineralization of M_1 (Figure 22). *Leontopithecus* was an exception, however, only one specimen was examined.

Given that at least some newborn *Leontopithecus* have M^1 commencing the late bell stage (Smith et al., 2015), we expect that may be the case for the mandibular counterpart. Our finding also put the more commonly studied hominid teeth in a broader perspective. In great apes and humans (Kraus & Jordan, 1965; Seibert & Swindler, 1991; Winkler et al., 1991), dp_4 is well mineralized but may have an unmineralized central basin or an isolated hypoconid, and M_1 is represented only by isolated cusps. In contrast, in all cercopithecoids the central basin and primary cusps have merged at birth, and in many newborns the two mesial cusps of M_1 are connected by a mineralized protocristid (Figure 22). In this manner, well-described hominids (noting that newborn *Gorilla* remains poorly investigated) are less advanced in mineralization of both of these teeth at birth. Platyrrhines vary more than catarrhines. *Cebuella* and most platyrrhines have complete, or nearly complete dp_4 crowns at birth, and M_1 is represented by two to three isolated cusps; in some cases the mesial cusp pair are bridged. Among platyrrhines we have examined, Pithecia *pithecia* has the most advanced development of M_1, with mineralization of the central basin underway (Figure 22).

Mineralization of permanent molars at birth in *T. syrichta* is entirely similar to *T. bancanus* (Luckett & Maier, 1982). M_2 is fully formed except for the center of the talonid basin; M_3 already has two mineralized cusps. No extant anthropoid that has been studied approaches this degree of advanced mineralization. Among strepsirrhines, there is an even starker disparity. *Varecia* spp. have the least mineralized crowns of all primates. On the other hand, lorisoids, indriids (see also Godfrey et al., 2004), and *Lepilemur* have more advanced permanent molar mineralization than any primate (Table 5, Figure 22).

4.4.2 | Replacement teeth—Extant anthropoids are revealed to have a unified tendency to delay mineralization of replacement teeth. Only *Callicebus, Pithecia*, and *Cebuella* possessed any mineralized portions of replacement teeth. As with the upper jaw (Smith et al., 2015), mineralization of replacement teeth in *Cebuella* is not observed in all newborns. Moreover, our previous histological work on maxillary teeth revealed that among all anthropoids, only callitrichines possess replacement tooth germs that were more advanced than the cap stage. Thus, we would generalize that (a) mineralization of replacement teeth is uncommon at birth in anthropoids broadly, (b) few anthropoids invest at all in prenatal mineralization of these teeth, and (c) only anterior replacement teeth, if any, may be mineralized at birth.

Strepsirrhines vary far more in the development of replacement teeth. Although teeth of *Varecia* spp. are undermineralized compared to all other true lemurs, it may be generalized that all lemurids delay mineralization of replacement teeth relative to other strepsirrhines. Only *Eulemur* spp. commonly (not always) have mineralized replacement teeth, and if so, only the cusp tips of the anterior teeth are seen. In loisoids, the anterior replacement teeth are the most advanced in mineralization. P2 has also has a mineralized cusp tip. *Lepilemur* and *Propithecus* have initiated mineralization of all replacement teeth.

4.4.3 | Degree of crown mineralization:

Patterns of HA density in newborn crowns: Anthropoids have a general pattern that distinguishes them from all other extant primates. Their anterior teeth and first deciduous

premolar (upper and lower dp2 or dp3) have the most surface area of relatively dense crown (as estimated by distribution of HA density—Figure 20) and are often the locus of MHD within the tooth row. In tarsiers and strepsirrhines, both anterior and postcanine teeth tend to have extensive parts of the crown at >50% MHD for the mandibular tooth row (Figures 19 and 20). In other words, the overall HA density is more evenly distributed among teeth in strepsirrhines (and also tarsiers) compared to anthropoids. In addition, the MHD among mandibular teeth most frequently occurs at the protoconid of dp_4, or more rarely at M_1 (*Propithecus, Lepilemur*, and some galagids).

Our preliminary comparison of MHD measurements in primate mandibular teeth shows that strepsirrhines, and especially small-bodied species, have higher dp_4 and M_1 MHD at birth than anthropoids. It remains of great interest how these data compare in an analysis that controls for phylogeny and body size. However, our results support a previous assertion based on maxillary tooth germs (Smith et al., 2017). Since M_1 volume is positively correlated with cranial length in all strepsirrhines, our finding of a *negative* correlation of MHD with cranial length supports our conclusion that tooth germ size and degree of mineralization at birth are highly independent, and that growth and mineralization proceed at different rate across gestational time.

Hominoid newborn samples remain unavailable to us at this time, and the relationship of their data to other primates remains of great interest. Still, we can at least assess peak densities newly reported here to previous work on humans using the same CT energy parameters. In human children of 4–5.8 years, dp_4 was reported to range from 1,345 to 2,077 mg/cc (Elfrink et al., 2013). Among strepsirrhines, specimens of several species (*Microcebus*, *Nycticebus*, *Lemur*) exhibit a MHD of dp_4 exceeding 1,500 mg/cc. In anthropoid monkeys studied here, no newborns exceed that density, and only one specimen (*Saimiri*) exceeds 1,400 mg/cc. The MHD of M_1 in humans from 18 to 25 years ranges from 2,006.5 to 2,281.8 mg/cc (He et al., 2011). The densest foci of M_1 crowns measured here are observed in *Tarsius* and *Nycticebus* (both >1,500 mg/cc), and *Propithecus* (> 1,400 mg/cc). In contrast, only one anthropoid measured here exceeds a MHD 800 mg/MHD. Of course, the published human data are from ontogenetically disparate samples. We may expect that MHD measured in the humans does not reveal true peaks, since some of the denser apical enamel likely wore away. Most certainly, most if not all primates studied here are still undergoing maturation of enamel. However, this comparison enables us to see that broadly, newborn anthropoids have lesser MHD of dp_4 and especially M_1 compared to the fully formed homologues in human children. In newborn strepsirrhines, dp_4 already falls within the range observed for the M_1 of young adult humans.

4.4.4 | Early postnatal rates of mineralization—Our small cross-sectional age samples suggest that mineralization rate shifts within the mandibular tooth row during early ontogeny. In the late fetal lemurids in our sample, MHD is located in more anterior deciduous teeth than at birth. MHD is found in d_1 to dc in fetal *Lemur* and Varecia, and shifts posteriorly in newborns. In Varecia this shift occurs over a longer time span (Days 0–12) than in *Lemur* (by Day 0). A similar transition occurs in *Propithecus*, but the MHD and overall crown density increase in the permanent molars rather than dps (Figure 21). This indicates shifting rates of mineralization. Initially, MHD likely reflects the timing at which

teeth enter the later bell stage, occurring in an anterior to posterior direction. A shift in MHD to teeth with greater importance in crushing food begins perinatally.

In galagids, as in lemurids, maps of HA density indicate a likely shift in mineralization rates. MHD is initially centered on cusps of dp_3 and dp_4. By 1 month of age, MHD is centered at the protoconid of M_1, suggesting an acceleration of mineralization in permanent molars.

Among anthropoids, there is a more limited representation of different age stages in our sample, however *Cebuella* and *Saguinus oedipus* provide useful contrasts to show the extent of variability. In newborn *Cebuella*, M_1 is more mineralized than in other callitrichines, and the cusp tips of two replacement teeth (I_1, I_2) are present. In an infant specimen (which resembles a specimen recorded at one-month-old) P_2 and P_4 have initiated mineralization. In *Saguinus* at 1 month of age, M_1 is still incompletely mineralized (lacks an entoconid) and only the very tip of I_1 is mineralized. In a specimen 117 days old, only the cusp tips of the three anterior replacement teeth are mineralized.

Our findings comparing MHD among species at age-matched time points reveals variation in postnatal rate of mineralization between and within primate suborders (Table 7). In the case of the most molariform teeth (dp_4 and M_1), only *Cebuella* is known to be as precocious as most strepsirrhines in terms of age at crown completion.

There is perhaps a greater range in timing of replacement teeth. As expected based on observations of maxillary cusp mineralization in newborns (Smith et al., 2015), cheirogaleids, indriids and galagids have more rapid mineralization of the first permanent molar and the first permanent incisor (the first replacement tooth to mineralize) compared to all other primates except tarsiers. Lemurids are delayed by comparison, but still may well reach these two dental milestones before weaning (Table 7).

Simply looking at newborns alone, it is apparent that strepsirrhines exhibit vastly different rates of mineralization of mandibular teeth, as reported for eruption rates. There appear to be strongly phylogenetic patterns as discussed above (Figure 19), and as recently discussed for eruption sequences (López-Torres, Schillaci, & Silcox, 2015; Monson, Coleman, & Hlusko, 2019). But it may also be the case that other factors may influence variation within families. In addition, the influence on primate social behaviors and group size are worth consideration. Primates with later weaning appear to be particularly variable in the rate of at which molariform crowns are completed (Table 6), and in which replacement teeth begin to mineralize (Table 7). Among strepsirrhines, those primates that are left in nests and/or “parked” while the mother forages tend to have advanced mineralization of replacement teeth at birth. In contrast, those that cling and then ride the mothers may or may not have mineralized replacement teeth at birth (Figure 23); what factors influence these patterns is a matter a future interest.

5 | CONCLUSIONS

5.1 | Phylogenetic implications

Because deciduous teeth were previously described in far fewer taxa relative to permanent teeth, their phylogenetic and functional importance has been rarely discussed. The findings herein may provide a better context to comparative and paleontological studies. While individual fossil deciduous teeth will continue to be described with regularity, we await opportunities to see more subadults with fully preserved deciduous dentition (e.g., Bloch, Boyer, Gingerich, & Gunnell, 2002; Franzen et al., 2009). Although it is difficult to assign precise ages to such fossils, and newborns are less likely to be well preserved than older subadults, knowing variability in the mineralization and eruption rates in extant primates provides a valuable comparative lens with which to view these fossils.

Of great interest in future studies is the antiquity of anthropoid patterns of dental development. Nearly all extant anthropoids have pronounced delays in mineralization of replacement teeth, especially premolars. Knowing the origin of these delays offers clues to life history characteristics of extinct relatives.

Lemurids require further exploration for similar reasons. The greater abundance of subfossil material may be of great comparative value to understand the deferred investment in mineralization of replacement teeth by lemurids.

In fossil primates, deciduous teeth have been used to infer relationships of extant species. Benefit (1994) compared deciduous premolars of extant cercopithecoids to a fossil cercopithecine, *Victoriapithecus*. The latter lacked distinct crests associated with bilophodont teeth; such observations have implication for the relationships of extant cercopithecoids to fossil species. The primitive dental eruption sequence for Primates is of great interest. Fossils of primates and other euarchontans may allow us to further explore how various factors influence developmental pacing of dental maturation and eruption (Bloch et al., 2002; Gingerich & Smith, 2010; López-Torres et al., 2015; Monson & Hlusko, 2018; Smith, 2000).

5.2 | Patterns of dental development

Strepsirrhines and anthropoids have clear differences in the relationship of MHD to cranial length. The relatively strong correlation of dp_4 and M_1 MHD in strepsirrhines is striking in several ways. First of all, dental germ volume of all strepsirrhines (and all primates) is positively correlated with head size (unsurprisingly, in absolute size, larger heads house larger teeth). This relationship is negative regarding MHD, suggesting that smaller species may be accelerating tooth mineralization. Secondly, this relationship in strepsirrhines contrasts clearly with anthropoids. Anthropoids show no clear pattern at all in MHD of dp_4, but have a strong *positive* correlation of M_1 MHD to cranial length. To the extent that cranial length includes both a neurocranial and midfacial component, it is presently difficult to explain this dichotomy. However, the positive relationship of anthropoid M_1, but not dp_4, to cranial length recalls that among all teeth, M_1 development bears a strong correlation to brain growth (Godfrey et al., 2001; Smith et al., 1994). A future study is needed to isolate the specific relationship of neonatal MHD to neurocranial measurements (e.g., endocranial

volume). Finally, the findings on MHD confirm our previous conclusion, based on qualitative observations, that dental mineralization and dental germ growth do not closely covary (Smith et al., 2017).

For now, we interpret the MHD data with caution as they may only measure how densely HA is deposited in cusps and crest of teeth, the portions of teeth that mineralize first (Tarrant & Swindler, 1973). We do not yet know whether the overall extent of mineralization at birth also differs, and this might best be assessed by measuring crown volumes relative to fully mineralized crowns of older specimens. Analysis of these two measurements in concert could elucidate whether primates vary in the pace of tooth maturation or simply in the pattern by which they mineralize.

5.3 | Factors influencing dental development

Diet, life history, and phylogeny have been discussed as the biggest factors in the pace of dental eruption (e.g., Godfrey et al., 2001; Monson & Hlusko, 2018; Smith et al., 1994; Smith et al., 2017). If defined based on dental eruption schedules, ontogenetic stages such as “infancy” do not always follow a similar duration across species, even in species of similar lifespans (Godfrey et al., 2001; Smith, 1994). Some primates are especially precocious in development of the permanent teeth, in some cases forecasting their dietary specialization (Godfrey et al., 2004). But, life history traits such as the duration of gestation have complex relationships with dental growth, and these affect development of the deciduous and permanent teeth differently. For example, relative deciduous premolar volume scales negatively with relative gestation length in strepsirrhines at birth, whereas M^1 scales positively (Smith et al., 2017). The convergence of dietary specialization adds additional complexity. Folivorous species are outliers with larger than predicted dp_4 (*Hapalemur*) or M_1 (Propithecus) volume when plotted against relative gestation length (Smith et al., 2017). Dental maturity during infancy reflects adaptation, even prior to use in mastication.

Our observations on the extent of crown mineralization and MHD do not reveal consistent patterns reflecting diet. The three highly folivorous strepsirrhines studied here (*Lepilemur, Propithecus*, and *Hapalemur*) are notable in the relative completeness of the M1 crown (Figure 22). *Lepilemur* and *Propithecus* have notably high MHD in M_1 at birth (relative to cranial length), but this is not apparent in *Hapalemur*. Among anthropoids, the seed-eating *Pithecia* is notable for the degree of completeness of its M1 crown, but *Colobus*, *Trachypithecus* and *Alouatta* are not more advanced in M1 crown formation than most nonfolivores (Figure 22). MHD of M1 in highly folivorous anthropoids does not appear notably higher than nonfolivores, relative to body size. However, all folivorous anthropoid species are only available to us as single specimens at this time.

The influence of life history variables such as gestation length and weaning age on dental mineralization in primates has not been studied. Generally, monkeys have a more prolonged process of dental mineralization that begins with nongrinding teeth, while mineralization of postcanine teeth, especially M_1, is delayed until after birth. This may in part be a result of relatively later weaning in most anthropoid primates. However, it is also striking that in some strepsirrhines the crowns of dp4 and M1 are poorly mineralized; an altricial state similar to hominoids. The departure of lemurids from the overall trend in strepsirrhines, of

relatively well-developed crowns at birth, suggests additional factors have an influence. Whether this is explained purely by phylogeny, life history, or perhaps infant care strategies requires a future phylogenetically-controlled quantitative study.

Supplementary Material

Refer to Web version on PubMed Central for supplementary material.

ACKNOWLEDGMENTS

Our study is supported in part by grant number P51 OD011132 to Yerkes Center. This project also used biological materials collected at SNPRC and funded by the Office of Research Infrastructure Programs/OD P51 OD011133. Specimens were also obtained through the Duke Lemur Center's Director's Fund. We also thank A.M. Burrows and L.T. Nash for providing selected samples. Thank you to E. Hoeger and N. Duncan for providing access to specimens from the AMNH. This is DLC publication # 1443.

Funding information

National Institutes of Health, Grant/Award Numbers: P40 OD010938, P51OD011106; National Science Foundation, Grant/Award Numbers: BCS-0959438, BCS-12-1728263, BCS-1231350, BCS-1231717, BCS-1830894, BCS-1830919; Duke Lemur Center's Director's Fund; Office of Research Infrastructure Programs, Grant/Award Number: P51 OD011133; Yerkes Center, Grant/Award Number: P51 OD011132

REFERENCES

Ahrens H. (1913). Die Entwicklung der menschlichen Zähne. Anatomische Hefte, 48, 169–257.

Anemone RL, Mooney MP, & Siegel MI (1996). Longitudinal study of dental development in chimpanzees of known chronological age: Implications for understanding age at death of Plio-Pleistocene hominids. American Journal of Physical Anthropology, 99, 119–133. [PubMed: 8928715]

Anemone RL, Skinner MM, & Dirks W. (2012). Are there two distinct types of hypocone in Eocene primates? The 'pseudohypocone' of notharctines revisited. Paleontologia Electronica, 15, 26A.

Avery JK (2002). Oral development and histology (3rd ed.). New York, NY: Thieme Medical Publishers.

Benefit BR (1994). Phylogenetic, paleodemographic, and taphonomic implications of Victoriapithecus deciduous teeth from Maboko, Kenya. American Journal of Physical Anthropology, 95, 277–331. [PubMed: 7856766]

Blechschmidt E. (1954). Rekonstruktionsverfahren mit Verwendung von Kunststoffen. Ein Verfahren zur Ermittlung und Rekonstruktion von Entwicklungsbewegungen. Zeitschrift für Anatomie und Entwicklungsgeschichte, 118, 170–174. [PubMed: 13227045]

Bloch JI, Boyer DM, Gingerich PD, & Gunnell GF (2002). New primitive paromomyid from the Clarkforkian of Wyoming and dental eruption in plesiadapiformes. The Journal of Vertebrate Paleontology, 22, 366–379.

Bouxsein MJ, Boyd SK, Christiansen BA, Guldberg RE, Jepsen KJ, & Muller R. (2010). Guideline for assessment of bone microstructure in rodents using micro-computed tomography. The Journal of Bone and Mineral Research, 25, 1468–1486. [PubMed: 20533309]

DeLeon VB, & Smith TD (2014). Mapping the nasal airways: Using histology to enhance CT-based three-dimensional reconstruction. The Anatomical Record, 297, 2113–2120. [PubMed: 25312369]

Elfrink MEC, ten Cate JM, van Ruijven LJ, & Veerkamp JSJ (2013). Mineral content in teeth with deciduous molar hypomineralisation (DMH). Journal of Dentistry, 41, 974–978. [PubMed: 24018462]

Fleagle JG (2013). Primate adaptation and evolution. New York, NY: Academic Press.

Franzen JL, Gingerich PD, Habersetzer J, Hurum JH, von Koenigswald W, & Smith BH (2009). Complete primate skeleton from the Middle Eocene of Messel in Germany: Morphology and paleobiology. PLoS One, 4, e5723. [PubMed: 19492084]

Garn SM, Lewis AB, & Polacheck DL (1959). Variability of tooth formation. Journal of Dental Research, 38, 135–148. [PubMed: 13631146]

Gingerich PD, Smith BH. 2010 Premolar development and eruption in the early Eocene adapoids Cantius ralstoni and Cantius abditus (Mammalia, Primates) Contributions from the Museum of Paleontology, University of Michigan pp. 3241–3247.

Godfrey LR, Samonds KE, Jungers WJ, Sutherland MR, & Irwin MT (2004). Ontogenetic correlates of diet in Malagasy lemurs. American Journal of Physical Anthropology, 123, 250–276. [PubMed: 14968422]

Godfrey LR, Samonds KE, Jungers WL, & Sutherland MR (2001). Teeth, brains, and primate life histories. American Journal of Physical Anthropology, 114, 192–214. [PubMed: 11241186]

He B, Huang S, Zhang C, Jing J, Hao Y, Xiao L, & Zhou X. (2011). Mineral densities and elemental content in different layers of healthy human enamel with varying teeth age. Archives of Oral Biology, 56, 997–1004. [PubMed: 21411061]

Hershkovitz P. (1977). Living New World monkeys (Platyrrhini) (Vol. 1). Chicago, IL: University of Chicago Press.

Jernvall J, Kettunen P, Karavanova I, Martin LB, & Thesleff I. (1994). Evidence for the role of the enamel knot as a control center in mammalian tooth cusp formation: Nondividing cells express growth stimulating Fgf-4 gene. The International Journal of Developmental Biology, 38, 463–469. [PubMed: 7848830]

Kappeler PM, & Pereira ME (2003). Primate life histories and socioecology. Chicago, IL: University of Chicago Press.

Kikugawa H, & Asaka T. (2004). Effect of long-term formalin preservation on bending properties and fracture toughness of bovine compact bone. Materials Transactions, JIM, 45, 3060–3064.

Kono RT, Suwa G, & Tanijiri T. (2002). A three-dimensional analysis of enamel distribution patterns in human permanent first molars. Archives of Oral Biology, 47, 867–875. [PubMed: 12450518]

Kraus BS, & Jordan R. (1965). The human dentition before birth. Philadelphia, PA: Lea and Febiger.

López-Torres S, Schillaci MA, & Silcox MT (2015). Life history of the most complete fossil primate skeleton: Exploring growth models for Darwinius. Royal Society Open Science, 2, 1–15.

Luckett WP, & Maier W. (1982). Development of deciduous and permanent dentition in Tarsius and its phylogenetic significance. Folia Primatologica, 37, 1–36.

Macchiarelli R, Bondioli L, Debénath A, Mazurier A, Tournepiche J-F, Birch W, & Dean C. (2006). How Neanderthal molar teeth grew. Nature, 444, 748–751. [PubMed: 17122777]

Mann A. (1988). The nature of Taung dental maturation. Nature, 333, 123. [PubMed: 3130577]

Monson TA, Coleman JL, & Hlusko LJ (2019). Craniodental allometry, prenatal growth rates, and the evolutionary loss of the third molars in New World monkeys. The Anatomical Record, 302, 1419–1433. [PubMed: 30315641]

Monson TA, & Hlusko LJ (2018). Breaking the rules: Phylogeny, not life history, explains dental eruptionsequence in primates. American Journal of Physical Anthropology, 167, 217–233. [PubMed: 30216408]

Nanci A. (2007). Ten Cate's oral histology: Development, structure, and function (9th ed.). St. Louis, MO: Elsevier.

Oka SW, & Kraus BS (1969). The circumnatal status of molar crown maturation among the Hominoidea. Archives of Oral Biology, 14, 639–659. [PubMed: 5257937]

Ooë T. (1979). Development of human first and second permanent molar, with special reference to the distal portmon of the dental lamina. Anatomy and Embryology, 155, 221–240. [PubMed: 420409]

Radlanski RJ (1995). Morphogenesis of human tooth primordia: The importance of 3D computer-assisted reconstruction. The International Journal of Developmental Biology, 39, 249–256. [PubMed: 7626413]

Reinholt LE, Burrows AM, Eiting TP, Dumont ER, & Smith TD (2009). Brief communication: Histology and microCT as methods for assessing facial suture patency. American Journal of Physical Anthropology, 138, 499–506. [PubMed: 19170212]

Rosenberger AL (2011). Evolutionary morphology, platyrrhine evolution, and systematics. The Anatomical Record, 294, 1955–1974. [PubMed: 22042518]

Schwartz JH (2007). Skeleton keys. New York, NY: Oxford University Press.

Schwartz JH, Tattersall I. (1985). Evolutionary relationships of living lemurs and lorises (Mammalia, Primates) and their potential affinities with European Eocene Adapidae. Anthropological Papers of the American Museum of Natural History, 60, 1–100.

Seibert JR, & Swindler DR (1991). Perinatal dental development in the chimpanzee (Pan troglodytes). American Journal of Physical Anthropology, 86, 287–294.

Selig KR, Sargis EKJ, & Silcox MT (2019). Three-dimensional geometric morphometric analysis of treeshrew (Scandentia) lower molars: Insight into dental variation and systematics. The Anatomical Record, 302, 1154–1168. [PubMed: 30809964]

Sirianni JE, & Swindler DR (1985). Growth and development of the pigtailed macaque. Boca Raton, FL: CRC Press.

Smith BH (1994). Patterns of dental development in Homo, Australopithecus, Pan, and Gorilla. American Journal of Physical Anthropology, 94, 307–325. [PubMed: 7943188]

Smith BH (2000). 'Schultz's Rule' and the evolution of tooth emergence and replacement patterns in primates and ungulates In Teaford M, Smith MM, & Ferguson MWJ (Eds.), Development, function and evolution of teeth (pp. 218–228). Cambridge, England: Cambridge University Press.

Smith BH, Crummett TL, & Brandt KL (1994). Ages of eruption of primate teeth: A compendium foraging individuals and comparing life histories. Yearbook of Physical Anthropology, 37, 177–231.

Smith TD, DeLeon VB, Vinyard CJ, & Young JW (in press) Skeletal anatomy of the newborn primate. Cambridge, England: Cambridge University Press.

Smith TD, Jankord KD, Progar AJ, Bonar CJ, Evans S, Williams L, … DeLeon VB (2015). Dental maturation, eruption, and gingival emergence in the upper jaw of newborn primates. The Anatomical Record, 298, 2098–2131. [PubMed: 26425925]

Smith TD, Muchlinski MN, Bucher WR, Vinyard CJ, Bonar CJ, Evans S, … DeLeon VB (2017). Relative tooth size at birth in primates: Life history correlates. American Journal of Physical Anthropology, 164, 623–634. [PubMed: 28832934]

Smith TD, Rossie JB, Cooper GM, Carmody KA, Schmieg RM, Bonar CJ, … Siegel MI (2011). Comparative micro CT and histological study of maxillary pneumatization in four species of New World monkeys: The perinatal period. American Journal of Physical Anthropology, 144, 392–410. [PubMed: 21302266]

Swarts JD (1988). Deciduous dentition: Implications for hominoid phylogeny In Schwatz JH (Ed.), Orang-utan biology (pp. 263–270). New York, NY: Oxford University Press.

Swindler DR (2002). Primate dentition. An introduction to the teeth of non-human primates. New York, NY: Cambridge University Press.

Swindler DR, & Beynon AD (1993). The development and microstructure of the dentition oin Theropithecus In Jablonski NG (Ed.), Theropithecus: The rise and fall of a primate genus (pp. 351–381). Cambridge, England: Cambridge University Press.

Swindler DR, & McCoy HA (1964). Calcification of deciduous teeth in rhesus monkeys. Science, 144, 1243–1244. [PubMed: 14150333]

Swindler DR, Orlosky FJ, & Hendrickx AG (1968). Calcification of the deciduous molars in baboons (Papio anubis) and other primates. Journal of Dental Research, 47, 167–170. [PubMed: 4966235]

Tarrant LH, & Swindler DR (1973). Prenatal dental development in the black howler monkey (Alouatta caraya). American Journal of Physical Anthropology, 38, 255–260. [PubMed: 4632074]

Tattersall I, & Schwartz JH (1974). Craniodental morphology and the systematics of the Malagasy lemurs (Primates, Pro-simii). Anthropological Papers of the American Museum of Natural History, 52, 139–192.

Winkler LA, Schwartz JH, & Swindler DR (1991). Aspects of dental development in the orangutan prior to eruption of the permanent dentition. American Journal of Physical Anthropology, 86, 255–271.

Zehr SM, Roach RG, Haring D, Taylor J, Cameron FH, & Yoder AD (2014). Life history profiles for 27 strepsirrhine primate taxa generated using captive data from the Duke Lemur Center. Scientific Data, 1, 140019. [PubMed: 25977776]

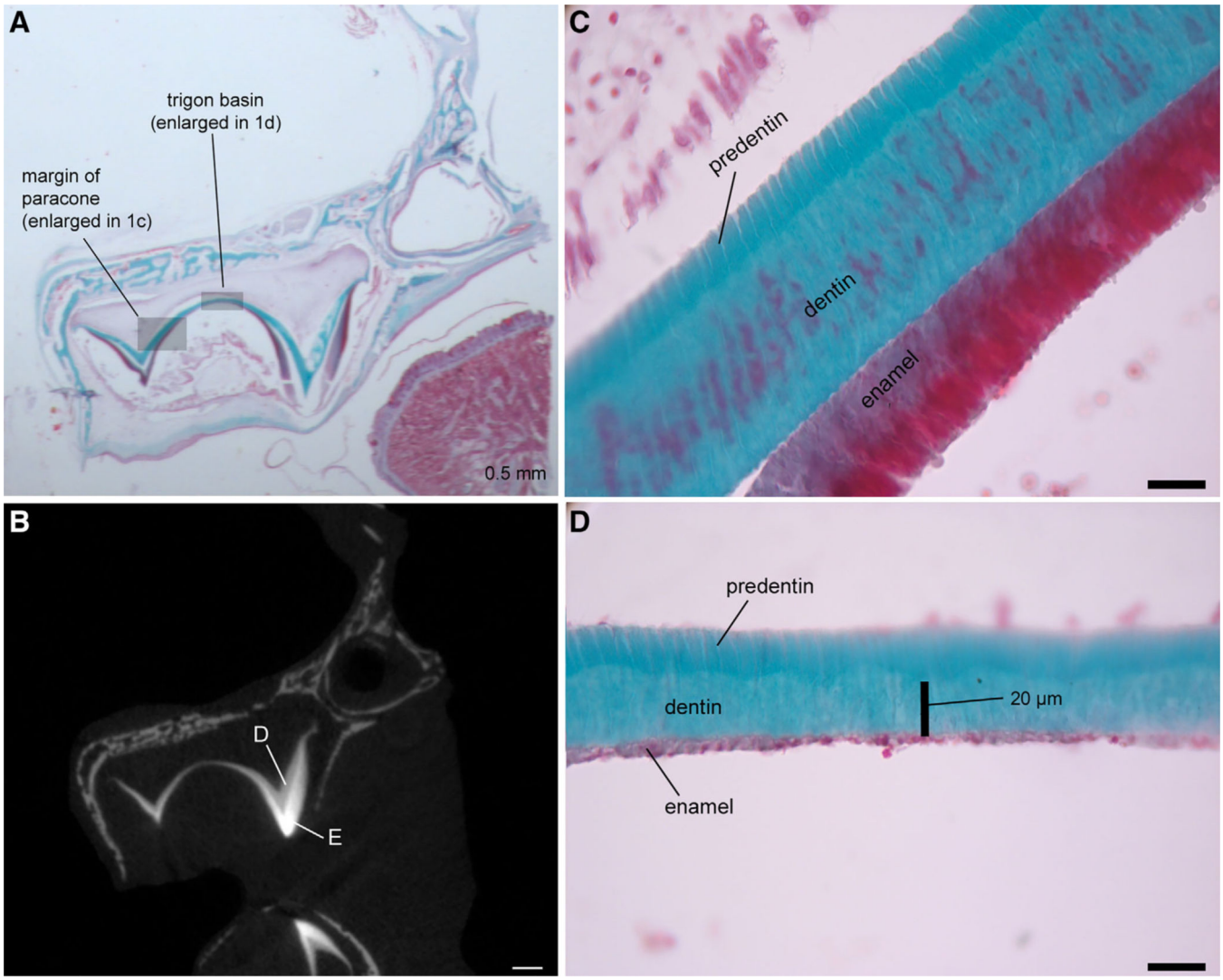

FIGURE 1.

Matching histology and µ-CT slices, following alignment (a, b), showing M^1 of *Tarsius syrichta*. Boxes indicate site of enlarged views (c, d). Enamel (E) and dentin (D) are distinct at the cusp tip (e.g., protocone shown in 1b). However, near the base of the cusps (e.g., paracone, 1c), or in the basins (1d) microCT cannot distinguish enamel and dentin. Scale bars: a,b, 0.5 mm; c,d 20 µm

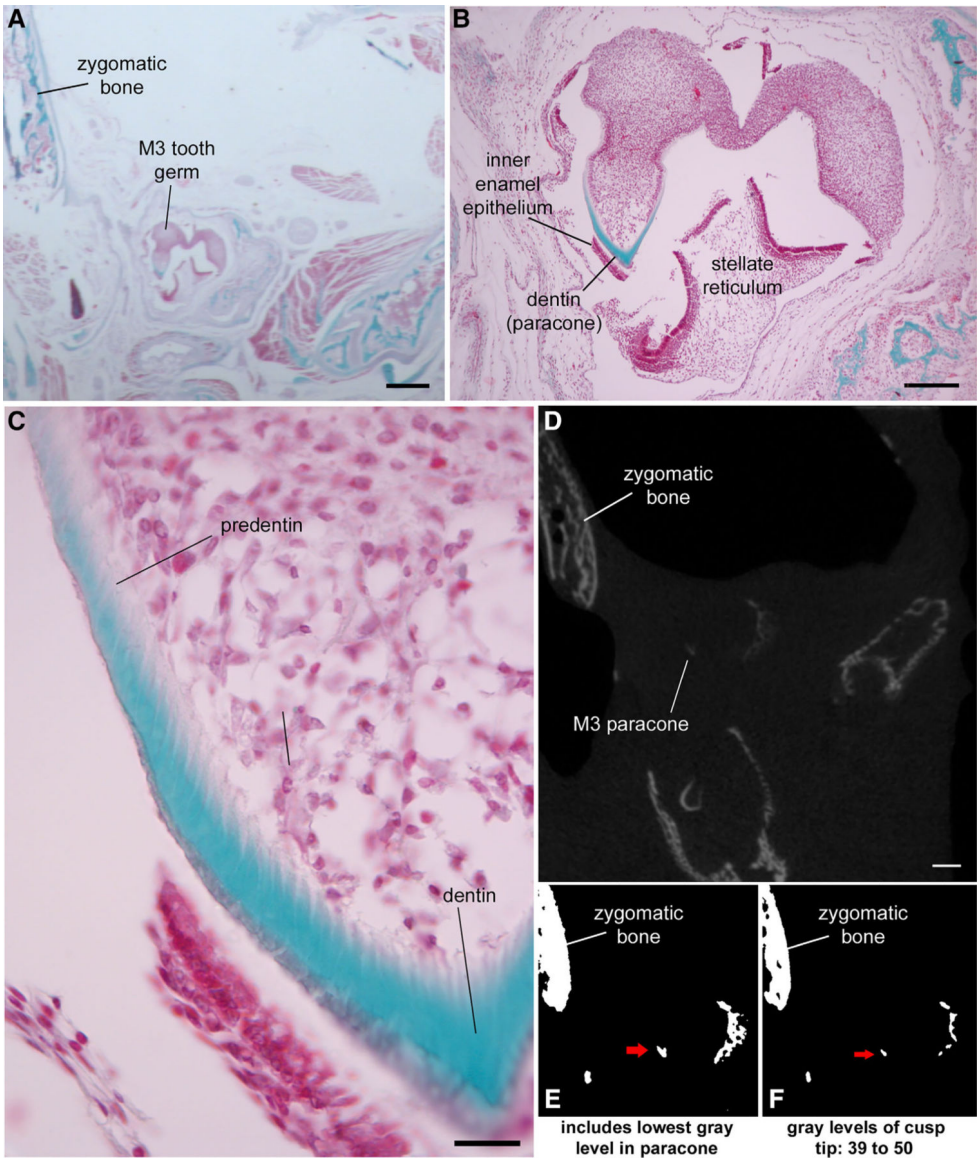

FIGURE 2.

(a,b) The M^3 tooth germ of *T. syrichta* has a mineralized paracone only. Histology confirms that the tip of the cusp is mature dentin, but tapers to only predentin approaching the base of the cusp (c). The cusp tip is easily detected via μ-CT (d). The cusp itself is barely thicker than voxel size. Low ranges of thresholds may detect less mineralized dentin (e), but may exaggerate the thickness of the cusp tip, which is identified by a narrower threshold range (f). Scale bars: a, 0.5 mm; b, 150 μm; c, 20 μm; d, 0.5 mm

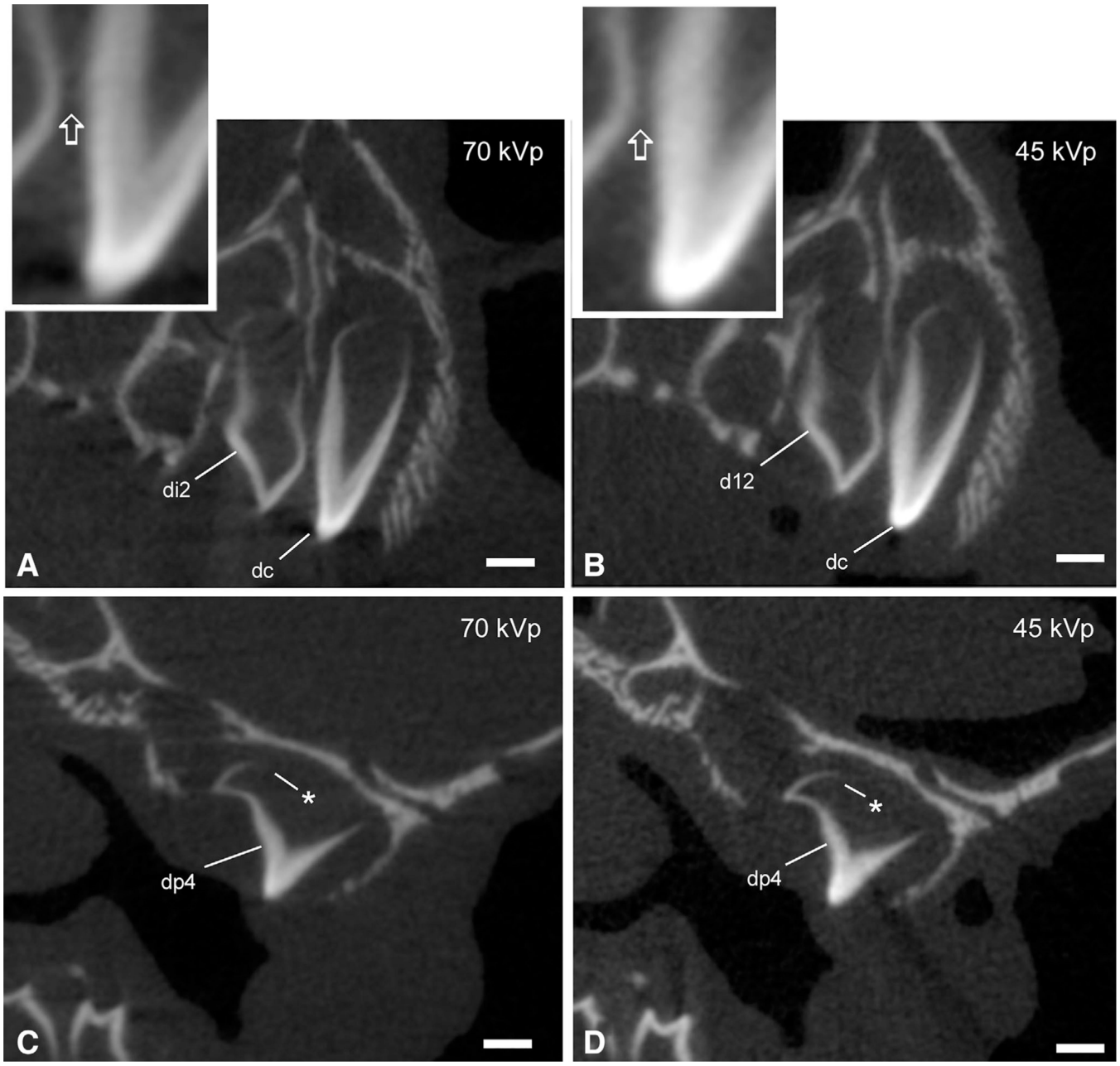

FIGURE 3.

μ-CT slices showing similar cross-sectional levels of deciduous anterior teeth (a,b,) and dp^4 (c,d) in a newborn *Callithrix jacchus* scanned using different energy levels. On the left side are slices with the head scanned at 70 kVp (a,c); on the right are slices with the head scanned at 45 kVp (b,d). The 70 kVp reveals a sharper boundary between adjacent teeth (see open arrow inset, a) compared to the 45 kVp scan (inset, b). Conversely, the 45 kVp was more effective at revealing the cervical region of the crown (c,d: *), where the cusp was least mineralized

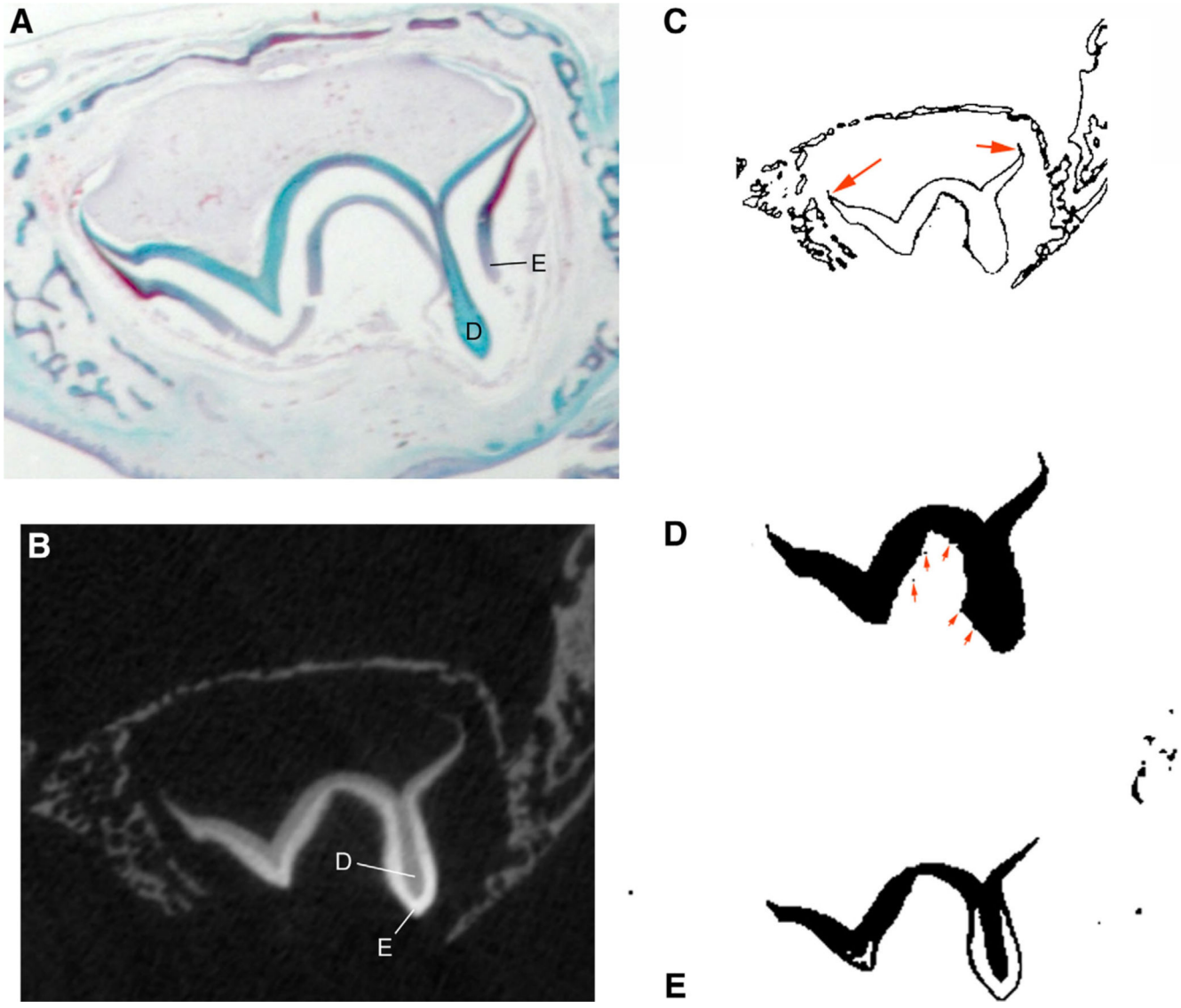

FIGURE 4.

(a) Histological section of dp^4 in a newborn squirrel monkey (*Saimiri*), showing the maxillary dp^4 in the region of the paracone. Note that enamel (E) is present, though fragmented near the cusp tip (D = dentin). (b) The same specimen shown as a μ-CT slice aligned to histology; enamel is distinctly more radio-opaque than the dentin, especially along the cusps. A low threshold range, such as that shown in Plate c (46–70 gray level range) is required to capture the least mineralized dentin found closest to the cervical region (red arrows). However, this range also captures a halo of noise surrounding the crown, including the occlusal surface. As a result, a slice segmented with a threshold that captures all gray levels above that which captures the least mineralized dentin results in a rough cusp surface, with artifactual complexity (red arrows). e) A more limited grayscale range of 99 to 174 captures a specific deeper part of the crown, but appears to exclude the densest enamel. Also, a comparison to the matching level of histology (right) suggests this threshold range isolates the full depth of dentin in the paracone

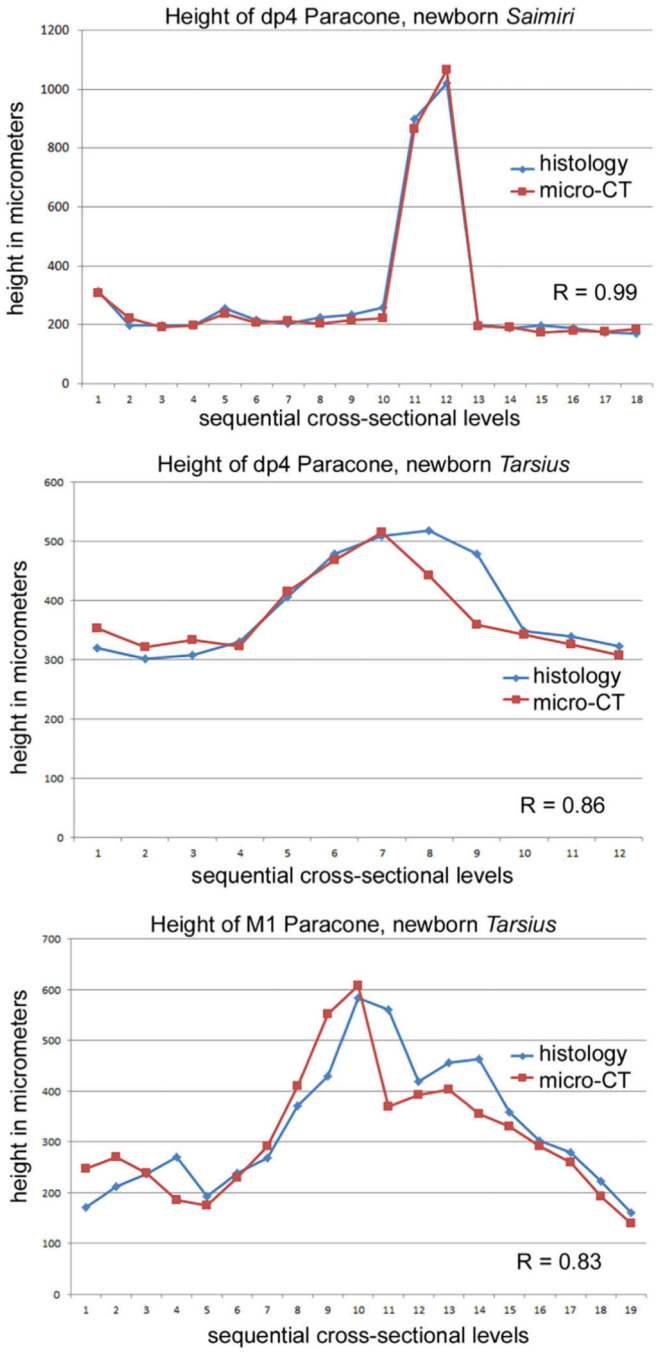

FIGURE 5.

Histology versus μ-CT-derived measurements. Graphs show measurements "height" (maximum apical-basal thickness) of dentin in the paracone of dp^4 or M^1, as measured using histology and μ-CT. In these specimens (newborn *Saimiri boliviensis* and *Tarsius syrichta*), the μ-CT scan volumes were aligned so that serial slices matched the same plan as histological sections of the same heads. Matching levels of histology and μ-CT slices were used for these measurements. Correlation coefficient for a comparison between methods is shown in the bottom right of each graph

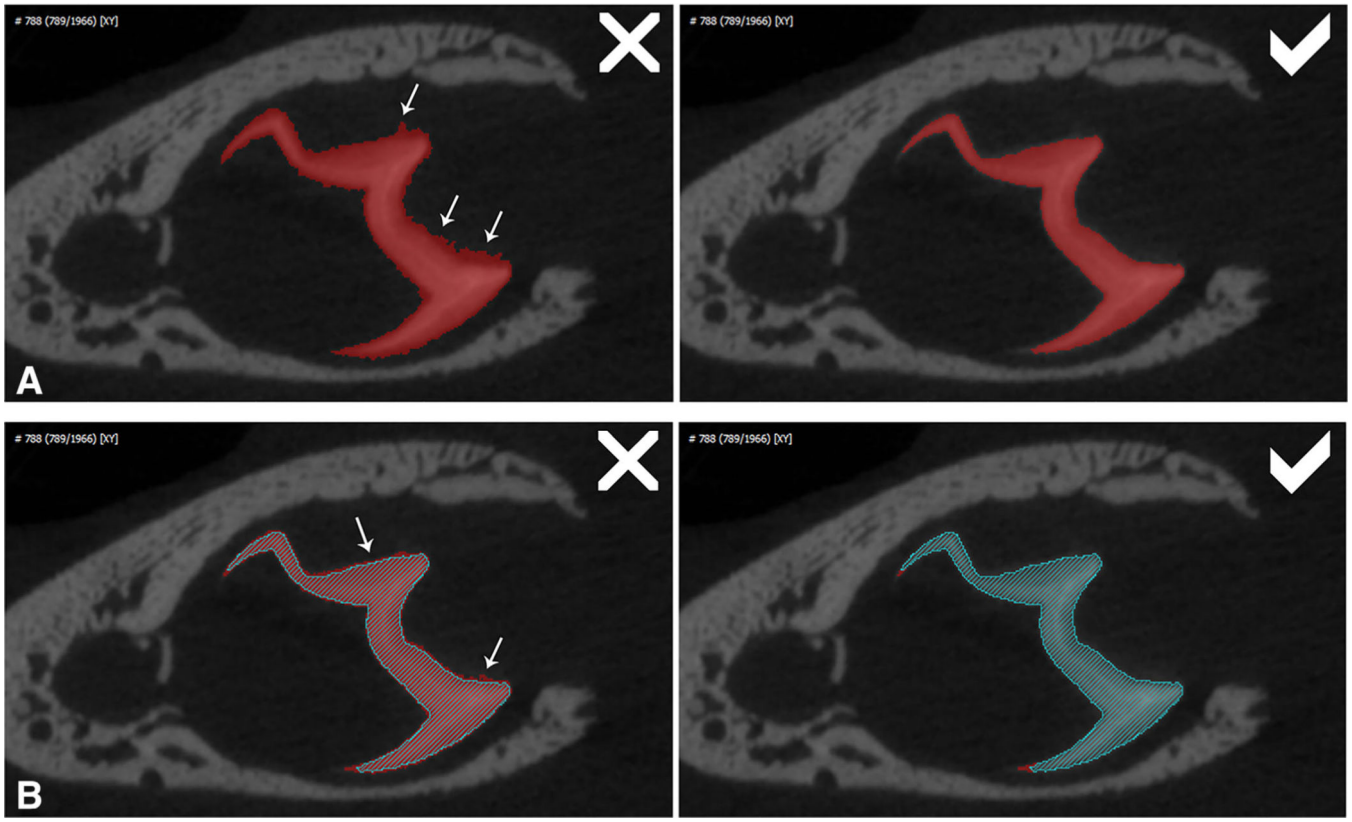

FIGURE 6.

Stepwise method of crown segmentation. In initial phases of segmentation (a), the range of gray levels is carefully selected to establish a relatively smooth occlusal surface (see right side image), and to avoid capturing artefactual “stray” voxels (left side, arrows). Subsequent phases of segmentation are similarly conducted by establishing incrementally lower ranges of gray levels (b), being careful not to allow captured ranges of voxels to “bleed” out onto the occlusal surface (left side, arrows), while adding more of the crown in less-mineralized areas (right side)

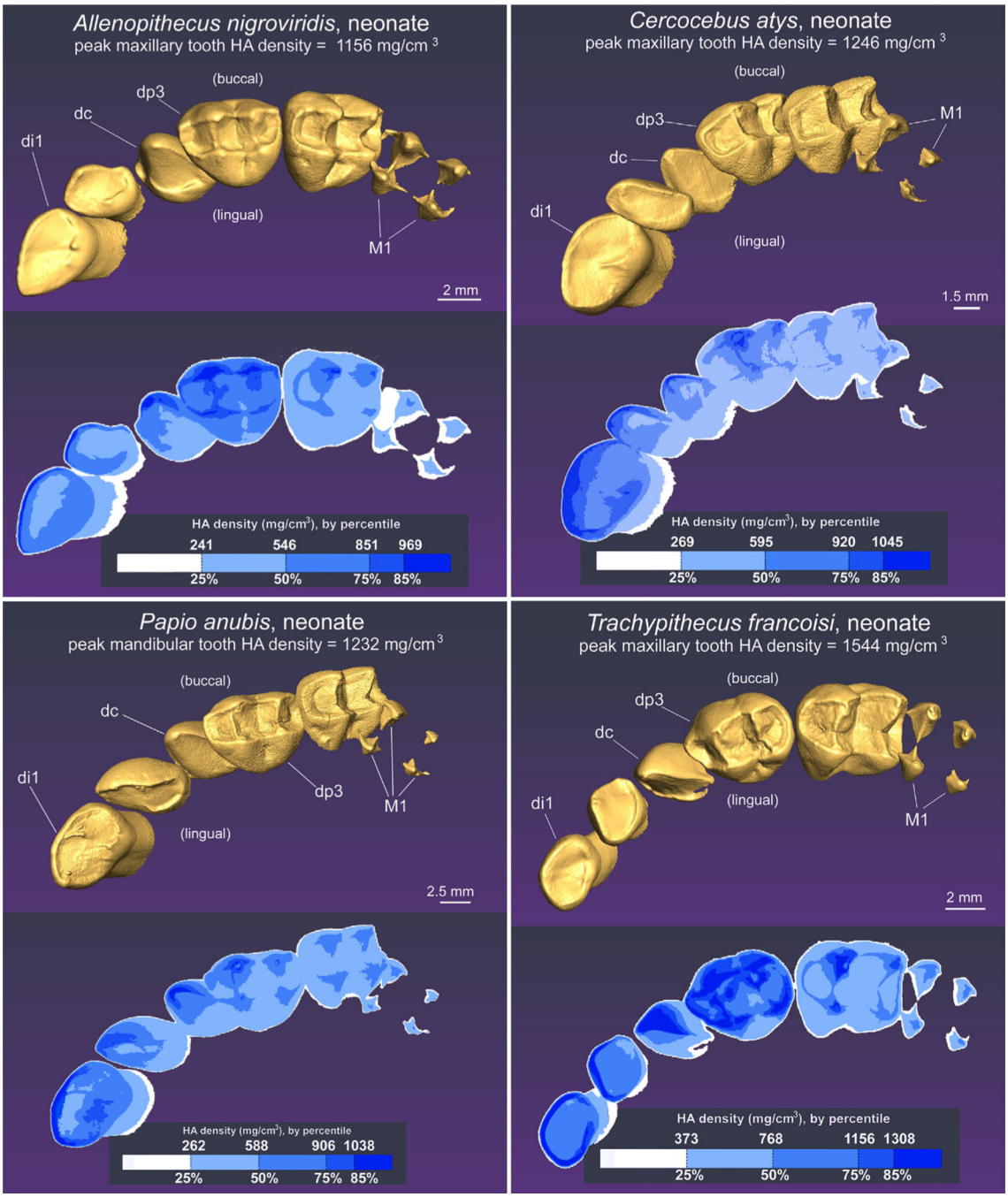

FIGURE 7.

Morphology and hydroxyapatite density in maxillary tooth crowns at birth in *Allenopithecus nigroviridis, Cercocebus atys, Papio anubis*, and *Trachypithecus francoisi*. In *Allenopithecus* and *Trachypithecus*, the right jaw is shown (inverted to facilitate comparison to other species) and the left jaw is shown in the other species. At the top of each image, the peak (or maximum) hydroxyapatite density for the pictured specimen is indicated

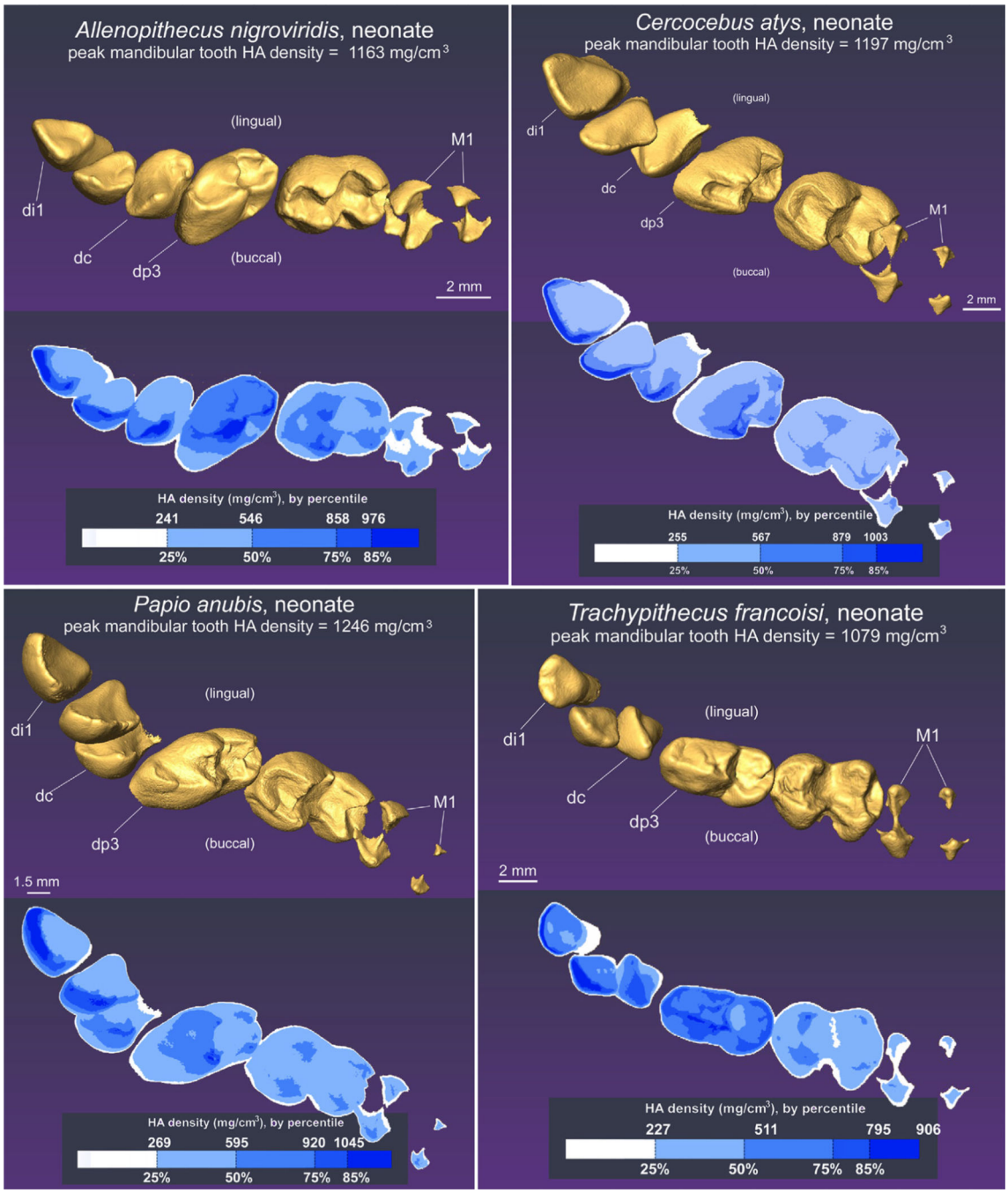

FIGURE 8.

Morphology and hydroxyapatite density in mandibular tooth crowns at birth in *Allenopithecus nigroviridis, Cercocebus atys, Papio anubis*, and *Trachypithecus francoisi*. In *Allenopithecus* the right jaw is shown (inverted to facilitate comparison to other species) and the left jaw is shown in the other species

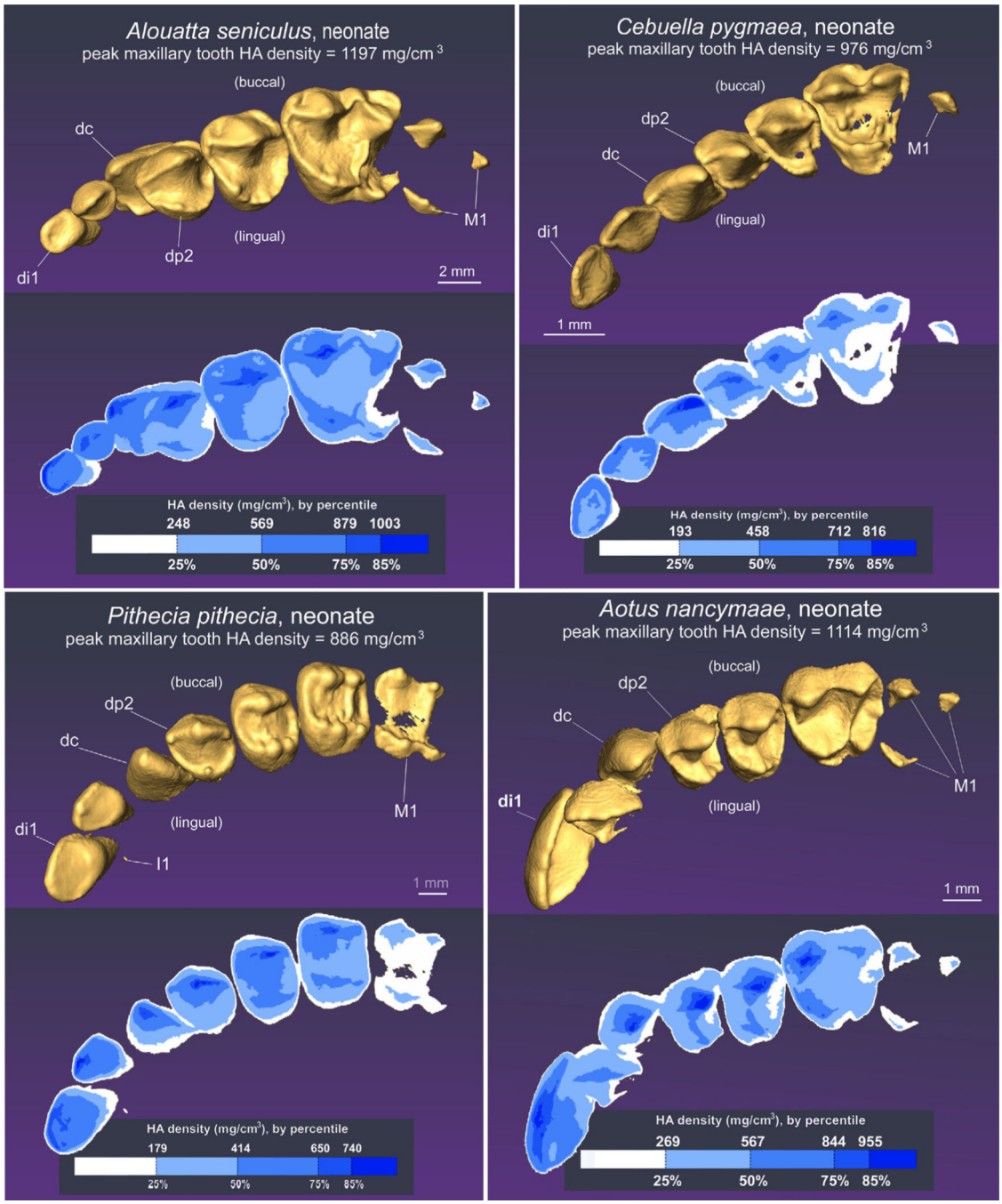

FIGURE 9.

Morphology and hydroxyapatite density in left maxillary tooth crowns at birth in *Alouatta seniculus, Cebuella pygmaea, Pithecia pithecia*, and *Aotus nancymaae*

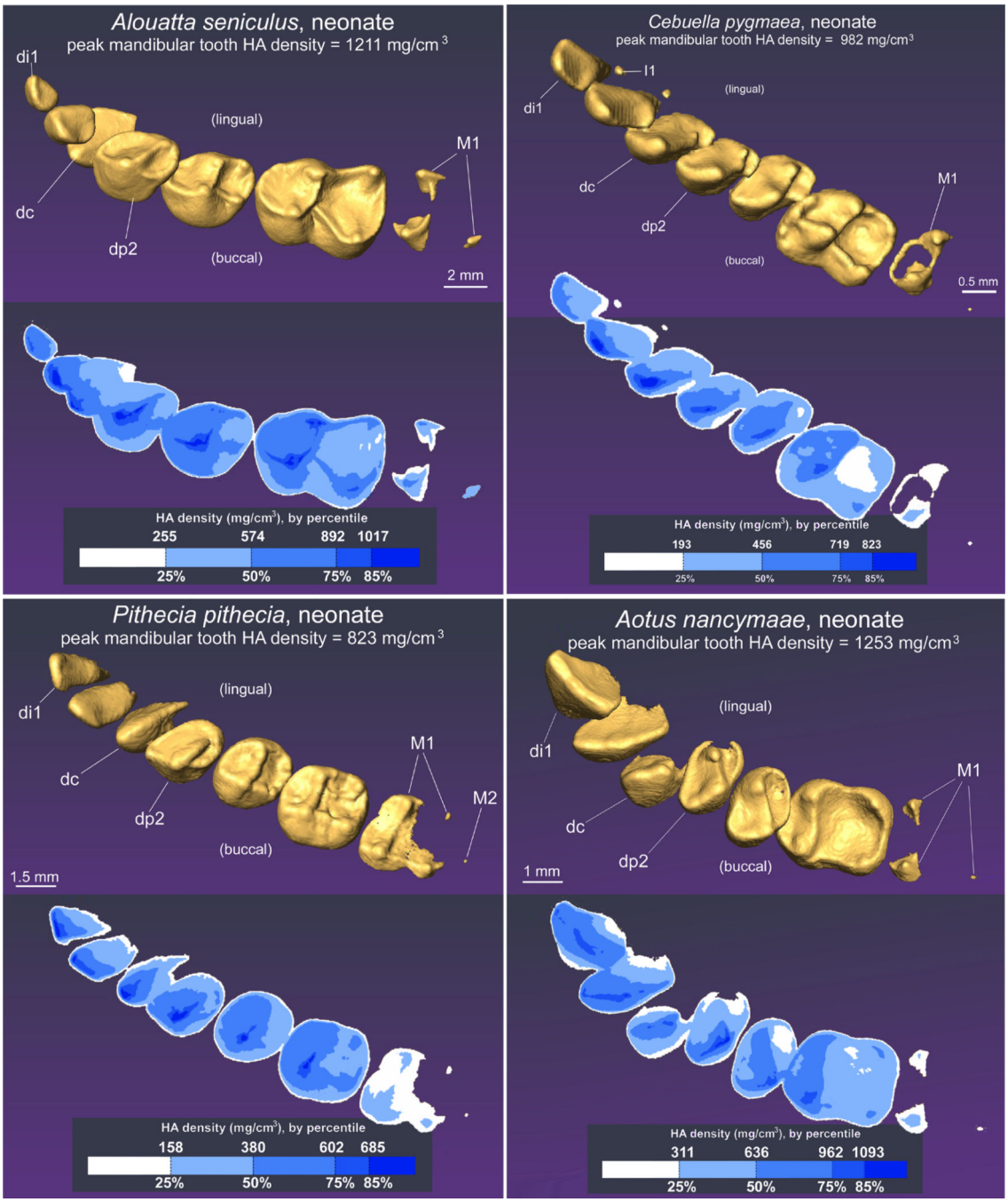

FIGURE 10.

Morphology and hydroxyapatite density in left mandibular tooth crowns at birth in *Alouatta seniculus, Cebuella pygmaea, Pithecia pithecia*, and *Aotus nancymaae*

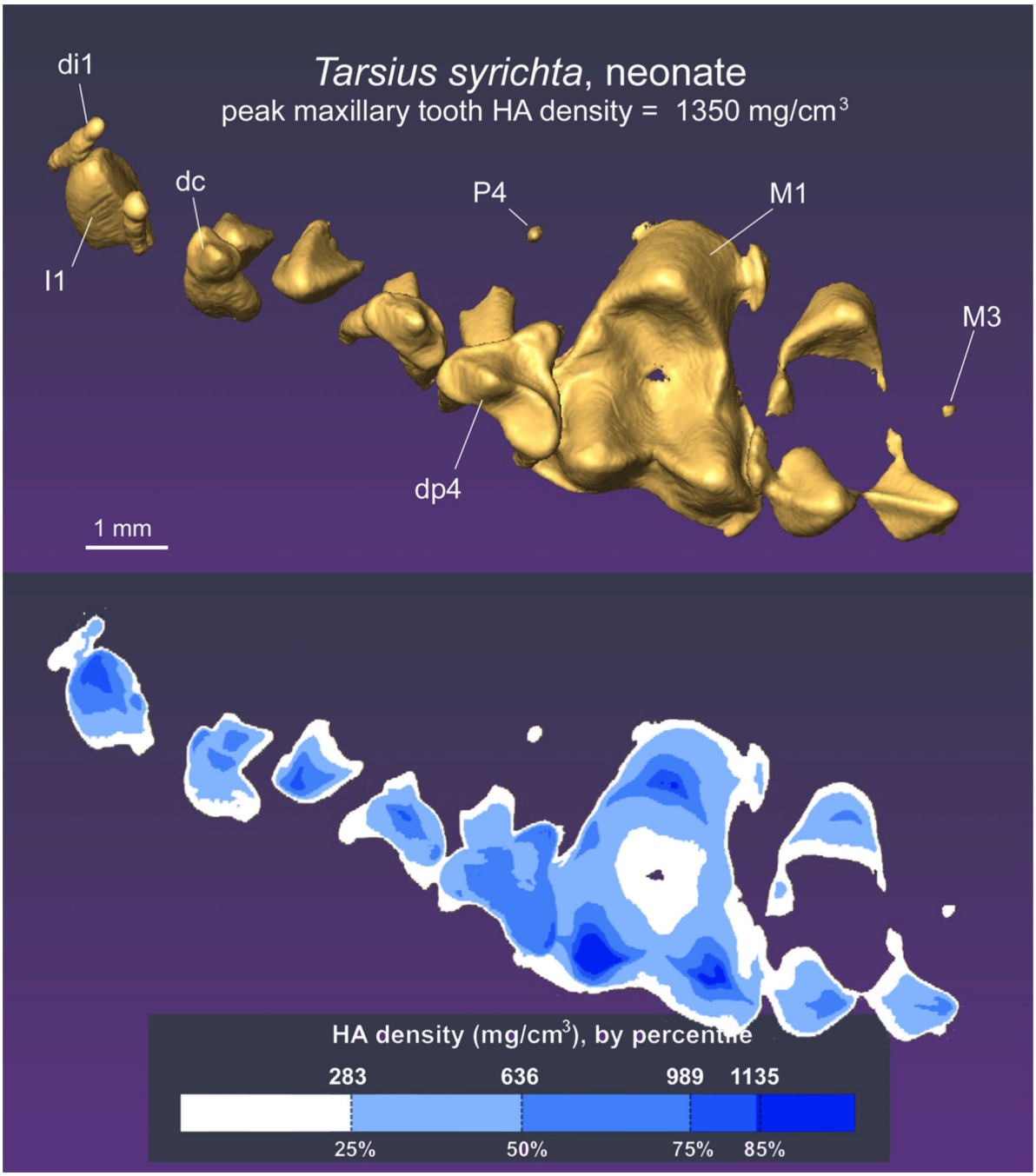

FIGURE 11.

Morphology and hydroxyapatite density in maxillary tooth crowns at birth in *Tarsius syrichta*. A Day 0 newborn is shown using the right jaw

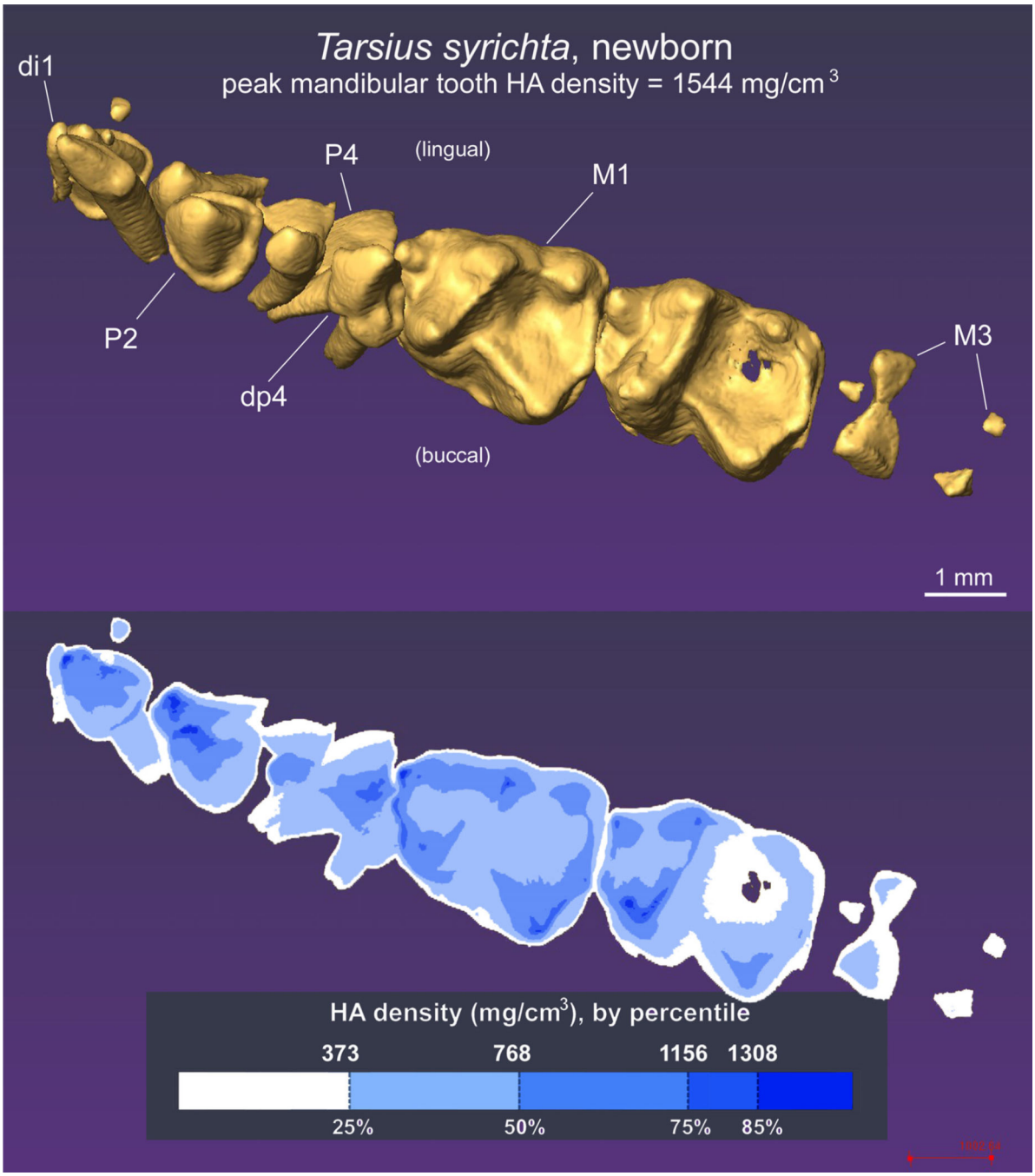

FIGURE 12.

Morphology and hydroxyapatite density in left mandibular tooth crowns at birth in *Tarsius syrichta*. A Day 6 newborn is shown

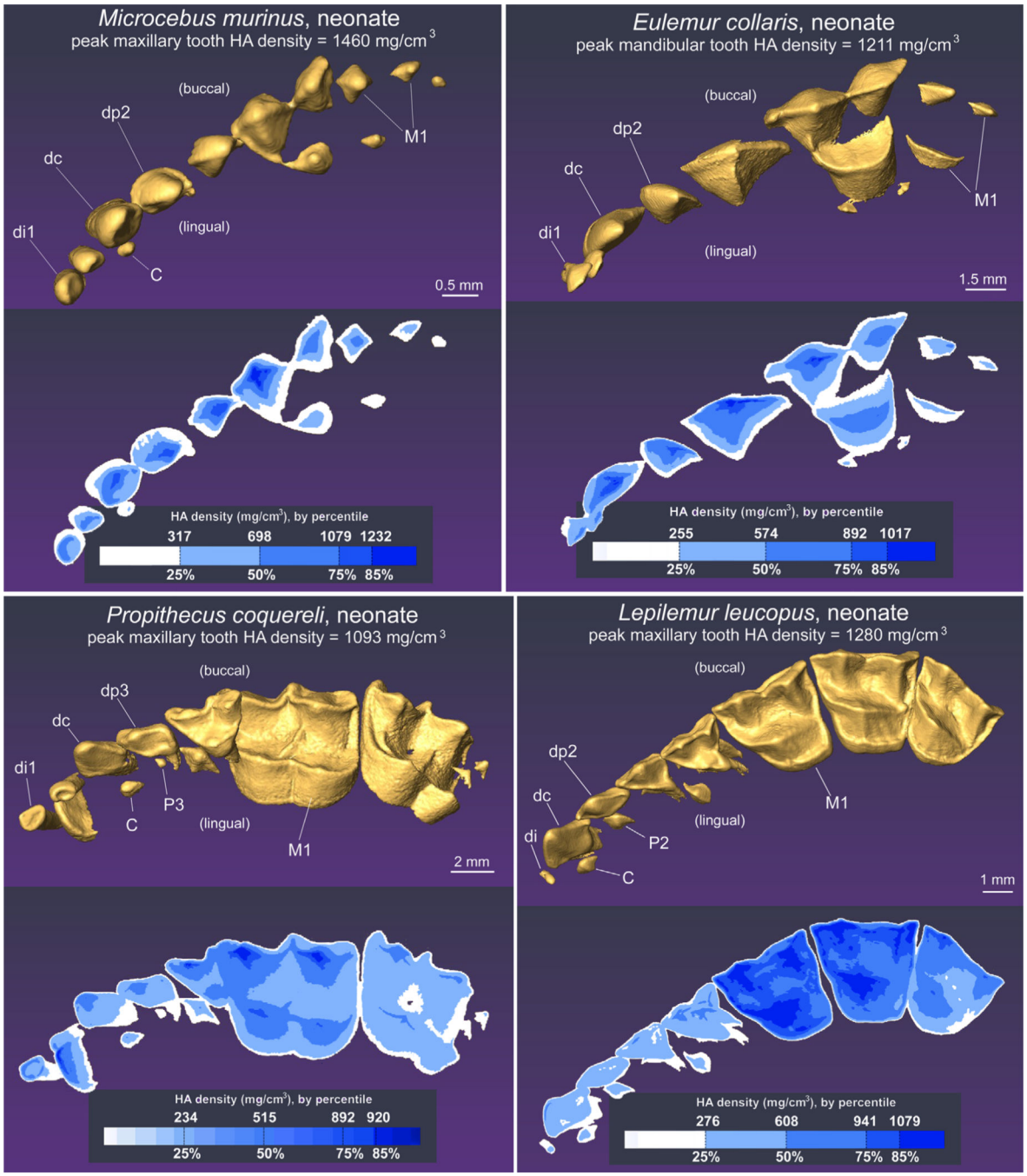

FIGURE 13.

Morphology and hydroxyapatite density in left maxillary tooth crowns at birth in *Microcebus murinus, Eulemur collaris, Propithecus coquereli*, and *Lepilemur leucopus*

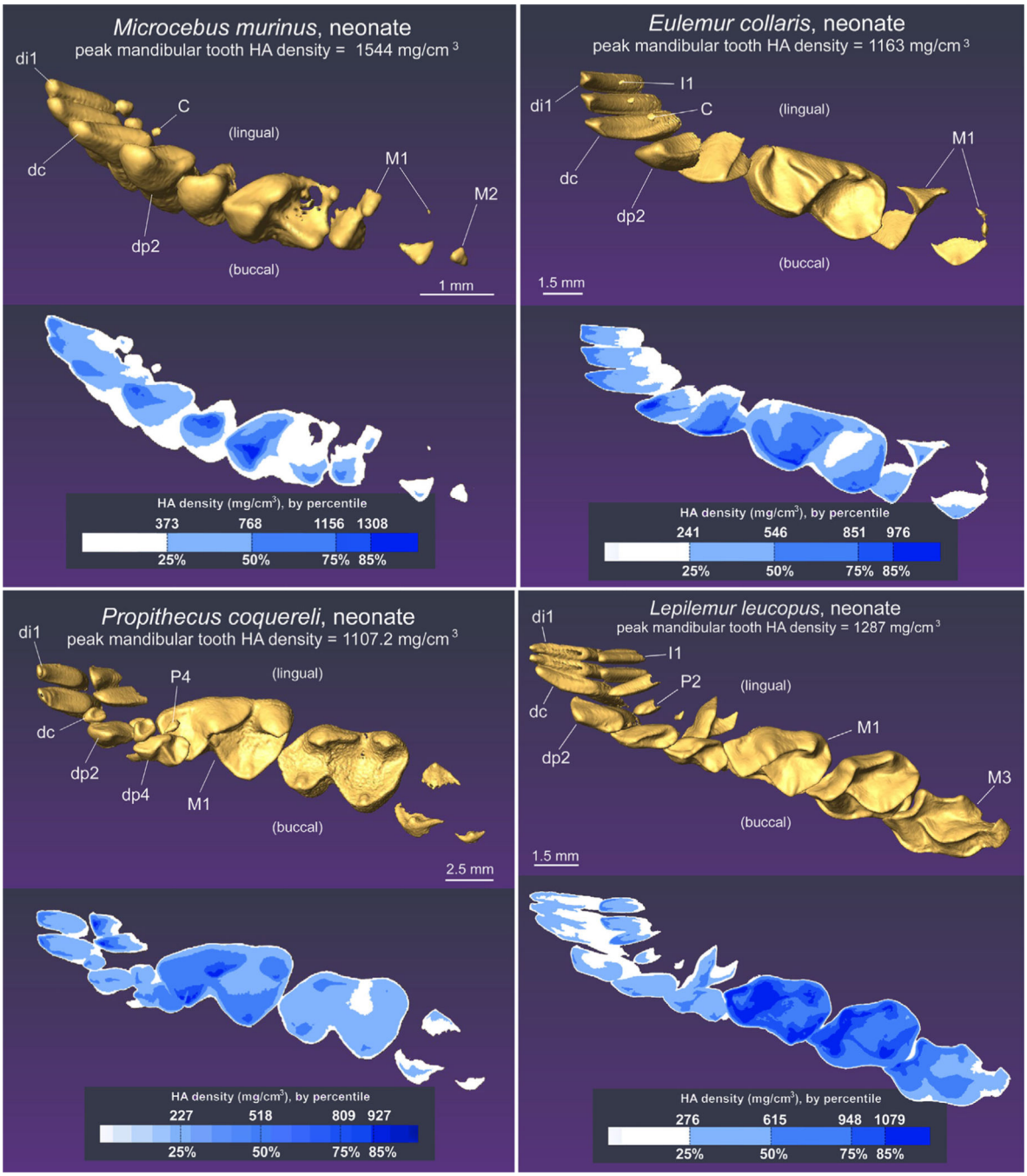

FIGURE 14.

Morphology and hydroxyapatite density in left mandibular tooth crowns at birth in *Microcebus murinus, Eulemur collaris, Propithecus coquereli*, and *Lepilemur leucopus*

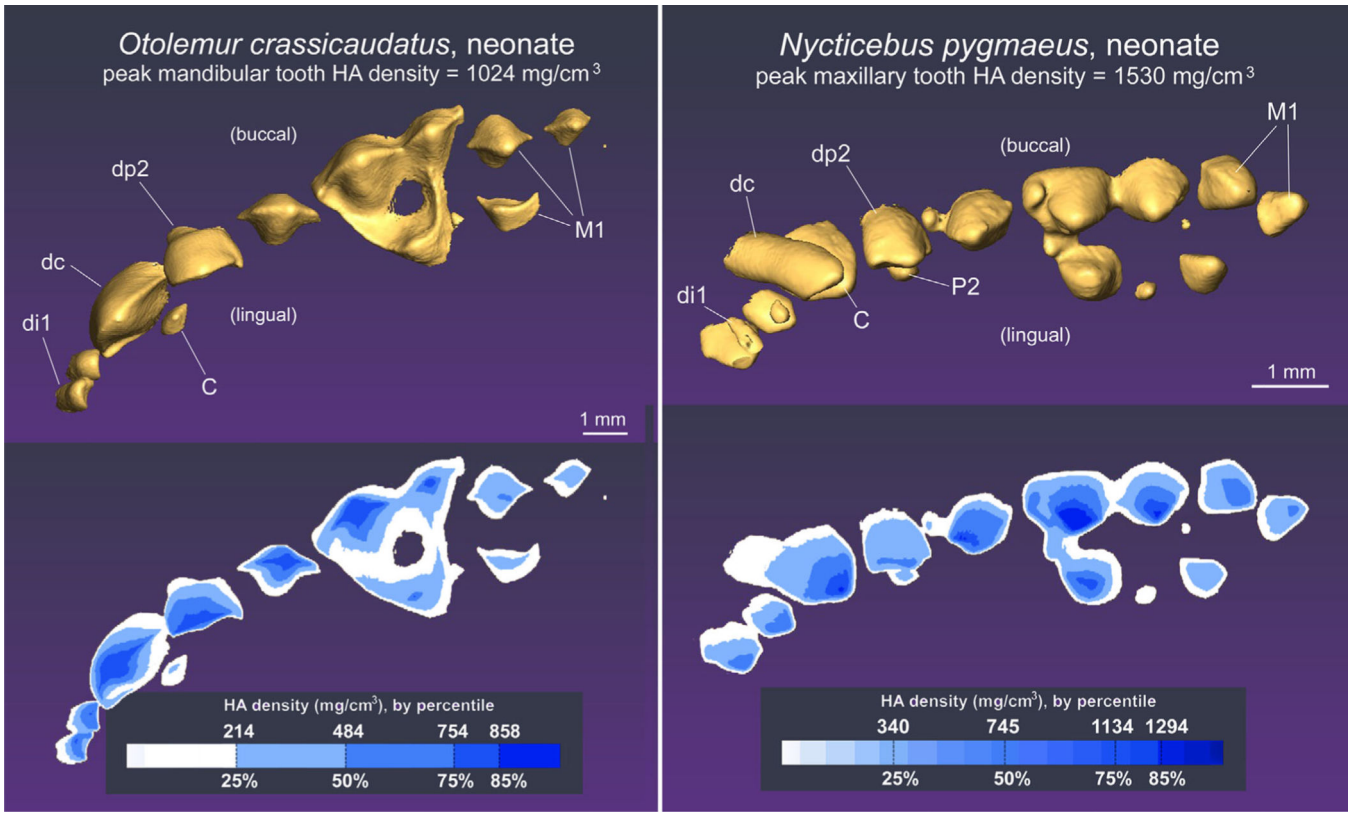

FIGURE 15.

Morphology and hydroxyapatite density in maxillary tooth crowns at birth in *Otolemur crassicaudatus* and *Nycticebus pygmaeus*. In *Otolemur crassicaudatus*, the right jaw is shown (inverted to facilitate comparison to other species) and the left jaw is shown in *Nycticebus pygmaeus*

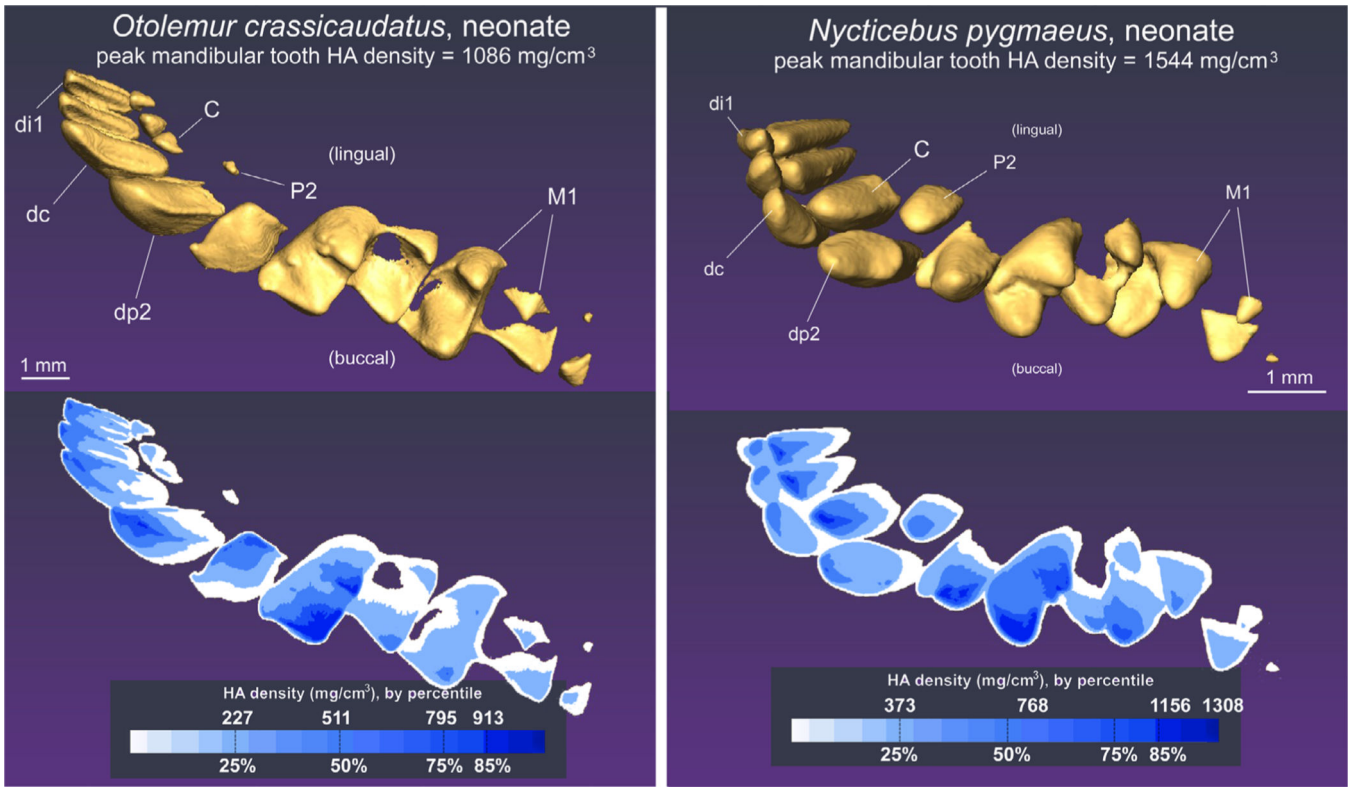

FIGURE 16.

Morphology and hydroxyapatite density in mandibular tooth crowns at birth in *Otolemur crassicaudatus* and *Nycticebus pygmaeus*. In *Otolemur crassicaudatus*, the right jaw is shown (inverted to facilitate comparison to other species) and the left jaw is shown in *Nycticebus pygmaeus*

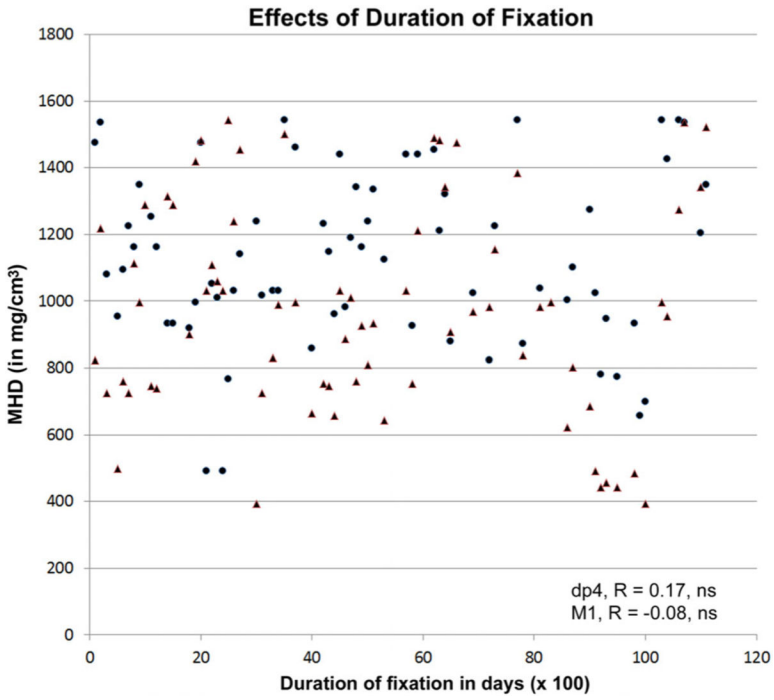

FIGURE 17.

Maximum hydroxyapatite density (MHD) of the last mandibular deciduous premolar (circles) and the first mandibular permanent molar (triangles) plotted against duration of fixation in formalin. All specimens are from the Duke Lemur Center

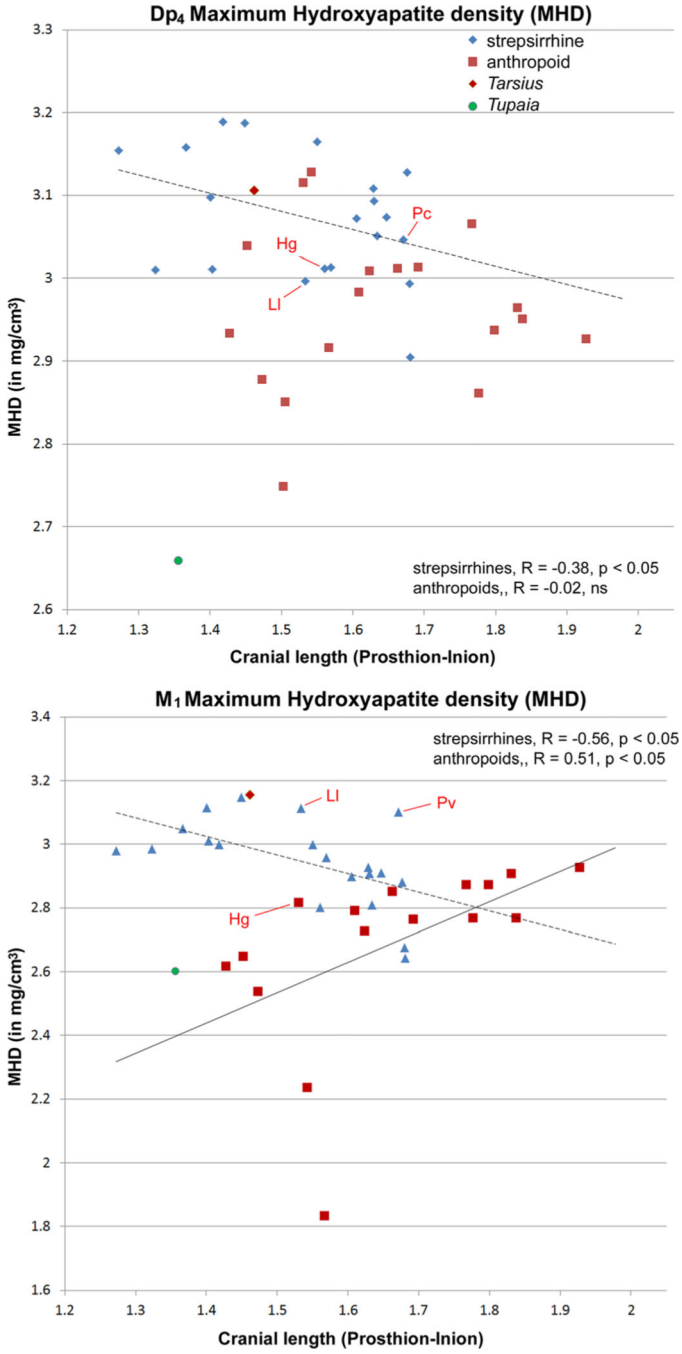

FIGURE 18.

(Top) MHD of dp_4 plotted against cranial length. The dashed line illustrates the negative slope for the significant correlation of dp_4 in strepsirrhines. (Bottom) MHD of M_1 plotted against cranial length. The dashed line illustrates the negative slope for the significant correlation of M_1 in strepsirrhines; the solid line illustrates the positive slope for the significant correlation of M_1 in Old and New World monkeys. *Hg, Hapalemur griseus; Ll, Lepilemur leucopus; Pc, Propithecus coquereli*

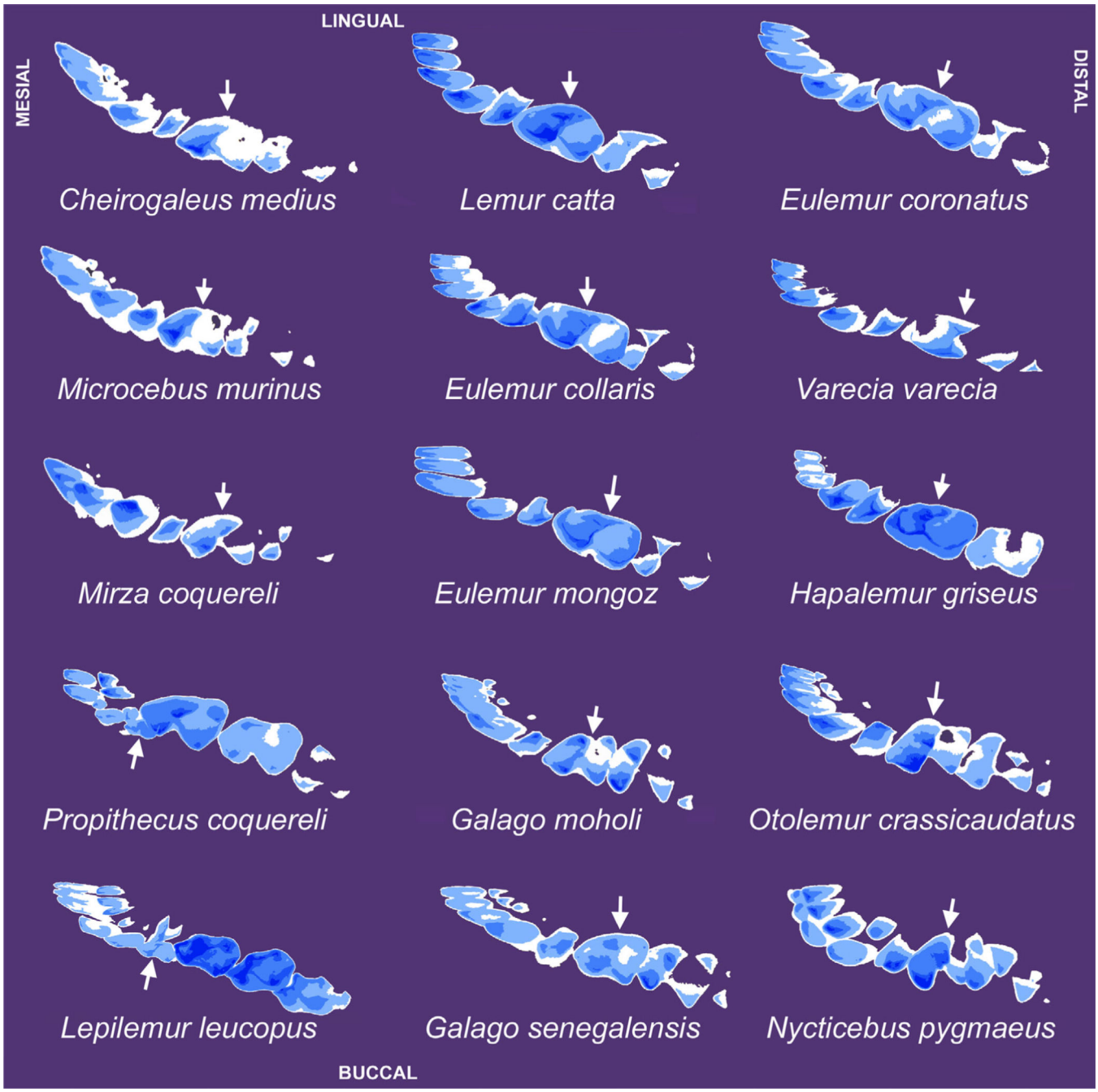

FIGURE 19.

Survey of hydroxyapatite density in mandibular teeth in newborn strepsirrhines. As in earlier plates, blue coding reveals the 25th, 50th, 75th, and 85th percentiles of MHD (light blue = 25th; darkest blue = 85th). Arrow indicates dp_4

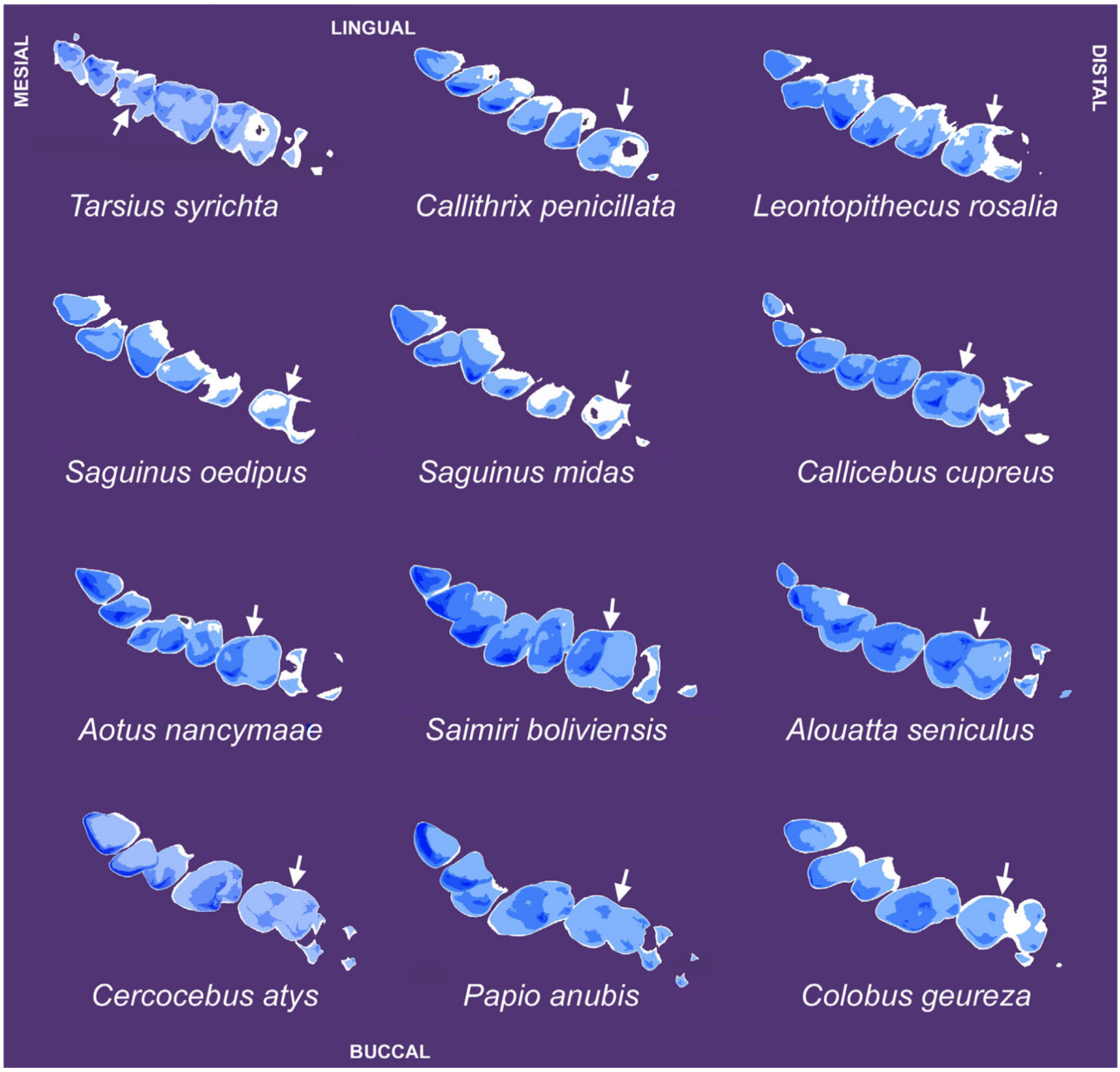

FIGURE 20.

Survey of MHD profiles of mandibular teeth in newborn haplorhines. As in earlier plates, blue coding reveals the 25th, 50th, 75th, and 85th percentiles of MHD (light blue = 25th; darkest blue = 85th). Arrow indicates dp_4

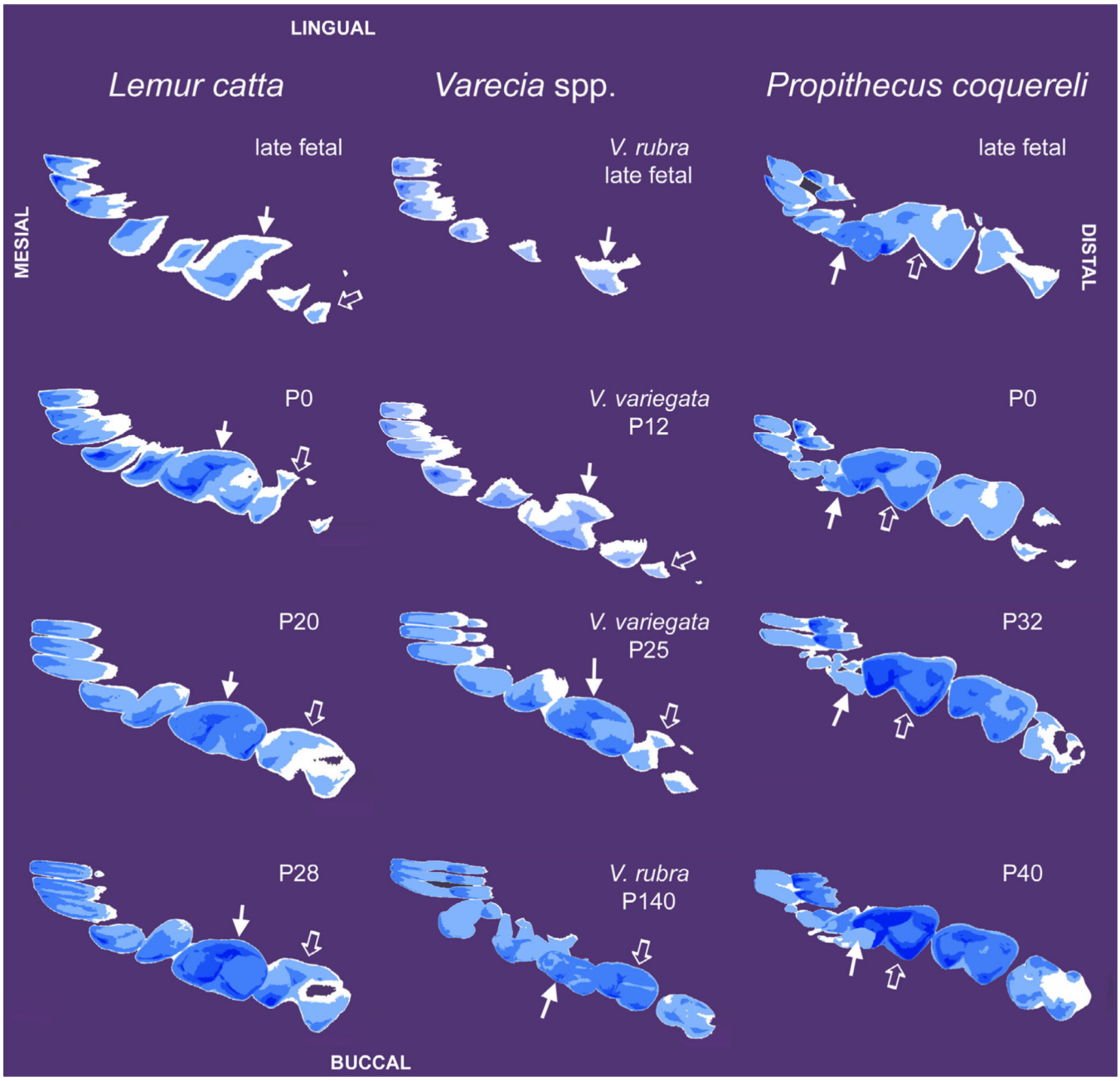

FIGURE 21.

Survey of cusp mineralization patterns in strepsirrhines at late fetal to subadult ages. As in earlier plates, blue coding reveals the 25th, 50th, 75th, and 85th percentiles of MHD (light blue = 25th; darkest blue = 85th). Note that hydroxyapatite density is initially highest anteriorly, and at older ages postcanine teeth contain the peaks in hydroxyapatite density. Solid arrow indicates dp_4; open arrow indicates M_1

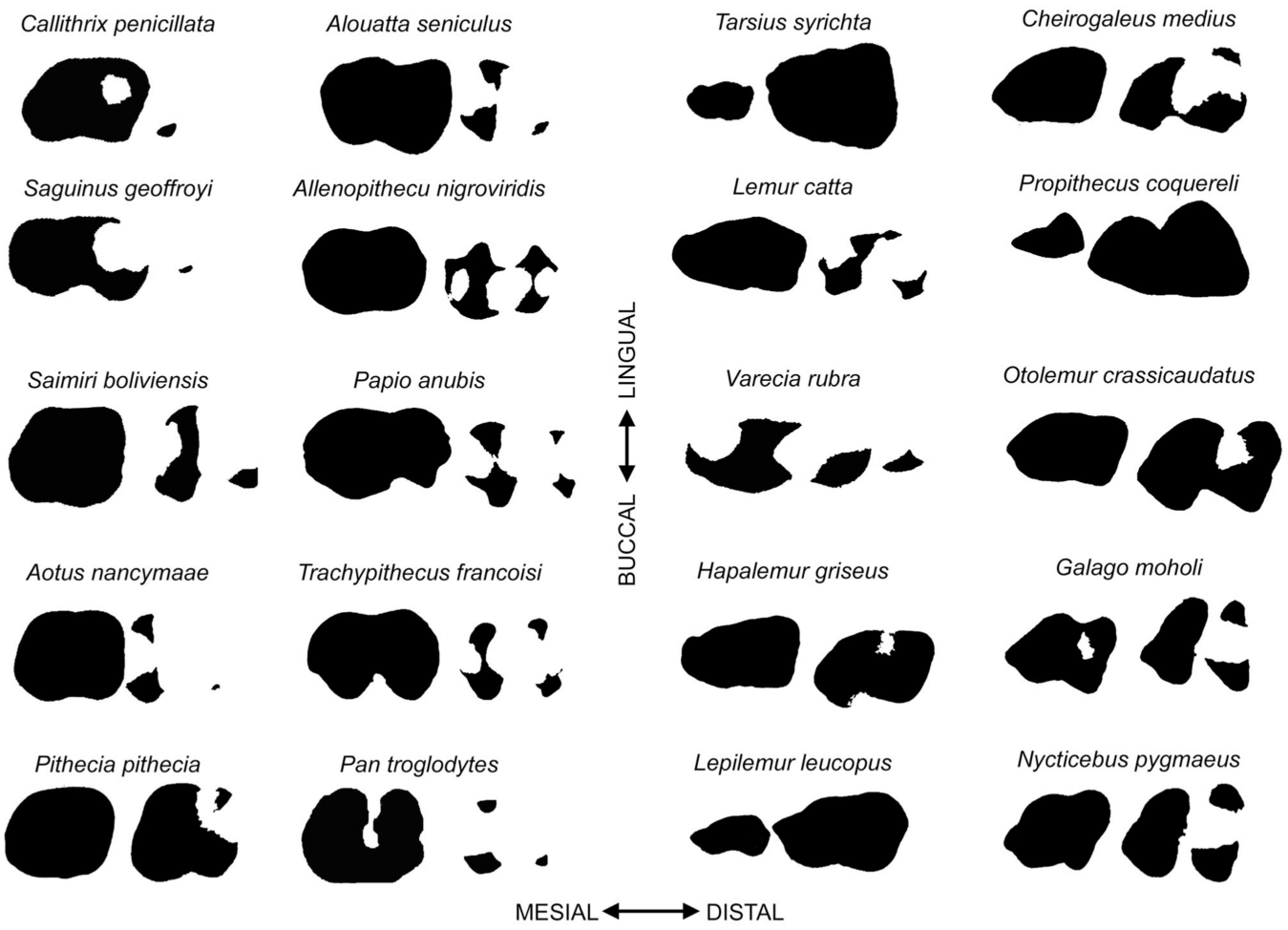

FIGURE 22.

Occlusal view showing extent of mineralization of mandibular dp_4 and M_1 in newborn primates

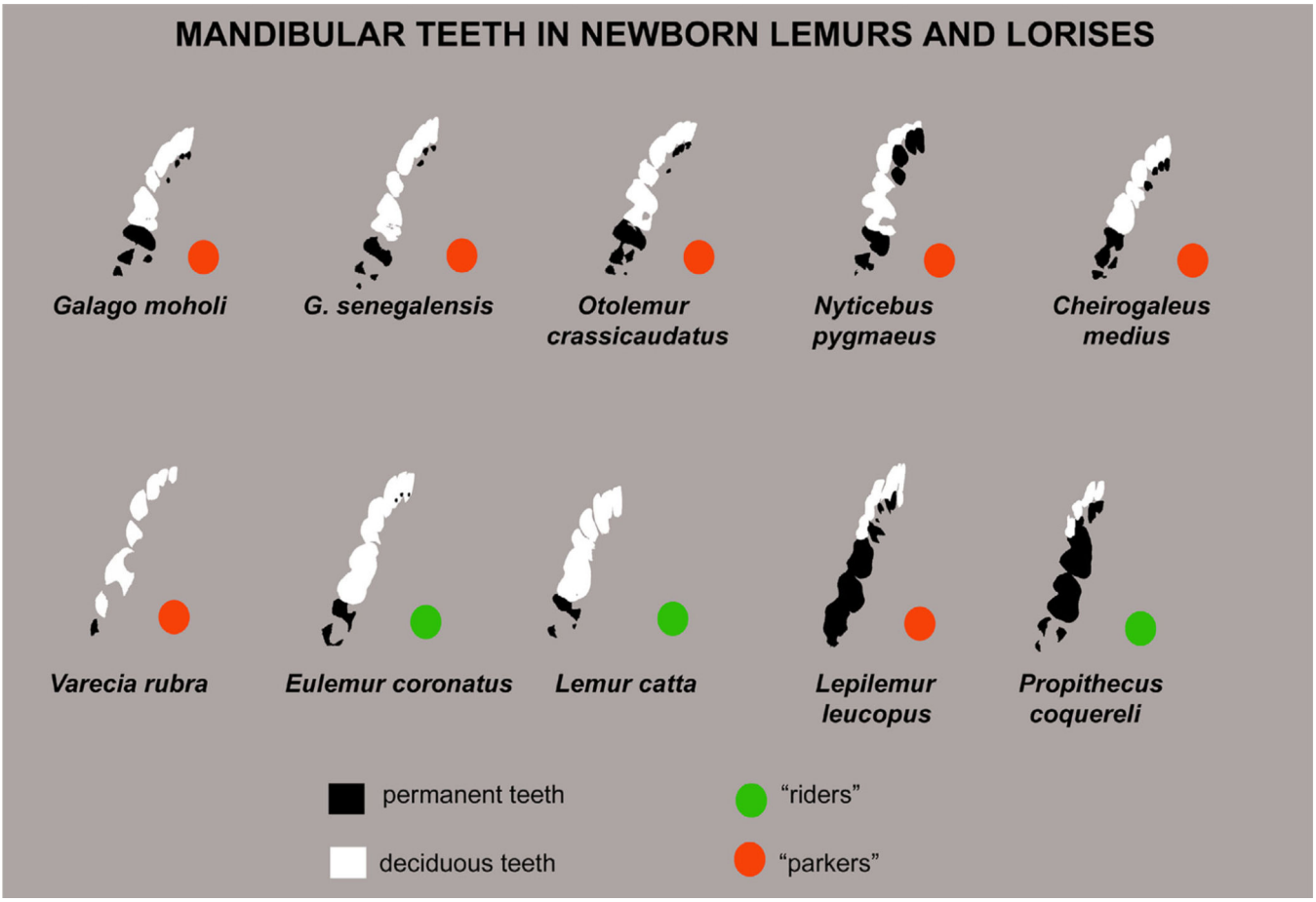

FIGURE 23.

Mineralized portions of deciduous (white) and replacement (black) tooth crowns at birth in newborn strepsirrhines with different parenting strategies

TABLE 1

Mineralized cusps of maxillary postcanine teeth at birth in primates and a sister-group

Species	Dp2		Dp3		Dp4		M1		M2		
	# primary cusps[a]	Crown mineralization[b]	# primary cusps	Crown mineralization	# primary cusps	Crown mineralization	# primary cusps	Crown mineralization[b]	# primary cusps	Crown mineralization[b]	Replacement teeth mineralized at birth?[c]
HAPLORHINES											
Catarrhini											
Cercopithecinae											
Allenopithecus nigroviridis	-	-	4	Crc	4	Crc	4	PC	-	-	None
Cercopithecus atys	-	-	4	Crc	4	Crc	4	PC	-	-	None
Macaca mulatta	-	-	4	Crc	4	Crc			-	-	None
Papio anubis	-	-	4	Crc	4	Crc	4	PC	-	-	None
Colobinae											
Colobus guereza	-	-	4	Crc	4	Crc			-	-	None
Trachypithecus spp.	-	-	4	Crc	4	Crc	4	PC	-	-	None
Platyrrhini											
Atelidae											
Alouatta spp.	1 to 2	Crc	1 to 2	Crc	4	PC	3	PC	-	-	-
Cebidae											
Callithrix spp.	1	PC	2	PC	3	PC	-	-	-	-	None
Cebuella pygmaea	1	Crc	2	PC	3	PC	0 to1	IC	-	-	(I1, C)
Leontopithecus rosalia	1	PC	2	PC	3	PC	-	-	-	-	None
Saguinus spp.	1	PC	1	PC	3	PC	-	-	-	-	None
Saimiri boliviensis	2	PC	2	PC	4	PC			-	-	None
Pithecidae											
Aotus nancymaae	2	PC/Crc	2	PC/Crc	4	Crc	3	PC	-	-	-
Callicebus cupreus	1	Crc	2	Crc	4	Crc	3 to 4	PC	-	-	-
Pithecia pithecia	1	Crc	2	Crc	4	Crc	4		-	-	I1
Tarsiiformes											

	Dp2		Dp3		Dp4		M1		M2		
Species	**# primary cusps[a]**	**Crown mineralization[b]**	**# primary cusps**	**Crown mineralization**	**# primary cusps**	**Crown mineralization**	**# primary cusps**	**Crown mineralization[b]**	**# primary cusps**	**Crown mineralization[b]**	**Replacement teeth mineralized at birth?[c]**
Tarsius syrichta	-	-	1	Crc	2	Crc	3	Crc	3	PC	I1,I2,P2 to P4
STREPSIRRHINES											
Lemuroidea Cheirogaleidae											
Cheirogaleus medius	1	Crc	1	PC	3	PC	3	PC	-	PC	I1, (I2), C, P2
Microcebus murinus	1	Crc	1	PC	3	PC	3	PC	1	PC	I1, C
Lemuridae											
Eulemur spp.	1	Crc	1	PC	3	PC	3	PC	-	-	(C)
Hapalemur griseus	1	PC	1	PC	3	Crc	3	PC	-	-	None
Lemur catta	1	Crc	1	PC	3	PC	3	PC	-	-	None
Varecia spp.	1	PC	1	PC	3	IC	1	PC	-	-	None
Indriidae											
Propithecus coquereli	-	-	1	C	3 to 4	C	4	Crc	4	Crc	I1, C, P3, P4
Lepilemuridae											
Lepilemur leucopus	1	Crc	1	Crc	3	Crc	3	Crc	3	Crc	C, P2, P3, P4
Lorisoidea											
Galagidae											
Galago spp.	1	Crc	1	Crc	4	PC	3	PC	1	PC	C, P2
Otolemur spp.	1	Crc	1	PC	4	PC	3		1		C, (P2)
Lorisidae											
Nycticebus pygmaeus	1	Crc	1	PC	4	PC	3	PC	-	-	I1, I2, C, P2
Scandentia											
Tupaia glis belangeri	1	IC	1	IC	3	IC	3	PC	-	-	None

[a] Number of primary cusps mineralized at birth.

[b] Crown mineralization at birth: -, tooth vestigial or not formed in this taxon; IC, isolated cusps; PC, Partial crown (e.g., crown base poorly mineralized or isolated cusp[s]); Crc, crown complete or nearly so (e.g., basin only incomplete); −, crown not yet mineralized;

[c] Replacement teeth mineralized at birth: parentheses indicate variably mineralized.

TABLE 2

Secondary cusps in maxillary deciduous premolars in selected primate species

Species	dp2			dp3			dp4		
HAPLORHINES	**Parastyle**	**Mesostyle**	**Metastyle/distostyle**	**Parastyle**	**Mesostyle**	**Metastyle/distostyle**	**Parastyle**	**Mesostyle**	**Metastyle**
Catarrhini									
Cercopithecinae									
Allenopithecus nigroviridis	-	-	-	P	A	A	P	A	A
Cercopithecus atys	-	-	-	W	A	A	W	A	A
Macaca mulatta	-	-	-	P	A	A	P	A	A
Papio anubis	-	-	-	P	A	A	P	A	A
Colobinae									
Colobus guereza	-	-	-	A	A	A	A	A	A
Trachypithecus spp.	-	-	-	P	A	A	P	A	A
Platyrrhini									
Atelidae									
Alouatta spp.	A	A	A	P	A	A	P	P	P
Cebidae									
Cebuella pygmaea	P	A	W	P	A	W	P	P	W
Cebus apella	P	A	A	P	A	A	P	A	A
Saimiri boliviensis	P	A	P	P	A	P	P	A	P
Pithecidae									
Aotus nancymaae	A	A	A	A	A	A	A	A	A
Callicebus cupreus	A	A	A	A	A	A	A	A	A
Pithecia pithecia	P	A	p	W	A	W	P	A	P
Tarsiiformes									
Tarsius syrichta	-	-	-	P	A	A	P	A	A
T. bancanus	-	-	-	P	A	A	P	A	A
STREPSIRRHINES									
Lemuroidea									
Lemuridae									
Eulemur spp.	P	A	W	P	A	W	P	A	P

Species	dp2			dp3			dp4		
HAPLORHINES	**Parastyle**	**Mesostyle**	**Metastyle/distostyle**	**Parastyle**	**Mesostyle**	**Metastyle/distostyle**	**Parastyle**	**Mesostyle**	**Metastyle**
Hapalemur griseus	P/W	A	?	P	A	?	P	P	P
Lemur catta	P	A	P	P	A	P	P	A	P
Varecia spp.	?	?	?	P	?	?	P	?	?
Indriidae									
Propithecus coquereli	-	-	-	W	A	W	P	P	P
Lepilemuridae									
Lepilemur leucopus	P	A	A	P	A	W	P	A	P
Lorisoidea									
Galagidae									
Galago spp.	P	A	P	P	A	P	P	A	P
Otolemur spp.	W	A	P	P	A	P	P	A	P

Abbreviations: A, absent; P, present; W, present but weakly expressed.

Anat Rec (Hoboken). Author manuscript; available in PMC 2020 September 01.

TABLE 3

Mineralized cusps of mandibular postcanine teeth at birth in primates and a sister-group

Species	dp2		dp3		dp4			M1		M2		
	# primary cusps[a]	Crown mineralization[b]	# primary cusps[c]	Crown mineralization	# primary cusps[d]	Paraconid?	Crown mineralization	# primary cusps[a]	Crown mineralization[b]	# primary cusps[a]	Crown mineralization[b]	Replacement teeth at birth?[e]
HAPLORHINES												
Catarrhini												
Cercopithecinae												
Allenopithecus nigroviridis	-	-	4	Crc	4	+	Crc	4	PC	-	-	None
Cercocebus atys	-	-	4	Crc	4	-	Crc	4	IC	-	-	None
Macaca mulatta	-	-	4	Crc	4	-	Crc	4	IC	-	-	None
Papio anubis	-	-	4	Crc	4	-	Crc	4	IC	-	-	None
Colobinae												
Colobus guereza	-	-	4	Crc	4	-	Crc	3	IC	-	-	None
Trachypithecus spp.	-	-	4	Crc	4	+	Crc	4	IC	-	-	None
Platyrrhini												
Atelidae												
Alouatta spp.	1	Crc	4	Crc	4	-	Crc	3	IC	-	-	None
Cebidae												
Callithrix spp.	1	PC/Crc	1	PC/Crc	4	-	Crc	1 to 2	IC	-	-	None
Cebuella pygmaea	1	PC/Crc	1	PC/Crc	4	+	Crc	0 to 3	IC	-	-	(I1,I2)
Leontopithecus rosalia	1	CRC	2	PC	4	-	PC	1	IC	-	-	None
Saguinus spp.	1	PC	1 to 2	PC	4	-	PC	3	PC/IC	0 to 1	IC	None
Saimiri boliviensis	1	Crc	2	Crc	4	-	Crc	2 to 3	IC	-	-	None
Pithecidae												
Aotus nancymaae	1 to 2	PC	2	Crc	4	-	Crc	3 to 4	IC	-	-	None
Callicebus cupreus	1	Crc	2	Crc	4	-	Crc	3	IC	-	-	(I1,I2)
Pithecia pithecia	1	Crc	2	Crc	4	-	Crc	4	PC	1	IC	-
Tarsiiformes												
Tarsius syrichta			1	Crc	5	+	Crc	5/5	Crc	5/5	PC	I1, C, P2-P4

Species	dp2 # primary cusps[a]	dp2 Crown mineralization[b]	dp3 # primary cusps[c]	dp3 Crown mineralization	dp4 # primary cusps[d]	dp4 Paraconid?	dp4 Crown mineralization	M1 # primary cusps[a]	M1 Crown mineralization[b]	M2 # primary cusps[a]	M2 Crown mineralization[b]	Replacement teeth at birth?[e]
STREPSIRRHINES												
Lemuroidea												
Cheirogaleidae												
Cheirogaleus medius	1	Crc	1	PC	4	-	Crc	¾	PC	1 to 2	IC	I1,I2,C,P2
Microcebus murinus	1	Crc	1	PC	4	-	Crc	4	PC	1	IC	I1,I2,C,P2
Mirza coquereli	1	PC	1	PC	4	-	PC	3	PC	-	-	I1, I2
Lemuridae												
Eulemur spp.	1	Crc	1	PC	3–4	+	Crc	4	IC	-	-	(I1, I2), C
Lemur catta	1	Crc	1	PC	4	+	Crc	3 to 4	IC	-	-	None
Hapalemur griseus	1	Crc	1	PC	4	+	Crc	4	PC	-	-	None
Varecia spp.	1	PC	1	PC	3	+	PC	1	IC	-	-	None
Indriidae												
Propithecus coquereli	1	Crc	-	PC	4	-	Crc	4	Crc	4	C/PC	I1,I2,P2,P4
Lepilemuridae												
Lepilemur leucopus	1	Crc	1	C	3	+	Crc	4	Crc	4	C	I1,I2,C,P2,P3,P4
Lorisoidea												
Galagidae												
Galago spp.	1	Crc	1	PC	4	+	Crc	4	IC	1 to 2	IC	I1,I2,C (P2)
Otolemur spp.	1	Crc	1	PC	4	+	Crc	4	IC/PC	1 to 2	IC	I1,I2,C,P2
Lorisidae												
Nycticebus pygmaeus	1	Crc	1	PC	4		PC	4	PC	1 to 3	IC	I1,I2,C,P2
Scandentia												
Tupaia belangeri	1	IC	1	IC	4	+	IC	3	IC	-	-	None

[a] Number of primary cusps mineralized at birth.

[b] Crown mineralization at birth (only described for neonates): IC, isolated cusps (at least two cusps isolated); PC, Partial crown (e.g., crown base poorly mineralized or isolated entoconid); Crc, crown complete or nearly so (e.g., basin only incomplete).

[c] For dp3, this number excludes a paraconid (except for *Tarsius* and *Tupaia*), which may be present in some species (see text).

[d] For dp4, this number excludes the paraconid, if present, but includes the hypoconulid in *Lemur* and *Hapalemur*.

[e] Replacement teeth mineralized at birth: parentheses indicate variably mineralized.

TABLE 4

Maximum hydroxyapatite density (MHD) of mandibular dp4 and M1 in primates, average, and range

	Dp_4 MHD		M_1 MHD	
	Average	**Range**	**Average**	**Range**
HAPLORHINI				
Catarrhini				
Cercopithecinae				
Allenopithecus nigroviridis	1,031	-	753.9	-
Cercocebus atys	920.1	-	809.3	-
Macaca mulatta	864.7	-	747	-
Papio anubis	843.9	-	843.9	-
Colobinae				
Colobus guereza	726.2	-	587.6	-
Trachypithecus francoisi	892.4	-	587.6	-
Platyrrhini				
Atelidae				
Alouatta seniculus	747	-	747	-
Cebidae				
Callithrix jacchus	1,093.3	795.5–1,273.4	445.7	2.82.9–643.1
Callithrix pencillata	753.9	-	345.2	-
Cebuella pygmaea	857.8	-	414.5	-
Leontopithecus rosalia	823.2	-	68.1	-
Saguinus bicolor	560	-	NP	-
Saguinus geoffroyi	1,342.7	-	172	-
Saguinus midas	708.9	608.4, 809.3	NP	-
Saguinus oedipus	1,303.4	1,238.8–1,349.6	656.9	-
Saimiri boliviensis	1,027.4	809–1,432.7	665.5	511–940.9
Pithecidae				
Aotus nancymaae	534.6	954.8–1,093	534.6	483.7–581
Callicebus cupreus	961.5	837,1,086	618.6	539.2,698
Pithecia pithecia	1,031	-	580.7	-

	Dp_4 MHD		M_1 MHD	
	Average	**Range**	**Average**	**Range**
Tarsiiformes				
Tarsius syrichta	1,277.1	1,204.1,1,350	1,432.8	1,342.7,1,522.8
STREPSIRRHINI				
Lemuroidea				
Cheirogaleidae				
Cheirogaleus medius	1,439.7	1,439.7, 1,439.7	1,121.1	1,031,1,211.1
Microcebus murinus	1,425.8	-	954.8	-
Mirza coquereli	1,543.6	-	996.3	-
Lemuridae				
Eulemur collaris	1,183.367	961.7–1,439.7	811.6333	656.9–1,031
Eulemur coronatus	1,124.2	-	643.1	-
Eulemur macaco	1,238.8	-	809.3	-
Eulemur mongoz	1,231.9	-	753.9	-
Eulemur rubriventer	1,342.7	-	760.8	-
Hapalemur griseus	1,026.7	976.6–1,102.2	633.8	476.8–802.4
Lemur catta	1,179.2	954.8–1,536.7	789.9	497.6–1,218
Varecia rubra	802.4	774.7–934	439.9	393.7–483.7
Varecia variegata	986.0	947.9,1,024	473.4	456,490.7
Indriidae				
Propithecus coquereli	1,112.7	996.3–1,474.3	1,261.1	1,058.7–1,481.9
Lepilemuridae				
Lepilemur leucopus	991.7	934–1,107.2	1,298.8	1,287.3–1,315
Lorisoidea				
Galagidae				
Galago moholi	1,218	878.6–1,321.9	1,302.9	906.3–1,488.2
Galago senegalensis	1,026.0	823.2–1,543.6	1,025.0	892–1,384.3
Galagoides demidovii	1,024	-	968.6	-
Otolemur crassicaudatus	1,031	1,031, 1,031	909.8	830.1, 989.4
Otolemur garnettii	1,460.4	-	996.3	-
Lorisidae				

	Dp_4 MHD		M_1 MHD	
	Average	**Range**	**Average**	**Range**
Nycticebus pygmaeus	1,540.1	1,536.6,1,543.6	1,405	1,273.4,1,536.6
Scandentia				
Tupaia belangeri	456	-	400.6	-

TABLE 5

Crown mineralization status in mandibular molarifom teeth of newborn primates

	Dp_4		M_1		M_2		M_3	
SPECIES	**Cusps**	**Basins**	**Cusps**	**Basins**	**Cusps**	**Basins**	**Cusps**	**Basins**
HAPLORHINI								
Catarrhini								
Cercopithecinae								
Allenopithecus nigroviridis	+++	+++	+++	−	NA	NA	NA	NA
Cercocebus atys	+++	+++	+++	−	NA	NA	NA	NA
Macaca mulatta	+++	+++	++	−	NA	NA	NA	NA
Papio anubis	+++	+++	++	−	NA	NA	NA	NA
Colobinae								
Colobus guereza	+++	+++	++	−	NA	NA	NA	NA
Trachypithecus francoisi	+++	+++	++	−	NA	NA	NA	NA
Platyrrhini								
Atelidae								
Alouatta seniculus	+++	+++	++	−	NA	NA	NA	NA
Cebidae								
Callithrix spp.	+++	++	+	−	NA	NA	NA	NA
Cebuella pygmaea	+++/++	+++/++	+/−	−	NA	NA	NA	NA
Leontopithecus rosalia	+++	++	+	−	NA	NA	NA	NA
Saguinus spp.	+++	++	+/−	−	NA	NA	NA	NA
Saimiri boliviensis	+++	+++	++	−	NA	NA	NA	NA
Pithecidae								
Aotus nancymaae	+++	+++	+	−	NA	NA	NA	NA
Callicebus cupreus	+++	+++	+	−	NA	NA	NA	NA
Pithecia pithecia	+++	+++	++	−	+	−	NA	NA
Hominidae								
Pan troglodytes	+++	+++	++	−	NA	NA	NA	NA
Pongo pygmaeus	+++?	+++	++	−	NA	NA	NA	NA
Tarsiiformes								

	Dp_4		M_1		M_2		M_3	
SPECIES	**Cusps**	**Basins**	**Cusps**	**Basins**	**Cusps**	**Basins**	**Cusps**	**Basins**
Tarsius syrichta	+++	+++	+++	+++	+++	++	++	−
STREPSIRRHINI								
Lemuroidea								
Cheirogaleidae								
Cheirogaleus medius	+++	+++	+++/++	++	++/+	−	NA	NA
Lemuridae								
Eulemur spp.	+++	+++	++	−	NA	NA	NA	NA
Hapalemur griseus	+++	+++			NA	NA	NA	NA
Lemur catta	+++	+++	++	−	NA	NA	NA	NA
Varecia spp.	++	++	+	−	NA	NA	NA	NA
Indriidae								
Propithecus coquereli	+++	+++	+++	+++	+++	+++	++	−
Lepilemuridae								
Lepilemur leucopus	+++	+++	+++	+++	+++	+++	+++	+++
Lorisoidea								
Galagidae								
Galago spp.	+++	+++	+++	++/+	+	−	NA	NA
Otolemur spp.	+++	+++	+++	++/+	+	−	NA	NA
Lorisidae								
Nycticebus pygmaeus	+++	+++	+++	++	++	−	NA	NA

Note. cusp mineralization: +++ all cusps mostly mineralized, ++ some cusps unmineralized, + most cusps unmineralized, − no mineralized cusps; [3]basins: +++ both basins mostly or completely mineralized, ++ one basin (e.g., talonid) mostly or completely unmineralized, + both basins mostly unmineralized, − no mineralization of basins; NA, not applicable (tooth germ not yet formed).

TABLE 6

Mandibular tooth calcification: last deciduous premolar (dp_4) and first permanent molar (M_1)

Species	dp_4 crown completion: At birth? Month?	dp_4 crown completion: At one	M_1: Age at crown completion (years)	References	Weaning age (years)	References
Pan troglodytes	Y[a]	Y	~2	Anemone, Mooney, and Siegel (1996)	4.6–5	Kappeler and Pereira (2003)
Macaca nemestrina	Y	Y	0.89–.97	Sirianni and Swindler (1985)	0.66–1	Kappeler and Pereira (2003)
Saguinus oedipus	N	Y	>0.083; < 0.32	New data	0.14	Kappeler and Pereira (2003)
Cebuella	N	Y	~0.083	New data	0.25	Kappeler and Pereira (2003)
Lemur catta	Y	Y	>0.083	New data	0.50	Zehr et al. (2014)
Varecia variegata	N	N	>0.083	New data	0.30	Zehr et al. (2014)
Propithecus coquereli	Y	Y	~Birth	New data	0.39	Zehr et al. (2014)
Galago moholi	Y[a]	Y	<0.083	New data	0.25	Zehr et al. (2014)

[a]Basin or distolingual crown may be poorly mineralized.

TABLE 7

Mandibular tooth calcification: first permanent molar (M_1) and incisors (I_1)[a]

Species	M_1: Age at crown completion (years)	I_1: Onset of calcification (years)	References	Weaning age (years)	References
Pan troglodytes	~2	0.5	Anenome et al. (1991)	4.6–5	Kappeler and Pereira (2003)
Macaca nemestrina	0.89–.97	2.11–2.28	Sirianni and Swindler (1985)	0.66–1	Kappeler and Pereira (2003)
Saguinus oedipus	>0.083, but <0.32	~ 0.083	New data	0.14	Kappeler and Pereira (2003)
Cebuella	~0.083	Perinatal[b]	New data	0.25	Kappeler and Pereira (2003)
Lemur catta	>0.083	>0.055, but <0.083	New data	0.50	Zehr et al. (2014)
Varecia variegata	>0.083	>0.033, but <0.068	New data	0.30	Zehr et al. (2014)
Propithecus coquereli	~Birth	Prenatal	New data	0.39	Zehr et al. (2014)
Galago moholi	<0.083	Prenatal	New data	0.25	Zehr et al. (2014)

[a] Table reproduced from Smith TD, DeLeon VB, Vinyard, CJ, & Young JW. (in press). *Skeletal anatomy of the newborn primate*. Cambridge, England: Cambridge University Press.

[b] Tooth cusp/crown is calcified in some but not all newborns.